The Journal of Antibiotics (2009) 62, 289–294

www.nature.com/ja

ORIGINAL ARTICLE

Enantioselective total synthesis of atpenin A5

Masaki Ohtawa[1], Satoru Ogihara[1], Kouhei Sugiyama[1], Kazuro Shiomi[2], Yoshihiro Harigaya[1], Tohru Nagamitsu[1] and Satoshi Ōmura[3]

Enantioselective total synthesis of atpenin A5, a potent mitochondrial complex II (succinate-ubiquinone oxidoreductase) inhibitor, has been achieved by a convergent approach through a coupling reaction between 5-iodo-2,3,4,6-tetraalkoxypyridine and a side-chain aldehyde. The two key segments were synthesized through *ortho*-metalation/boronation with $(MeO)_3B$/oxidation with *m*CPBA, *ortho*-iodination, halogen dance reaction, Sharpless epoxidation and regioselective epoxide-opening reaction. This synthetic study resulted in the revision of the earlier reported ^{1}H-NMR data of the natural atpenin A5 and the confirmation of the stereochemical assignment.
The Journal of Antibiotics (2009) **62,** 289–294; doi:10.1038/ja.2009.29; published online 17 April 2009

Keywords: atpenin A5; complex II inhibitor; enantioselective total synthesis

INTRODUCTION

Atpenins[1,2] were first isolated from the fermentation broth of a fungal strain, *Penicillium* sp. FO-125, as growth inhibitors of both fatty acid synthase-deficient (A-1) and acyl-CoA synthase I-deficient (L-7) mutants of *Candida lipolytica* and atpenin B were shown to inhibit the ATP-generating system of Raji cells (Figure 1). They inhibited the growth of filamentous fungi. The absolute configuration of atpenin A4 (**2**) was confirmed by X-ray crystallographic analysis.[3] The total synthesis of (±)-atpenin B (**1**) was reported by Quéguiner and co-workers.[4] Recently, atpenins were rediscovered as a result of microbial screening for mitochondrial complex II (succinate-ubiquinone oxidoreductase) inhibitors.[5] Among them, atpenin A5 (**3**) proved to be much more potent against bovine heart complex II than known complex II inhibitors. Furthermore, the crystal structure analysis of *Escherichia coli* complex II–atpenin A5 (**3**) complex has been achieved, and catalytic reduction of quinone was suggested to occur at the atpenin-binding site of *E. coli* complex II.[6] As described, atpenins are expected to be useful as biochemical tools in the molecular-biological research of complex II. We report herein the enantioselective total synthesis of atpenin A5 (**3**) by a convergent strategy through a coupling reaction between 2,3,4,6-tetraalkoxypyridine (**4a**) and a side-chain aldehyde (**5**), as shown in Figure 2. The 2,3,4,6-tetraalkoxypyridine (**4a**) would be constructed from 2-chloro-3-pyridinol (**6**) through the modified Quéguiner's procedure as follows: (1) directed *ortho*-lithiation/iodination, (2) halogen dance reaction[7] and (3) installation of a hydroxy group on the pyridine ring through a one-pot procedure by a sequence of reactions, and halo–lithium exchange/quenching with $(MeO)_3B$/oxidation. The side-chain aldehyde **5** could be synthesized from a commercially available chiral ester **7** by Sharpless asymmetric epoxidation[8] and regioselective epoxide opening as key reactions.

RESULTS AND DISCUSSION

The synthesis of **4a** began with the conversion of the commercially available 2-chloro-3-pyridinol **6** into a known 4-hydroxypyridine **8** (51%, 3 steps), according to the Quéguiner's atpenin B synthesis[4] (Scheme 1). In the earlier synthesis, the next key reaction was a directed *ortho*-lithiation, followed by bromination, in which the use of a diisopropyl carbamate group as a protecting group for the 4-hydroxy group was essential for the directed *ortho*-lithiation. However, the treatment required to deprotect the diisopropyl carbamate group in the final stage of total synthesis (5 M solution of KOH in methanol under reflux) would lead to significant epimerization at the C8 position (in atpenin A5 numbering). Therefore, we looked at other approaches to provide 5-halogenation and protection of the 4-hydroxy group. After various unfruitful trials, the problem was solved by a very simple and mild method, in which **8** was treated with K_2CO_3 and I_2 in water (for similar reaction conditions, see Kay *et al.*[9]) to afford the desired 4-hydroxy-5-iodopyridine **9** in 75% yield. This modification allowed the use of an easily removable protecting group and led us to the synthesis of an MOM ether **10** (90% yield). Subsequent halogen dance reaction of **10** with lithium diisopropylamide smoothly proceeded to afford 6-iodopyridine **11** in 75% yield. Treatment of **11** with *n*-butyl lithium for halo–lithium exchange, boronation with $(MeO)_3B$ and oxidation with *m*CPBA (used instead of trifluoroperacetic acid because of its ease in handling) gave 6-hydroxy-5-iodopyridine **13**, not **12**, in 76% yield with good reproducibility. The iodopyridinol **13** would be obtained by *ortho*-iodination of **12** with iodine, which was easily generated *in situ* by oxidation of the iodide with *m*CPBA under

[1]School of Pharmacy, Kitasato University, Shirokane, Minato-ku, Tokyo, Japan; [2]Kitasato Institute for Life Sciences and Graduate School of Infection Control Sciences, Kitasato University, Shirokane, Minato-ku, Tokyo, Japan and [3]Kitasato Institute for Life Sciences, Kitasato University, Shirokane, Minato-ku, Tokyo, Japan
Correspondence: Dr T Nagamitsu, School of Pharmacy, Kitasato University, 5-9-1 Shirokane, Minato-ku, Tokyo 108-8641, Japan.
E-mail: nagamitsut@pharm.kitasato-u.ac.jp or Professor S Ōmura, Kitasato Institute for Life Sciences, Kitasato University, 5-9-1 Shirokane, Minato-ku, Tokyo 108-8641, Japan.
E-mail: omura-s@kitasato.or.jp
Received 4 February 2009; revised 11 March 2009; accepted 16 March 2009; published online 17 April 2009

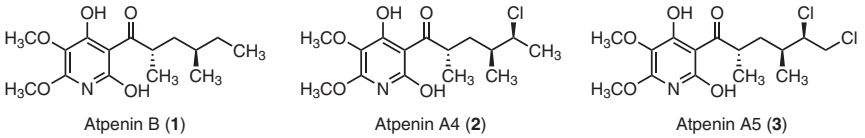

Figure 1 Structures of atpenins B (**1**), A4 (**2**) and A5 (**3**).

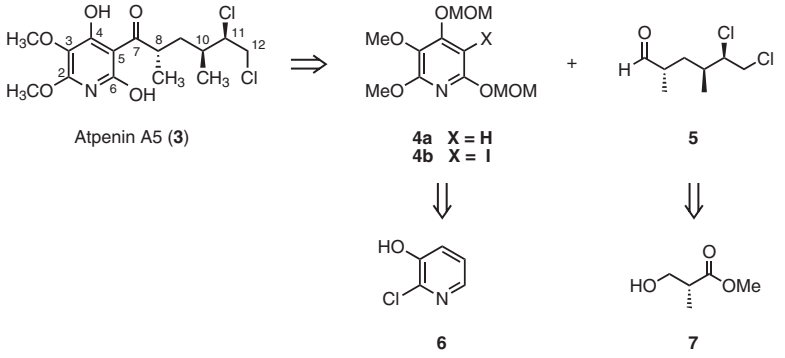

Figure 2 Retrosynthesis of atpenin A5 (**3**).

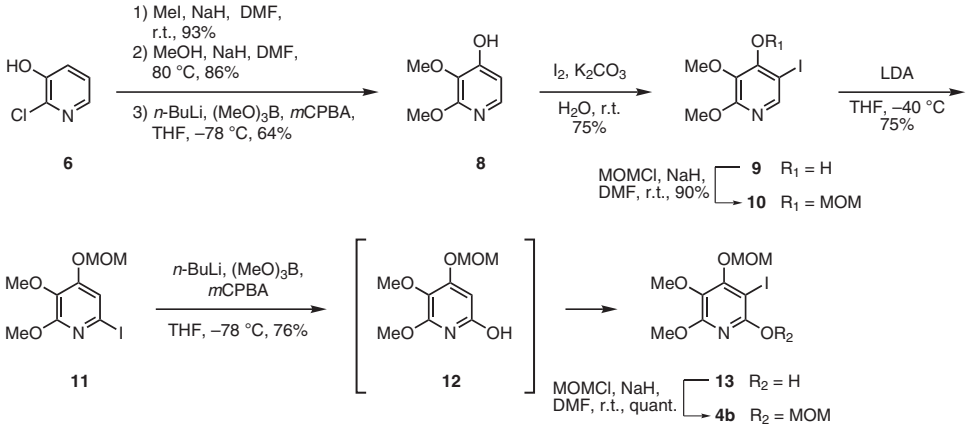

Scheme 1 Synthesis of 5-iodo-2,3,4,6-tetraalkoxypyridine **4b**.

basic conditions. The iodopyridinol **13** was protected as an MOM ether to furnish 5-iodo-2,3,4,6-tetraalkoxypyridine **4b** in a quantitative yield, which is the desirable alternative to 2,3,4,6-tetraalkoxypyridine **4a** in terms of the coupling reaction with the side chain **5**.

The stereoselective construction of the other required fragment, aldehyde **5**, was carried out as summarized in Scheme 2. A readily available alcohol **14** (Komatsu *et al.*,[10] enantiomeric excess was determined by ^{19}F-NMR spectroscopy after esterification with Mosher's acid.), derived from the commercially available ester **7**, was subjected to tosylation, followed by a nucleophilic substitution reaction with potassium cyanide to give nitrile **16** quantitatively over two steps. The cyano group in **16** was reduced with DIBAL to afford a known aldehyde **17** in 73% yield.[11] Subsequent two-carbon elongation with $Ph_3P{=}CHCO_2Et$ provided **18** in 85% yield. Reduction of the ethyl ester **18** with DIBAL, followed by Sharpless asymmetric epoxidation with (−)-DET, afforded the desired epoxy alcohol **20** as a single diastereomer in 91% yield over two steps. (The epoxidation of the corresponding allyl alcohol with *m*CPBA as a simple achiral epoxidizing agent gave a 1:1 diastereomixture of the epoxy alcohol.) Alcohol **20** was protected as a trityl ether and subjected to the regioselective epoxide-opening reaction with Me_2CuLi and $BF_3{\bullet}Et_2O$[12] to furnish alcohol **22** as a single diastereomer in 94% yield over two steps. Birch reduction to remove the trityl group gave diol **23** in 85% yield. Bischlorination by treatment of diol **23** with NCS and PPh_3 followed by deprotection of the TIPS ether with TBAF, gave **24** in 65% yield over two steps.[13] Oxidation of alcohol **24** with TEMPO and $PhI(OAc)_2$ afforded the key fragment **5** in 81% yield.

With the required fragments, **4b** and **5,** in hand, coupling reaction was attempted as the next key step (Scheme 3). Halo–lithium exchange of **4b** with *n*-BuLi, followed by treatment of aldehyde **5** gave the desired coupled product **25** as a diastereomixture in 83% yield. Oxidation of **25** with Dess–Martin periodinane provided **26** in 86% yield. Finally, cleavage of the bis-MOM ether in **26** with TFA afforded atpenin A5 (**3**) in 93% yield. However, the ^{1}H-NMR spectrum of our synthetic atpenin A5 (**3**) had different chemical shifts from those reported in the literature for the natural product, although the peak patterns were quite similar. As a result, we re-measured the ^{1}H-NMR spectrum of the natural atpenin A5 (**3**) and found that the earlier reported data were incorrect. In fact, our synthetic atpenin A5 (**3**) was completely identical to an authentic sample in all respects.

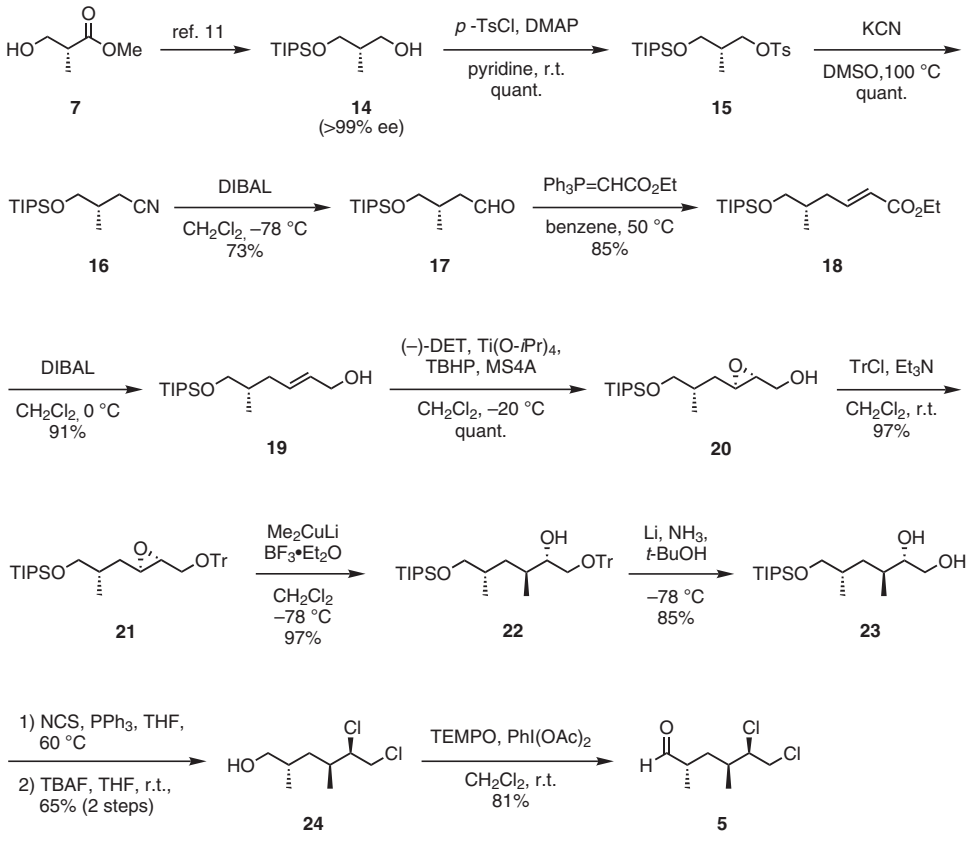

Scheme 2 Synthesis of aldehyde **5**.

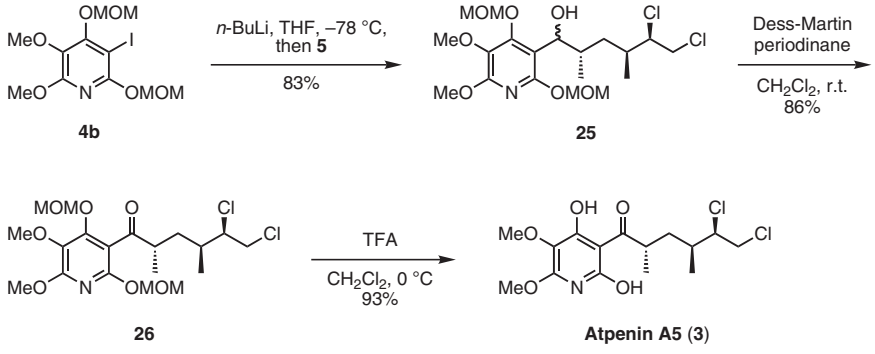

Scheme 3 Completion of the total synthesis of atpenin A5 (**3**).

In summary, the first enantioselective total synthesis of atpenin A5 has been achieved by a convergent approach. The syntheses of the other congeners (A4 and B), and the analogs as well as the biological evaluation of **3**, are currently in progress in our laboratories.

EXPERIMENTAL SECTION

General

Melting points were measured with a Yanagimoto MP apparatus (Yanagimoto, Kyoto, Japan) and remain uncorrected. UV and IR spectra were obtained using an Agilent 8453 spectrophotometer (Agilent Technologies, Waldbornn, Germany) and a Horiba FT-710 spectrophotometer (Horiba, Kyoto, Japan) respectively. ^{1}H- and ^{13}C-NMR spectra were obtained on JEOL JNM-EX-270 (JEOL, Tokyo, Japan), Mercury-300 (Varian, Palo Alto, CA, USA), UNITY-400 (Varian) and INOVA-600 (Varian) spectrometers, and chemical shifts were reported on the δ scale from internal TMS. MS spectra were measured with JEOL JMS-700 (JEOL) and JEOL JMS-AX505HA (JEOL) spectrometers. Optical rotations were recorded on a JASCO DIP-1000 polarimeter (JASCO, Tokyo, Japan). Elemental analyses were performed on a Yanako-MT5 (Yanako, Kyoto, Japan). Commercial reagents were used without further purification unless otherwise indicated. Organic solvents were distilled and dried over molecular sieves (3 or 4 Å). Reactions were carried out in a flame-dried glassware under positive Ar pressure while stirring with a magnetic stirbar unless otherwise indicated. Flash chromatography was carried out on silica gel 60N (spherical, neutral, particle size 40–50 mm). TLC was performed on 0.25 mm E Merck silica gel 60 F254 plates and visualized by UV (254 nm) and cerium ammonium molybdenate.

5-Iodo-2,3-dimethoxypyridin-4-ol (9)

A solution of 2,3-dimethoxypyridin-4-ol **8** (440 mg, 2.84 mmol) in H_2O (6.3 ml) was treated with K_2CO_3 (785 mg, 5.68 mmol) and I_2 (742 mg, 2.93 mmol). The reaction mixture was stirred at room temperature for 1 h,

quenched with saturated aqueous NH_4Cl and extracted with CH_2Cl_2. The organic layers were combined, dried over Na_2SO_4, filtered and concentrated *in vacuo*. The residue was purified by silica gel flash column chromatography (10 : 1 hexanes/EtOAc) to afford **9** (598 mg, 75%) as a yellow solid. mp 134–136°C; IR (KBr) 2998, 2942, 1571, 1473, 1403, 1319, 1261, 1191, 1002, 761, 651 cm^{-1}; ^{1}H-NMR (270 MHz, $CDCl_3$) δ 8.02 (s, 1H), 3.97 (s, 3H), 3.88 (s, 3H); ^{13}C-NMR (150 MHz, $CDCl_3$) δ 157.3, 155.0, 147.2, 130.1, 73.0, 60.7, 53.9; HRMS (FAB, *m*-NBA) $[M+H]^+$ calcd for $C_7H_9NO_3I$ 281.9627, found 281.9627.

5-Iodo-2,3-dimethoxy-4-(methoxymethoxy)pyridine (10)

A solution of **9** (58.0 mg, 206 μmol) in DMF (2.0 ml) was treated with NaH (60%, 12.4 mg, 309 μmol) and MOMCl (24 μl, 309 μmol). The reaction mixture was stirred at room temperature for 1 h, quenched with H_2O and extracted with CH_2Cl_2. The organic layers were combined, dried over Na_2SO_4, filtered and concentrated *in vacuo*. The residue was purified by silica gel flash column chromatography (20 : 1 hexanes/EtOAc) to afford **10** (60.3 mg, 90%) as a yellow solid. mp 57–59 °C; IR (KBr) 3062, 2989, 2944, 2836, 1735, 1563, 1467, 1400, 1211, 1164, 1105, 904, 617, 586 cm^{-1}; ^{1}H-NMR (270 MHz, $CDCl_3$) δ 8.10 (s, 1H), 5.36 (s, 2H) 3.95 (s, 3H), 3.81 (s, 3H), 3.60 (s, 3H); ^{13}C-NMR (150 MHz, $CDCl_3$) δ 159.6, 155.2, 147.6, 135.6, 98.7, 80.9, 60.5, 58.1, 53.9; HRMS (FAB, *m*-NBA) $[M+H]^+$ calcd for $C_9H_{13}NO_4I$ 325.9890, found 325.9890.

6-Iodo-2,3-dimethoxy-4-(methoxymethoxy)pyridine (11)

To a solution of iPr_2NH (67 μl, 471 μmol) in THF (0.4 ml) was added dropwise *n*-BuLi (1.61 M in hexane, 293 μl, 471 μmol). After stirring for 30 min at 0 °C, a solution of **10** (51.0 mg, 157 μmol) in THF (0.4 ml) was added at −40 °C, and the resulting mixture was further stirred for 1 h at −40 °C. EtOH was added, and the resulting solution was partitioned between EtOAc and H_2O. The aqueous layer was extracted with EtOAc, and the organic layers were combined, dried over Na_2SO_4, filtered and concentrated *in vacuo*. The residue was purified by silica gel flash column chromatography (10 : 1 hexanes/EtOAc) to afford **11** (38.3 mg, 75%) as a yellow solid. mp 59–61 °C; IR (KBr) 3097, 2944, 1571, 1479, 1367, 1240, 1162, 1114, 1072, 995, 912, 844, 740, 441 cm^{-1}; ^{1}H-NMR (270 MHz, $CDCl_3$) δ 7.15 (s, 1H), 5.21 (s, 2H), 3.95 (s, 3H), 3.82 (s, 3H), 3.48 (s, 3H); ^{13}C-NMR (150 MHz, $CDCl_3$) δ 157.8, 156.9, 132.8, 116.5, 105.0, 94.7, 60.7, 56.6, 54.4; HRMS (FAB, *m*-NBA) $[M+H]^+$ calcd for $C_9H_{13}NO_4I$ 325.9890, found 325.9894.

3-Iodo-5,6-dimethoxy-4-(methoxymethoxy)pyridin-2-ol (13)

A solution of *n*-BuLi (1.59 M in hexane, 2.38 ml, 1.51 mmol) in THF (15 ml) was treated with a solution of **13** (491 mg, 1.51 mmol) in THF (15 ml) at −78 °C. Trimethylborate (507 μl, 4.53 mmol) was added and the mixture was stirred for 5 min at –78 °C. In addition, *m*CPBA (60%, 1.74 g, 6.04 mmol) was added and the mixture was stirred for 30 min. Saturated aqueous $Na_2S_2O_3$ was added, and the resulting solution was partitioned between EtOAc and H_2O. The aqueous layer was extracted with EtOAc, and the organic layers were combined, dried over Na_2SO_4, filtered and concentrated *in vacuo*. The residue was purified by silica gel flash column chromatography (20 : 1 hexanes/EtOAc) to afford **13** (393 mg, 76%) as a white solid. mp 119–121 °C; IR (KBr) 3116, 2987, 2832, 2547, 1600, 1467, 1386, 1112, 894, 819, 767 cm^{-1}; ^{1}H-NMR (270 MHz, $CDCl_3$) δ 5.40 (s, 2H), 3.93 (s, 3H), 3.75 (s, 3H), 3.63 (s, 3H); ^{13}C-NMR (150 MHz, $CDCl_3$) δ 158.6, 157.6. 155.9, 129.6, 99.0, 61.9, 61.0, 58.5, 54.6; HRMS (FAB, *m*-NBA) $[M+H]^+$ calcd for $C_9H_{13}NO_5I$ 341.9838, found 341.9843.

3-Iodo-5,6-dimethoxy-2,4-bis(methoxymethoxy)pyridine (4b)

A solution of **13** (29.3 mg, 85.9 μmol) in DMF (1.0 ml) was treated with NaH (60%, 5.0 mg, 129 μmol) and MOMCl (8 μl, 103 μmol), and the mixture was stirred at room temperature for 1 h. The resulting solution was partitioned between EtOAc and H_2O. The aqueous layer was extracted with EtOAc, and the organic layers were combined, dried over Na_2SO_4, filtered and concentrated *in vacuo*. The residue was purified by silica gel flash column chromatography (15 : 1 hexanes/EtOAc) to afford **4b** (33.4 mg, quant.) as a yellow oil. mp 62–64 °C; IR (KBr) 2954, 2838, 2362, 1735, 1562, 1467, 1378, 1214, 1159, 1105, 995, 877 cm^{-1}; ^{1}H-NMR (270 MHz, $CDCl_3$) δ 5.52 (s, 2H), 5.38 (s, 2H), 3.95 (s, 3H), 3.76 (s, 3H), 3.63 (s, 3H) 3.55 (s, 3H); ^{13}C-NMR (150 MHz, $CDCl_3$) δ 158.5, 157.0, 155.2, 130.4, 99.0, 92.7, 65.0, 60.9, 58.4, 57.3, 54.1; HRMS (FAB, *m*-NBA) $[M+H]^+$ calcd for $C_{11}H_{18}NO_6I$ 386.0101, found 386.0107; Anal. calcd for $C_{11}H_{18}NO_6I$: C, 4.19; H, 34.30; O, 3.64, found: C, 4.10; H, 34.51; O, 3.67.

(*R*)-2-Methyl-3-(triisopropylsilyloxy)propyl 4-methylbenzenesulfonate (15)

A solution of **14** (870 mg, 3.45 mmol) in pyridine (6.9 ml) was treated with *p*-TsCl (990 mg, 5.18 mmol) and a catalytic amount of DMAP. The mixture was stirred at room temperature for 2 h. The resulting solution was partitioned between EtOAc and H_2O. The aqueous layer was extracted with EtOAc, and the organic layers were combined, dried over Na_2SO_4, filtered and concentrated *in vacuo*. The residue was purified by silica gel flash column chromatography (50 : 1 hexanes/EtOAc) to afford **15** (1.31 g, quant.) as a colorless oil. $[\alpha]_D^{27}$ −6.31 (*c* 1.0, $CHCl_3$); IR (KBr) 2952, 2867, 1600, 1463, 1367, 1182, 1105, 977, 786, 675, 561 cm^{-1}; ^{1}H-NMR (270 MHz, $CDCl_3$) δ 7.78 (d, 2H, *J*=8.3 Hz), 7.33 (d, 2H, *J*=8.3 Hz), 4.06 (dd, 1H, *J*=9.2, 6.0 Hz), 3.95 (dd, 1H, *J*=9.2, 6.0 Hz), 3.59 (dd, 1H, *J*=9.9, 5.8 Hz), 3.49 (dd, 1H, *J*=9.9, 5.8 Hz), 2.43 (s, 3H), 2.00−1.94 (m, 1H), 1.05−0.94 (m, 3H), 0.99 (bs, 18H), 0.90 (d, 3H, *J*=6.9 Hz); ^{13}C-NMR (150 MHz, $CDCl_3$) δ 144.5, 133.0, 129.7, 127.8, 72.2, 64.2, 35.9, 21.6, 17.9, 13.2, 11.8; LRMS (FAB, *m*-NBA) $[M+H]^+$ 401, $[M+Na]^+$ 423.

(*S*)-3-Methyl-4-(triisopropylsilyloxy)butanenitrile (16)

A solution of **15** (1.31 g, 3.25 mmol) in DMSO (3.3 ml) was treated with KCN (210 mg, 3.25 mmol). After stirring at 100 °C for 1.5 h, the resulting solution was partitioned between EtOAc and H_2O. The aqueous layer was extracted with EtOAc, and the organic layers were combined, dried over Na_2SO_4, filtered and concentrated *in vacuo*. The residue was purified by silica gel flash column chromatography (20 : 1 hexanes/EtOAc) to afford **16** (850 mg, quant.) as a colorless oil. $[\alpha]_D^{27}$ −18.0 (*c* 1.0, $CHCl_3$); IR (KBr) 2952, 2867, 2246, 1463, 1108, 883, 788, 680 cm^{-1}; ^{1}H-NMR (270 MHz, $CDCl_3$) δ 3.71 (dd, 1H, *J*=8.4, 4.3 Hz), 3.51 (dd, 1H, *J*=8.4, 4.3 Hz), 2.53 (dd, 1H, *J*=16.5, 6.5 Hz), 3.49 (dd, 1H, *J*=16.5, 6.5 Hz), 2.10−2.02 (m, 1H), 1.11−1.00 (m, 3H), 1.06 (bs, 18H), 0.98 (d, 3H, *J*=3.3 Hz); ^{13}C-NMR (150 MHz, $CDCl_3$) δ 118.9, 66.4, 33.5, 20.8, 17.9, 15.8, 11.8; HRMS (FAB, *m*-NBA) $[M+H]^+$ calcd for $C_{14}H_{30}NOSi$ 256.2100, found 256.2096.

(*S*)-3-Methyl-4-(triisopropylsilyloxy)butanal (17)

A solution of **16** (850 mg, 3.33 mmol) in CH_2Cl_2 (16 ml) was treated with DIBAL (1.02 M in hexane, 7.5 ml, 7.65 mmol) at −78 °C. After stirring for 1 h at −78 °C, 3 N aqueous HCl solution was added to the mixture. The aqueous layer was extracted with EtOAc, and the organic layers were combined, dried over Na_2SO_4, filtered and concentrated *in vacuo*. The residue was purified by silica gel flash column chromatography (20 : 1 hexanes/EtOAc) to afford **17** (630 mg, 73%) as a colorless oil. The physical properties of **17** were completely identical to those reported in the literature.[11]

(*S*,*E*)-Ethyl 5-methyl-6-(triisopropylsilyloxy)hex-2-enoate (18)

A solution of **17** (630 mg, 2.44 mmol) in benzene (24 ml) was treated with (carbethoxymethylene)triphenylphosphorane (1.70 g, 4.88 mmol). After stirring at 50 °C for 24 h, the resulting solution was partitioned between EtOAc and H_2O. The aqueous layer was extracted with EtOAc, and the organic layers were combined, dried over Na_2SO_4, filtered and concentrated *in vacuo*. The residue was purified by silica gel flash column chromatography (20 : 1 hexanes/EtOAc) to afford **18** (680 mg, 85%) as a colorless oil. $[\alpha]_D^{28}$ −1.80 (*c* 1.0, $CHCl_3$); IR (KBr) 2950, 2867, 2350, 2337, 1724, 1654, 1463, 1263, 1174, 1108, 1049, 883, 790, 678 cm^{-1}; ^{1}H-NMR (300 MHz, $CDCl_3$) δ 7.02−6.92 (m, 1H), 5.83 (d, 1H, *J*=15.6, 1.4 Hz), 4.18 (q, 2H, *J*=7.1 Hz), 3.56 (dd, 1H, *J*=9.7, 6.0 Hz), 3.48 (dd, 1H, *J*=9.7, 6.0 Hz), 2.47−2.37 (m, 1H), 2.07−1.97 (m, 1H), 1.85−1.78 (m, 1H), 1.28 (t, 3H, *J*=7.1 Hz), 1.09−1.02 (m, 3H), 1.06 (bs, 18H), 0.90 (d, 3H, *J*=6.8 Hz); ^{13}C-NMR (150 MHz, $CDCl_3$) δ 166.5, 148.0, 122.4, 67.8, 60.0, 36.0, 35.7, 18.0, 16.4, 14.2, 11.9; HRMS (FAB, *m*-NBA) $[M+H]^+$ calcd for $C_{18}H_{37}O_3Si$ 329.2512, found 329.2511.

(*S*,*E*)-5-Methyl-6-(triisopropylsilyloxy)hex-2-en-1-ol (19)

A solution of **18** (650 mg, 1.98 mmol) in CH_2Cl_2 (20 ml) was treated with DIBAL (1.02 M in hexane, 4.85 ml, 4.95 mmol) at −78 °C. After stirring for 1 h at 0 °C, MeOH was added dropwise at −78 °C to the resulting solution until the evolution of gas ceased. The mixture was diluted with CH_2Cl_2, treated with celite (1.50 g) and Na_2SO_4•$10H_2O$ (1.60 g) and then stirred for 12 h at room temperature. The resulting solution was filtered through a pad of celite, and the filtrate was concentrated *in vacuo*. The residue was purified by silica gel flash column chromatography (20 : 1 hexanes/EtOAc) to afford **19** (510 mg, 91%) as a colorless oil. $[\alpha]_D^{28}$ −4.27 (*c* 1.0, $CHCl_3$); IR (KBr) 3334, 2950, 2865, 1463, 1105, 1006, 883, 794, 678, 595 cm^{-1}; ^{1}H-NMR (270 MHz, $CDCl_3$) δ 5.75−5.60 (m, 2H), 4.09 (d, 2H, *J*=4.0 Hz), 3.50 (d, 2H, *J*=3.2 Hz), 2.27−2.20 (m, 1H), 1.91−1.81 (m, 1H), 1.75−1.65 (m, 1H), 1.12−1.02 (m, 3H), 1.06 (bs, 18H), 0.88 (d, 3H, *J*=6.6 Hz); ^{13}C-NMR (150 MHz, $CDCl_3$) δ 131.7, 130.3, 68.0, 63.7, 36.1, 35.9, 18.0, 16.4, 12.0; HRMS (FAB, *m*-NBA) $[M+H]^+$ calcd for $C_{16}H_{35}O_3Si$ 287.2403, found 287.2408.

{(2*R*,3*R*)-3-[(*S*)-2-Methyl-3-(triisopropylsilyloxy)propyl] oxiran-2-yl}methanol (20)

A mixture of Ti(O*i*Pr)$_4$ (3.2 ml, 10.8 mmol) and 4 Å MS (1.24 g) in CH_2Cl_2 (50 ml) was treated with (−)-DET (1.9 ml, 10.8 mmol), and the solution was vigorously stirred at −5 °C for 0.5 h. TBHP (5.0–6.0 M in decane, 4.4 ml, 21.6 mmol) was slowly added to the above mixture, and the solution was stirred at −20 °C for 20 min. A solution of **19** (3.10 g, 10.8 mmol) in CH_2Cl_2 (58 ml) was added to the above mixture, and the solution was stirred at −20 °C for 10.5 h. After Me_2S (1.19 ml, 16.2 mmol) was added, the mixture was further stirred at −20 °C for 1 h. The resulting mixture was diluted with Et_2O, treated with celite (6.50 g) and Na_2SO_4•$10H_2O$ (6.50 g), and then stirred for 2 h at room temperature. The resulting suspension was filtered through a pad of celite, and the filtrate was concentrated *in vacuo*. The residue was purified by silica gel flash column chromatography (5 : 1 hexanes/EtOAc) to afford **20** (3.27 g, quant.) as a colorless oil. $[\alpha]_D^{28}$ +16.1 (*c* 1.0, $CHCl_3$); IR (KBr) 3432, 2944, 2865, 1463, 1382, 1103, 887, 792, 678, 653 cm^{-1}; ^{1}H-NMR (270 MHz, $CDCl_3$) δ 3.56 (m, 4H), 3.09−3.02 (m, 1H), 2.90−2.88 (m, 1H), 1.85−1.75 (m, 3H), 1.11−1.02 (m, 3H), 1.06 (bs, 18H), 0.99 (d, 3H, *J*=6.6 Hz); ^{13}C-NMR (150 MHz, $CDCl_3$) δ 68.0, 61.7, 58.4, 55.1, 35.4, 34.5, 18.0, 17.0, 11.9; HRMS (ESI) $[M+Na]^+$ calcd for $C_{16}H_{34}O_3SiNa$ 325.2175, found 325.2212.

Triisopropyl{[(*S*)-2-methyl-3-(2*R*,3*R*)-3-(triphenylmethyloxymethyl) oxiran-2-yl]propoxy}silane (21)

A solution of **20** (496 mg, 1.46 mmol) in CH_2Cl_2 (16 ml) was treated with TrCl (914 mg, 3.28 mmol) and Et_3N (680 µl, 4.92 mmol), and the mixture was stirred at room temperature for 8.5 h. The resulting solution was partitioned between CH_2Cl_2 and H_2O. The aqueous layer was extracted with CH_2Cl_2, and the organic layers were combined, dried over Na_2SO_4, filtered and concentrated *in vacuo*. The residue was purified by silica gel flash column chromatography (150 : 1 hexanes/EtOAc) to afford **21** (869 mg, 97%) as a colorless oil. $[\alpha]_D^{28}$ +4.76 (*c* 1.0, $CHCl_3$); IR (KBr) 2942, 2865, 1596, 1490, 1448, 1091, 1070, 883, 702 cm^{-1}; ^{1}H-NMR (300 MHz, $CDCl_3$) δ 7.48−7.12(m, 15H), 3.57 (dd, 1H, *J*=9.6, 5.7 Hz), 3.51 (dd, 1H, *J*=9.6, 6.0 Hz), 3.26 (dd, 1H, *J*=10.6, 3.2 Hz), 3.12 (dd, 1H, *J*=10.6, 5.4 Hz) 2.92−2.84 (m, 2H), 1.88−1.78 (m, 1H), 1.77−1.69 (m, 1H), 1.41−1.31 (m, 1H), 1.10−0.95 (m, 3H), 1.03 (bs, 18H), 0.99 (d, 3H, *J*=6.7 Hz); ^{13}C-NMR (150 MHz, $CDCl_3$) δ 143.8, 128.6, 127.8, 127.0, 86.6, 68.0, 64.6, 57.1, 55.4, 35.6, 34.5, 18.0, 17.1, 11.9; HRMS (FAB, *m*-NBA) $[M+Na]^+$ calcd for $C_{35}H_{48}O_3SiNa$ 567.3271, found 567.3248.

(2*S*,3*S*,5*S*)-3,5-Dimethyl-6-(triisopropylsilyloxy)-1-(trityloxy) hexan-2-ol (22)

A mixture of CuI (1.57 g, 8.25 mmol) in CH_2Cl_2 (8.0 ml) was treated with MeLi (1.04 M in Et_2O, 15.8 ml, 16.5 mmol), and the solution was stirred at −78 °C for 5 min. BF_3•OEt_2 (314 µl, 2.48 mmol) was added to the above mixture, and the solution was stirred at −78 °C for 5 min. A solution of **21** (900 mg, 1.65 mmol) in CH_2Cl_2 (8.5 ml) was added to the above mixture, and the solution was stirred at −78 °C for 2 h. The reaction mixture was warmed to room temperature and treated with saturated aqueous NH_4Cl. The resulting solution was partitioned between EtOAc and H_2O. The aqueous layer was extracted with EtOAc, and the organic layers were combined, dried over Na_2SO_4, filtered and concentrated *in vacuo*. The residue was purified by silica gel flash column chromatography (50 : 1 hexanes/EtOAc) to afford **22** (720 mg, 97%) as a colorless oil. $[\alpha]_D^{26}$ –4.09 (*c* 1.0, $CHCl_3$); IR (KBr) 3478, 2950, 2865, 1712, 1596, 1455, 1378, 1097, 1074, 887, 773, 698 cm^{-1}; ^{1}H-NMR (270 MHz, $CDCl_3$) δ 7.47−7.20 (m, 15H), 3.58−3.53 (m, 1H), 3.43 (d, 2H, *J*=6.3 Hz), 3.26 (dd, 1H, *J*=9.4, 3.2 Hz), 3.08 (dd, 1H, *J*=9.4, 7.9 Hz), 2.38 (d, 1H, *J*=3.3 Hz), 1.72−1.56 (m, 2H), 1.26−1.13 (m, 2H), 1.07−1.01 (m, 3H), 1.04 (bs, 18H), 0.81 (d, 3H, *J*=6.6 Hz), 0.72 (d, 3H, *J*=6.8 Hz); ^{13}C-NMR (150 MHz, $CDCl_3$) δ 143.9, 128.6, 127.8, 127.0, 86.7, 75.2, 69.4, 65.6, 35.5, 33.4, 33.3, 18.0, 16.1, 15.0, 12.0; HRMS (FAB, *m*-NBA) $[M+Na]^+$ calcd for $C_{36}H_{52}O_3SiNa$ 583.3583, found 583.3607.

(2*S*,3*S*,5*S*)-3,5-Dimethyl-6-(triisopropylsilyloxy)hexan-1,2-diol (23)

To a mixture of Li (57.7 mg, 8.89 mmol) in liquid ammonia (9.0 ml, 0.1 M) was added a solution of **22** (498 mg, 0.890 mmol) in THF (5.0 ml) and *t*BuOH (0.21 ml, 2.22 mmol) at −78 °C, and the resulting solution was stirred at −78 °C for 30 min. MeOH was added at −78 °C until the color of the solution changed, and after complete volatilization of ammonia, the resulting solution was partitioned between EtOAc and H_2O. The aqueous layer was extracted with EtOAc, and the organic layers were combined, dried over Na_2SO_4, filtered and concentrated *in vacuo*. The residue was purified by silica gel flash column chromatography (5 : 1 hexanes/EtOAc) to afford **23** (241 mg, 85%) as a colorless oil. $[\alpha]_D^{27}$ –17.8 (*c* 1.0, $CHCl_3$); IR (KBr) 3419, 2948, 2867, 1625, 1461, 1382, 1105, 1068, 881, 790, 678 cm^{-1}; ^{1}H-NMR (300 MHz, $CDCl_3$) δ 3.75−3.68 (m, 1H), 3.54−3.44 (m, 4H), 1.76−1.65 (m, 2H), 1.42−1.23 (m, 2H), 1.13−1.02 (m, 3H), 1.07 (bs, 18H), 0.88 (d, 3H, *J*=6.6 Hz), 0.85 (d, 3H, *J*=6.6 Hz); ^{13}C-NMR (150 MHz, $CDCl_3$) δ 78.8, 71.9, 67.9, 36.3, 34.7, 32.4, 17.9, 17.3, 15.1, 12.1; HRMS (FAB, *m*-NBA) $[M+Na]^+$ calcd for $C_{17}H_{38}O_3SiNa$ 341.2488, found 341.2490.

(2*S*,4*S*,5*R*)-5,6-Dichloro-2,4-dimethylhexan-1-ol (24)

A solution of **23** (211 mg, 0.660 mmol) in THF (3.3 ml) was treated with NCS (266 mg, 1.99 mmol) and PPh_3 (552 mg, 1.99 mmol), and the mixture was stirred at 60 °C for 3 h. The resulting solution was partitioned between CH_2Cl_2 and H_2O. The aqueous layer was extracted with CH_2Cl_2. The organic layer was combined, dried over Na_2SO_4, filtered and concentrated *in vacuo*. The residue was semi-purified by flash silica gel column chromatography (5 : 1 hexanes/EtOAc) to afford the crude dichloride as a colorless oil. A solution of the crude dichloride in THF (6.6 ml) was treated with TBAF (1.0 M THF, 1.32 ml, 1.32 mmol), and the reaction mixture was stirred at room temperature for 1 h and quenched with saturated aqueous NH_4Cl. The resulting solution was partitioned between EtOAc and H_2O. The aqueous layer was extracted with EtOAc, and the organic layers were combined, dried over Na_2SO_4, filtered and concentrated *in vacuo*. The residue was purified by silica gel flash column chromatography (5 : 1 hexanes/EtOAc) to afford **24** (86.0 mg, 65% for 2 steps) as a colorless oil. $[\alpha]_D^{27}$ –11.3 (*c* 1.0, $CHCl_3$); IR (KBr) 3365, 2964, 2925, 1457, 1380, 1037, 738, 686 cm^{-1}; ^{1}H-NMR (270 MHz, $CDCl_3$) δ 4.12−4.06 (m, 1H), 3.81−3.66 (m, 2H), 3.56−3.41 (m, 2H), 2.32−2.25 (m, 1H), 1.78−1.69 (m, 1H), 1.55–1.45 (m, 2H), 0.94 (d, 3H, *J*=6.6 Hz), 0.93 (d, 3H, *J*=6.6 Hz); ^{13}C-NMR (150 MHz, $CDCl_3$) δ 73.1, 61.6, 46.0, 35.0, 33.8, 31.8, 18.0, 17.6, 15.4, 12.0; HRMS (FAB, *m*-NBA) $[M+H]^+$ calcd for $C_8H_{17}Cl_2O$ 199.0656, found 199.0647.

(2*S*,4*S*,5*R*)-5,6-Dichloro-2,4-dimethylhexanal (5)

A solution of **24** (54.0 mg, 0.270 mmol) in CH_2Cl_2 (2.7 ml) was treated with TEMPO (4.3 mg, 27.1 µmol) and PhI(OAc)$_2$ (131 mg, 0.410 mmol). The reaction mixture was then stirred at room temperature for 2.5 h and quenched with saturated aqueous $Na_2S_2O_3$. The resulting solution was partitioned between CH_2Cl_2 and H_2O. The aqueous layer was extracted with CH_2Cl_2, and the organic layers were combined, dried over Na_2SO_4, filtered and concentrated *in vacuo*. The residue was purified by silica gel flash column chromatography (20 : 1 hexanes/EtOAc) to afford **5** (43.0 mg, 81%) as a colorless oil. $[\alpha]_D^{27}$ +1.13 (*c* 1.0, $CHCl_3$); IR (KBr) 2971, 2715, 1725, 1457, 1382, 1257, 925, 815, 740, 688 cm^{-1}; ^{1}H-NMR (300 MHz, $CDCl_3$) δ 9.64 (d, 1H, *J*=8.6 Hz), 4.13−4.07 (m, 1H), 3.78 (dd, 1H, *J*=11.3, 5.7 Hz), 3.70 (dd, 1H,

J=11.3, 8.8 Hz), 2.48–2.39 (dq, 1H, *J*=7.0, 1.8 Hz), 2.33–2.25 (m, 1H), 1.89–1.79 (m, 1H), 1.48–1.38 (m, 1H), 1.14 (d, 3H, *J*=7.0 Hz), 0.95 (d, 3H, *J*=6.6 Hz); HRMS (FAB, *m*-NBA) $[M+Na]^+$ calcd for $C_8H_{14}Cl_2O$ 196.0422, found 199.0431.

(2*S*,4*S*,5*R*)-5,6-Dichloro-1-(5,6-dimethoxy-2,4-bis(methoxymethoxy) pyridin-3-yl)-2,4-dimethylhexan-1-ol (25)

To a solution of *n*-BuLi (1.59 M in hexane, 672 µl, 1.07 mmol) in THF (3.6 ml) was added a solution of **4b** (138 mg, 359 µmol) in THF (1.8 ml) at −78 °C. A solution of **5** (58.0 mg, 299 µmol) in THF (1.8 ml) was then added and the mixture was stirred for 15 min at −78 °C. MeOH was added, and the resulting solution was partitioned between EtOAc and H_2O. The aqueous layer was extracted with EtOAc, and the organic layers were combined, dried over Na_2SO_4, filtered and concentrated *in vacuo*. The residue was purified by silica gel flash column chromatography (3 : 1 hexanes/EtOAc) to afford a diastereomixture of **25** (101 mg, 83%) as a colorless oil. $[\alpha]_D^{20}$ −11.8 (*c* 1.0, $CHCl_3$); IR (KBr) 3561, 2962, 1590, 1469, 1392, 1160, 1116, 1060, 1025, 904 cm^{-1}; ^{1}H-NMR (300 MHz, $CDCl_3$) δ 5.60–5.47 (m, 2H), 5.38–5.27 (m, 2H), 4.16–4.05 (m, 1H), 3.93 (s, 3H), 3.83–3.65 (m, 2H), 3.75 (s, 3H), 3.74 (s, 3H), 3.58–3.50 (m, 1H), 3.57 (s, 3H), 3.56 (s, 3H), 3.52 (s, 6H), 2.37–2.25 (m, 1H), 2.21–2.10 (m, 1H), 2.08–2.00 (m, 1H), 1.64–1.51 (m, 1H), 1.07 (d, 3H, *J*=6.6 Hz), 0.96 (d, 3H, *J*=6.5 Hz), 0.82 (d, 3H, *J*=6.9 Hz), 0.73 (d, 3H, *J*=6.7 Hz); ^{13}C-NMR (150 MHz, $CDCl_3$) δ 157.3, 157.2, 155.2×2, 153.2, 153.1, 130.0×2, 110.0×2, 99.4×2, 92.1×2, 72.4, 71.9, 67.7, 66.9, 60.8×2, 58.1×2, 57.7×2, 53.9, 53.8, 46.5, 45.4, 38.7, 38.3, 36.7, 36.6, 33.2, 32.6, 16.6, 16.2, 13.0, 12.6; HRMS (FAB, *m*-NBA) $[M+Na]^+$ calcd for $C_{19}H_{31}Cl_2NO_7$ 478.1373, found 478.1378.

(2*S*,4*S*,5*R*)-5,6-Dichloro-1-(5,6-dimethoxy-2,4-bis(methoxymethoxy) pyridin-3-yl)-2,4-dimethylhexan-1-one (26)

A solution of **25** (93.3 mg, 205 µmol) in CH_2Cl_2 (2.0 ml) was treated with Dess–Martin periodinane (130 mg, 307 µmol). The mixture was then stirred at room temperature for 15 min and quenched with saturated aqueous $Na_2S_2O_3$ and saturated aqueous $NaHCO_3$. The resulting solution was partitioned between CH_2Cl_2 and H_2O. The aqueous layer was extracted with CH_2Cl_2, and the organic layers were combined, dried over Na_2SO_4, filtered and concentrated *in vacuo*. The residue was purified by silica gel flash column chromatography (10 : 1 hexanes/EtOAc) to afford **26** (79.5 mg, 86%) as a colorless oil. $[\alpha]_D^{27}$ −2.91 (*c* 1.0, $CHCl_3$); IR (KBr) 2971, 2715, 1725, 1457, 1382, 1257, 925, 815, 740, 688 cm^{-1}; ^{1}H-NMR (300 MHz, $CDCl_3$) δ 5.50 (s, 2H), 5.30 (s, 2H), 4.19 (ddd, 1H, *J*=7.6, 6.3, 2.9 Hz), 3.97 (s, 3H), 3.77 (s, 3H), 3.78–3.63 (m, 2H), 3.49 (s, 6H), 3.24–3.12 (m, 1H), 2.37–2.26 (m, 1H), 1.94–1.84 (m, 1H), 1.51–1.46 (m, 1H), 1.17 (d, 3H, *J*=7.0 Hz), 0.93 (d, 3H, *J*=6.6 Hz); ^{13}C-NMR (150 MHz, $CDCl_3$) δ 204.8, 157.3, 156.3, 152.9, 130.1, 110.7, 99.1, 92.0, 66.2, 60.9, 57.9, 57.6, 54.2, 46.5, 44.2, 37.3, 32.7, 16.8, 13.0; HRMS (FAB, *m*-NBA) $[M+Na]^+$ calcd for $C_{19}H_{29}Cl_2N$ Na O_7 476.1219, found 476.1210.

Atpenin A5 (3)

A solution of **26** (76.7 mg, 169 µmol) in CH_2Cl_2 (1.7 ml) was treated with TFA (1.7 ml) at 0 °C, and the mixture was stirred at 0 °C for 0.5 h. The reaction mixture was concentrated *in vacuo*. The residue was purified by silica gel flash column chromatography (5 : 1 hexanes/EtOAc) to afford atpenin A5 (**3**) (57.4 mg, 93%) as a white solid.

Synthetic atpenin A5 (3). mp 83–85 °C; $[\alpha]_D^{25}$ −0.82 (*c* 1.0, EtOH); IR (KBr) 1648, 1602, 1454, 1324, 1199, 1160, 993 cm^{-1}; ^{1}H-NMR (400 MHz, $CDCl_3$) δ 4.13 (s, 3H), 4.14–4.10 (m, 2H), 3.82 (s, 3H), 3.74 (dd, 1H, *J*=11.1, 6.1 Hz), 3.65 (dd, 1H, *J*=11.3, 8.5 Hz), 2.21 (dq, 1H, *J*=7.1, 2.4 Hz), 1.91 (ddd, 1H, *J*=14.2, 6.9, 6.9 Hz), 1.55–1.47 (m, 1H), 1.18 (d, 3H, *J*=6.7 Hz), 0.95 (d, 3H, *J*=6.6 Hz); ^{13}C-NMR (150 MHz, $CDCl_3$) δ 210.0, 172.8, 162.2, 155.6, 121.2, 101.1, 65.7, 61.8, 58.6, 46.1, 39.6, 37.7, 32.8, 18.3, 13.2; HRMS (FAB, *m*-NBA) $[M+H]^+$ calcd for $C_{15}H_{22}NO_5Cl_2$ 366.0875, found 366.0876; Anal. calcd for $C_{15}H_{22}NO_5Cl_2$: C, 5.78; H, 49.19; O, 3.82, found: C, 5.64; H, 49.37; O, 3.92; UVλ_{max}^{EtOH} nm (ε (cm^2 $mmol^{-1}$)) 239 (3160), 277 (2220), 333 (1450).

Revised data of natural atpenin A5 (3). ^{1}H-NMR (400 MHz, $CDCl_3$) δ 4.13 (s, H), 4.14–4.10 (m, 2H), 3.82 (s, 3H), 3.73 (dd, 1H, *J*=11.2, 5.9 Hz), 3.65 (dd, 1H, *J*=11.3, 8.9 Hz), 2.20 (dq, 1H, *J*=7.0, 2.7 Hz), 1.91 (ddd, 1H, *J*=14.3, 7.0, 7.0 Hz), 1.55–1.47 (m, 1H), 1.18 (d, 3H, *J*=6.7 Hz), 0.95 (d, 3H, *J*=6.5 Hz).

ACKNOWLEDGEMENTS

We thank Ms N Sato, Ms A Nakagawa and Dr K Nagai (Kitasato University) for kindly measuring NMR and MS spectra and Elemental analytical data. We also acknowledge Dr T Izuhara for helpful discussions. MO acknowledges a Kitasato University research grant for young researchers.

1 Ōmura, S. *et al.* Atpenins, new antifungal antibiotics produced by *Penicillium* sp. Production, isolation, physico-chemical and biological properties. *J. Antibiot.* **41,** 1769–1773 (1988).
2 Oshino, K., Kumagai, H., Tomoda, H. & Ōmura, S. Mechanism of action of atpenin B on Raji cells. *J. Antibiot.* **43,** 1064–1068 (1990).
3 Kumagai, H. *et al.* The structures of atpenins A4, A5 and B, new antifungal antibiotics produced by *Penicillium* sp. *J. Antibiot.* **43,** 1553–1558 (1990).
4 Trécourt, F., Mallet, M., Mongin, O. & Quéguiner, G. Total synthesis of (±)-Atpenin B. An original 'Clockwise' functionalization of 2-chloropyridine. *J. Org. Chem.* **59,** 6173–6178 (1994).
5 Miyadera, H. *et al.* Atpenins, potent and specific inhibitors of mitochondrial complex II (succinate-ubiquinone oxidoreductase). *Proc. Natl Acad. Sci. USA* **100,** 473–477 (2003).
6 Horsefield, R. *et al.* Structural and computational analysis of the quinone-binding site of complex II (succinate-ubiquinone oxidoreductase). *J. Biol. Chem.* **281,** 7309–7316 (2006).
7 Schnürch, M., Spina, M., Khan, A. F., Milhovilovic, M. D. & Stanetty, P. Halogen dance reactions—A review. *Chem. Soc. Rev.* **36,** 1046–1057 (2007) Recent review.
8 Katsuki, T. & Sharpless, K. B. The first practical method for asymmetric epoxidation. *J. Am. Chem. Soc.* **102,** 5974–5976 (1980).
9 Kay, A. J. *et al.* Simple zwitterionic merocyanines as potential NLO chromophores. *J. Mater. Chem.* **11,** 2271–2281 (2001).
10 Komatsu, K., Tanino, K. & Miyashita, M. Stereoselective total synthesis of the ionophore antibiotic zincophorin. *Angew. Chem. Int. Ed.* **43,** 4341–4345 (2004).
11 Ouellet, S. G., Tuttle, J. B. & MacMillan, D. W. C. Enantioselective organocatalytic hydride reduction. *J. Am. Chem. Soc.* **127,** 32–33 (2005).
12 Brondel, N., Renoux, B. & Gesson, J. P. New strategy for the synthesis of phosphatase inhibitors TMC-69-6H and analogs. *Tetrahedron Lett.* **47,** 9305–9308 (2006).
13 Schiavi, B. *et al.* Synthesis of 5-deazathiogirollines: analogs of a natural antitumor agent. *Tetrahedron* **58,** 4201–4215 (2002).

The Journal of Antibiotics (2009) 62, 295–302

www.nature.com/ja

ORIGINAL ARTICLE

Identification of a new antimicrobial lysine-rich cyclolipopeptide family from *Xenorhabdus nematophila*

Maxime Gualtieri[1,2,3], André Aumelas[4] and Jacques-Olivier Thaler[5]

Entomopathogenic bacteria of the genus *Xenorhabdus* are known to be symbiotically associated with soil dwelling nematodes of the *Steinernematidae* family. These bacteria are transported by their nematode hosts into the hemocoel of the insect larvae, where they proliferate and produce insecticidal proteins, inhibitors of the insect immune system and antimicrobial molecules. In this study, we describe the discovery of a new family (PAX) of five antimicrobial compounds produced by fermentation of the *Xenorhabdus nematophila* F1 strain and purified by cation exchange chromatography and reversed phase chromatography. The chemical structure of PAX 3, a lysine-rich cyclolipopetide, was obtained from the analysis of homo and heteronuclear 2D NMR and confirmed by MS-MS experiments. The five members of the PAX family showed significant activity against plants and human fungal pathogens and moderate activity against few bacteria and yeast. No cytotoxicity was observed on CHO or insect cells.
The Journal of Antibiotics (2009) **62,** 295–302; doi:10.1038/ja.2009.31; published online 17 April 2009

Keywords: antimicrobial; cyclolipopetide; *Xenorhabdus*

INTRODUCTION

Gram-negative bacterial strains of the genus *Xenorhabdus* are known to be symbiotically associated with soil dwelling nematodes of the *Steinernematidae* family.[1–3] After entering the insect larvae through natural openings, nematodes release bacteria from their intestine to the host's hemocoel.[4] Bacteria are involved in killing the insect host by producing insecticidal proteins[5] and inhibitors of the insect immune system.[6–8] The bacteria proliferate in the killed host and favor the reproduction of the nematode by degrading the insect biomass[9] and by producing antibiotics that inhibits the development of the other microorganisms present in the insects corpse (bacteria, fungi).[10] Boemare *et al.*[11] classified the antibiotic activities of *Xenorhabdus* into two categories: (i) antimicrobial molecules with broad spectrum and (ii) bacteriocins with very narrow spectrum and active only against bacteria closely related to *X. nematophila*. Only a few families of antimicrobial compounds have been described from *Xenorhabdus* in the literature: xenocoumacins,[12] xenorhabdins,[13] indole derivatives,[14,15] puromycin,[16] benzylidenacetone,[17] proteinaceous bacteriocins,[11,18] and xenortide and xenematide.[19] All *Xenorhabdus* strains spontaneously produce two distinct physiological states *in vitro*,[20] phase I and II variants.[21] Phase I variants produce several antibiotics and secrete a variety of proteins, whereas these properties are apparently absent or greatly reduced in phase II variants.

In our screening program, we found new cyclolipopeptidic antimicrobial compounds in the culture supernatant of the *X. nematophila* F1/1. These compounds possess significant activity against fungi and moderate activity against few Gram-negative and Gram-positive bacteria.

Nonribosomaly antimicrobial lipopetides are produced in bacteria and fungi during cultivation.[22–24] They are composed of a cationic or an anionic peptide covalently bound to a specifically modified aliphatic chain. Most of the peptidic moieties have complex cyclic structures. Some of these molecules are highly active against bacteria including multiresistant strains.[25–28] Others display solely antifungal activity[22,29] and a few both antifungal and antimicrobial activities.[22] Members of this family were approved for clinical use by the Food and Drug Administration: daptomycine, polymixine, echinochandine.[30,31]

This article describes the fermentation of the *X. nematophila* F1/1 strain, the isolation and biological activities of these active compounds named PAX (for peptide antimicrobial from *Xenorhabdus)*, and the chemical structure elucidation of PAX 3. This is the first example of lysine-rich cyclolipopetide characterized from the genus *Xenorhabdus*.

RESULTS AND DISCUSSION

Fermentation

Xenorhabdus nematophila F1/1 was cultivated for 48 h, at 28 °C with shaking in a 5 l Erlenmeyer flask containing 1 l of LB broth. The

[1]Selectbiotics, Nîmes, France; [2]Université Montpellier 1, Centre d'études d'agents Pathogènes et Biotechnologies pour la Santé, CNRS, UMR 5236, CPBS, 4 Bd Henri IV, CS 69033, Montpellier, France; [3]Université Montpellier 2, Centre d'études d'agents Pathogènes et Biotechnologies pour la Santé, Montpellier, France; [4]CNRS UMR5048, INSERM, U554, Centre de Biochimie Structurale, Université Montpellier 1 et 2, 29 rue de Navacelles, Montpellier, Cedex 9, France and [5]Ecologie Microbienne des Insectes et Interactions Hôtes-Pathogène, UMR 1133, INRA UMII, Montpellier, France
Correspondence: Dr M Gualtieri, Centre d'études d'agents Pathogènes et Biotechnologies pour la Santé, CNRS, UMR 5236, Faculté de pharmacie, Avenue Charles Flahault, Montpellier 34093, France.
E-mail: maxime.gualtieri@univ-montp1.fr
Received 6 November 2008; accepted 18 March 2009; published online 17 April 2009

culture was inoculated with 0.1% (v/v) of a 24 h preculture in the same medium. The antibiotic production was controlled and quantified by diffusion test agar against *Micrococcus luteus*, and by analytical HPLC.

Isolation

Bacterial cells were removed by low-speed centrifugation (6000 *g*, 10 min at 4 °C) and supernatant was sterilized on 0.22 µm pore size filter. Supernatant was added (1:1; v/v) to a 0.1 M NaCl, 0.02 M Tris buffer (pH 9) and subjected to cation-exchange chromatography on a Sep Pack CarboxyMethyl cartridge (Acell Plus CM, Waters, Milford, MA, USA). Unbound material was removed by washes with a 0.1 M NaCl, 0.02 M Tris buffer (pH 9) and the antibiotic eluted with 0.5 M NaCl, 0.02 M Tris buffer (pH 9). This eluate was acidified with 0.1% (v/v) trifluoroacetic acid (TFA) and was then subjected to reversed-phase chromatography on a Sep Pack C18 cartridge (Sep-Pak Plus C18, Waters). Unbound material was removed by washing with H_2O-TFA 0.1%, and the antibiotic pool was eluted with acetonitrile. The eluate was concentrated by evaporation under reduced pressure and diluted in water (1:5; v/v). Pure compounds were isolated from the crude extract by reverse-phase HPLC using a semi-preparative C18 column (Waters; Symmetry Prep C18; 7 µm; 7.8×300 mm), a linear gradient of H_2O, 0.1% TFA-acetonitrile, 0.1% TFA starting from 20 to 80% in 30 min, a flow rate of 5 ml min^{-1} and an UV detection at 214 nm, yielding pure PAX compounds with the following HPLC-retention times: PAX 1=19.9 min, PAX 2=20.94 min, PAX 3=21.1 min, PAX 4=21.3 min and PAX 5=22.3 min with roughly the 30/10/50/9/1 percentages. The collected fractions were freeze-dried.

Biological properties

The PAX compounds show antifungal and antibacterial activities. They were tested for antimicrobial activity against a wide range of bacteria and fungi involved in nosocomial infection and phytopathologies (Tables 1 and 2). Regarding human pathogens (Table 1), PAX 1 and 2 did not show antibacterial activity except against *Staphylococcus epidermidis and M. luteus.* PAX 3 and 4 have weak activity against only few Gram-negative bacteria (*Pseudomonas aeruginosa*, *Escherichia coli* and *Salmonella typhimurium*), moderate activity against *S. epidermidis* and *B. cereus* and high activity against *M. luteus.* PAX 5 has moderate activity against few Gram-negative (*E. coli, P. aeruginosa and S. typhimurium*) including multiresistant strains and against few Gram-positive bacteria. However, high activity against the fungus *Fusarium oxysporum* was observed for PAX 1–5, whereas weak activity was observed against *Candida albicans*. The fungi belonging to the genus *Fusarium* are well-known plant pathogens and food contaminants that also cause superficial and subcutaneous infections in humans, such as onychomycosis and keratomycosis.[32] They have recently emerged as major opportunistic agents in immunocompromised hosts, especially in patients with hemopathy.[33,34] They are now considered as the third most common fungal genus (after *Candida* and *Aspergillus*) isolated from systemic infections in bone marrow transplantation patients.[35] *F. oxysporum* is responsible for about 30% of the human infection caused by this genus.[36] Regarding phytopathogenic fungi (Table 2), only PAX 1–3 were tested. At 10, 20 and 40 µg ml^{-1}, PAX 1 and 3 have strong activity against majority of fungi except *Botrytis cinerea myc* and *Piricularia oryzae sp.* PAX 2 has similar activity as PAX 1 and 3 against *Cladosporium sp.*, *F. culmorum sp.* and *Phytophthora*. Nevertheless, at 10 and 20 µg ml^{-1}, this molecule was less active against other fungi.

No cytotoxic activity with doses up to 1 mg ml^{-1} against CHO cells was measured. Injections of the five PAX into the hemocoels of different species of insects did not result in increased mortality. Moreover, these molecules did not exhibit cytolytic activities against sheep erythrocytes or insect hemocytes. These results show that the PAX had no entomotoxic effects (data not shown).

Chemical structure elucidation of PAXs

Five compounds referred as PAX 1–5 were isolated, purified to homogeneity as a white powder and characterized by mass spectrometry. ESI-MS experiments revealed the molecular weights of different PAXs (PAX 1: 1051 Da, PAX 2: 1079 Da, PAX 3: 1065 Da, PAX 4: 1093 Da). PAXs are soluble in water and alcohols and show an UV λmax of 214 nm (methanol).

Structure elucidation of PAX 3

The acid hydrolysate of PAX 3 yielded seven amino acids, one glycine (Gly) and six lysine (Lys). Its NMR analysis carried out by homo and hetero nuclear experiments is described below.

The NMR data of PAX 3 (1065 Da) were recorded in DMSO-*d6* (Table 3). Its 1D spectrum showed eight amide signals spanning the 8.5–7.3 p.p.m. chemical shift area. Among them, one is a triplet (8.18 p.p.m., 5.7 and 5.7 Hz) thus suggesting the presence of a glycine and another displays an unusual doublet of doublet (7.36 p.p.m., 6.5 and 4.0 Hz) indicating that this amide group is bound with a methylene group. The six other amide signals are doublets with a $^3J_{HN\text{-}CH}$ coupling constant ranging from 5.2 to 7.1 Hz. The natural abundance ^1H-^{15}N HSQC confirmed the presence of these eight amide protons and the absence of a C-terminal amide group (data not shown). In agreement with the acid hydrolysis, the TOCSY experiment allowed us to unambiguously identify a glycine and six lysine residues (Figure 1a). These later being also characterized from the intense signal at 2.74 p.p.m. typical of the CεH_2 protons. Surprisingly, the two-amide signals at 8.38 (doublet) and at 7.36 p.p.m. (doublet of doublet) were found to share the same spin system indicating that the ζ amino group of this lysine was involved in an amide bond to be identified. From the analysis of the DQF-COSY, TOCSY and NOESY data the assignment of the peptidic part was established on the basis of the classical sequential NOEs and is reported in Figure 1. The peptidic sequence was shown to consist of seven residues as following: $G^1K^2K^3K^4K^5K^6K^7$. Unexpectedly, this lysine-rich peptide includes an unusual 5-lysine macrocycle closed by an amide bond between the K^7 carboxyl group and the ζK^3 amino group. Such a cyclization which gives rise to a 5-residue macrolactame ring was mainly supported by the strong intensity dNN NOE between the K^7 and the ζK^3 amide protons and by the successive dNN NOEs observed all around the cycle. Owing to the overlap of the K^6 and K^7 amide signals, the dNN_{6-7} NOE could not be observed in pure DMSO-*d6*. The addition of 17% water was enough to separate these two resonances and observe this essential NOE to confirm the cyclic structure giving rise to a 5-residue macrolactame ring. As a result, this cyclization constrains the K^3 side chain. This is in agreement with the strong inequivalency observed for the CεH_2 resonances of K^3 at 3.45 and 2.77 p.p.m. (Figure 1a).

Clearly, several remaining resonances in the ^1H spectrum do not belong to the peptidic part. In particular, the doublet at 0.84 p.p.m. and the multiplet at 1.49 p.p.m. belong to an isopropyl group. By using both homonuclear and heteronuclear data, starting from the sole methyl signal of the spectrum, the $(CH_3)_2$-CH-$(CH_2)_3$- spin system was unambiguously characterized (Figure 2). This is also the case for the proton resonance at 3.81 p.p.m. that belongs to a CH group whose ^{13}C signal is at 67.58 p.p.m.. These chemical shifts are typical for an alcohol or ether function indicating the presence of an

Table 1 Chemical structure characteristics of PAX and minimal inhibitory concentration (MIC)[a] against bacteria and fungi including human pathogens

	PAX 1	*PAX 2*	*PAX 3*	*PAX 4*	*PAX 5*	*Vancomycin*	*Polymixin B*
Molecular weight (Da)	1051	1079	1065	1093	1079		
Chemical structure characteristics							
Peptidic part: position 2 residue	K	R	K	R	ND		
3-hydroxy fatty acid part: isomerization and length	iso-14:0	iso-14:0	iso-15:0	iso-15:0			
Activity against Gram-negative bacteria							
P. aeruginosa CIP 76.*110*	>100[a]	>100	100	50	25	>100	1.56
P. aeruginosa H41308 (L, Q)	>100	>100	100	100	50	>100	0.78
E. coli CIP 76.24	100	>100	100	50	12.5	>100	0.78
E. coli H35393 (L,C,Q)[b]	>100	100	50	100	25	>100	1.56
S. typhimurium H23212	100	100	100	100	50	>100	1.56
S. maltophilia H38058	>100	>100	>100	>100	>100	50	1.56
Klebsiella pneumoniae H35150	>100	>100	>100	>100	>100	>100	1.56
E. aerogenes H35956	>100	>100	>100	>100	>100	>100	1.56
M. morganii H45543	>100	>100	>100	>100	>100	>100	>100
P. vulgaris CIP 58.60	>100	>100	>100	>100	>100	>100	>100
Activity against Gram-positive bacteria							
S. aureus CIP 76.25	>100	100	50	50	50	1.56	>100
S. epidermidis CIP 68.21	100	50	25	12.5	12.5	1.56	100
E. faecalis H37812	>100	>100	>100	>100	>100	1.56	>100
B. cereus ATCC 14579			25	25		1.56	>100
S. pneumoniae CIP 103.566	>100	>100	>100	>100	>100	1.56	>100
M. luteus CIP 53.45	3.125	3.125	3.125	3.125	1.56	0.78	6.25
Activity against fungi and yeast							
F. oxysporum H3012	1.56	1.56	1.56	3.12	0.78		
C. albicans CIP 48.72	50	50	50	50	50		

Abbreviation: ND, not determined.
[a]In $\mu g\,ml^{-1}$.
[b]Resistance to L: β lactam, Q: quinolone, C: Cycline.

Table 2 Antifungal activity of PAX (percent inhibition of fungal growth)

	PAX 1			*PAX 2*			*PAX 3*		
	10 $\mu g\,ml^{-1}$	*20 $\mu g\,ml^{-1}$*	*40 $\mu g\,ml^{-1}$*	*10 $\mu g\,ml^{-1}$*	*20 $\mu g\,ml^{-1}$*	*40 $\mu g\,ml^{-1}$*	*10 $\mu g\,ml^{-1}$*	*20 $\mu g\,ml^{-1}$*	*40 $\mu g\,ml^{-1}$*
Alternaria brassicae	82	84	83	25	47	83	82	82	83
Botrytis cinerea	38	95	95	12	53	83	52	95	94
Botrytis cinerea myc	21	34	60	0	6	34	40	70	93
Cladosporium sp	94	94	94	74	95	95	94	94	94
Cladosporium myc	89	90	89	0	40	91	70	92	91
F. culmorum	96	96	96	66	97	97	96	96	96
Helminthosporium teres	70	91	95	33	47	80	76	94	92
Rhizoctonia solani myc	9.7	85	93	6	7	64	56	91	93
Phytophthora myc	79	78	77	71	81	78	76	78	77
P. oryzae	18	22	45	12	15	21	30	35	45
S. tritici	88	88	85	0	86	89	87	88	86

-CH(OH)- or -CH(OR)- group. In addition, from this alcohol or ether group the CO-CH_2-CH(O)-$(CH_2)_3$- spin system was clearly characterized (Figure 2). Interestingly, these two well-identified spin systems share an identical intense cross-peak at (^{1}H) 1.24/(^{13}C) 28.86 p.p.m. corresponding to several -CH_2- groups, suggesting that the two spin systems could be linked together by an aliphatic chain. Thus, the acyl fragment would be a 3-hydroxy fatty acid. Owing to the overlap of several methylene groups the acyl chain length was deduced

Table 3 NMR data of PAX 3 (dimethyl sulfoxide, 32 °C) and of PAX 4 (dimethyl sulfoxide, 27 °C)

	Pax 3		*Pax 4*	
Residue	*^{13}C (p.p.m.)*	*^{1}H (p.p.m.)*	*Residue*	*^{1}H (p.p.m.)*
iso-15:0 (3-hydroxy) fatty acid			*iso-15:0 (3-hydroxy) fatty acid*	
$(CH_3)2$	22.29	0.845	$(CH_3)2$	0.841
$C_{13}H$	27.15	1.489	$C_{13}H$	1.500
$C_{12}H2$	38.21	1.140	$C_{12}H2$	1.135
$C_{11}H2$	26.55	1.124	$C_{11}H2$	1.240
$C_{6-10}H2$	28.86	1.249	$C_{6-10}H2$	1.250
C_5H2	24.78	1.243	C_5H2	1.238
C_4H2	36.78	1.356	C_4H2	1.354
$C_3H(OH)$	67.58	3.807	$C_3H(OH)$	3.803
C_2H2	43.25	2.233	C_2H2	2.228
C_1O	171.45			
Gly[1]			*Gly[1]*	
HN		8.178	HN	8.190
H_α	41.92	3.738	H_α	3.755
$H_{\alpha'}$		3.700	$H_{\alpha'}$	3.688
Lys[2]			*Arg[2]*	
HN		8.015	HN	8.063
H_α	52.68	4.180	H_α	4.199
$C_\beta H2$	30.41	1.615/1.557	$C_\beta H2$	1.662/1.563
$C_\gamma H2$	21.96	1.320	$C_\gamma H2$	1.499/1.420
$C_\delta H2$	26.35	1.518	$C_\delta H2$	3.097
$C_\varepsilon H2$	38.38	2.740	HN_ε	7.768
Lys[3]			*Lys[3]*	
HN		8.377	HN	8.423
H_α	53.53	4.093	H_α	4.104
$C_\beta H2$	30.77	1.653	$C_\beta H2$	1.646
$C_\gamma H2$	22.18	1.430	$C_\gamma H2$	1.325/1.233
$C_\delta H2$	28.68	1.455/1.324	$C_\delta H2$	1.420
$C_\varepsilon H2$	37.95	3.448/2.774	$C_\varepsilon H2$	3.458/2.756
HN_ε		7.358	$H_\varepsilon N$	7.353
Lys[4]			*Lys[4]*	
HN		7.589	HN	7.600
H_α	52.76	4.097	H_α	4.087
$C_\beta H2$	29.68	1.656/1.628	$C_\beta H2$	1.645
$C_\gamma H2$	21.67	1.213	$C_\gamma H2$	1.293/1.212
$C_\delta H2$	26.25	1.518	$C_\delta H2$	1.517
$C_\varepsilon H2$	38.38	2.740	$C_\varepsilon H2$	2.750
Lys[5]			*Lys[5]*	
HN		8.165	HN	8.174
H_α	52.86	4.073	H_α	4.064
$C_\beta H2$	30.52	1.750	$C_\beta H2$	1.745/1.590
$C_\gamma H2$	21.69	1.320	$C_\gamma H2$	1.321
$C_\delta H2$	26.25		$C_\delta H2$	1.543
$C_\varepsilon H2$	38.38	2.740	$C_\varepsilon H2$	2.740
Lys[6]			*Lys[6]*	
HN		7.922	HN	7.926
H_α	52.15	4.077	H_α	4.064
$C_\beta H2$	29.35	1.765/1.512	$C_\beta H2$	1.700
$C_\gamma H2$	22.02	1.318/1.264	$C_\gamma H2$	1.324
$C_\delta H2$	26.23	1.518	$C_\delta H2$	1.525
$C_\varepsilon H2$	38.38	2.740	$C_\varepsilon H2$	2.760
Lys[7]			*Lys[7]*	
HN		7.904	HN	7.926
H_α	53.23	4.077	H_α	4.064
$C_\beta H2$	30.04	1.717/1.640	$C_\beta H2$	1.700
$C_\gamma H2$	22.12	1.378	$C_\gamma H2$	1.324
$C_\delta H2$	26.23	1.518	$C_\delta H2$	1.525
$C_\varepsilon H2$	38.38	2.740	$C_\varepsilon H2$	2.762

from the molecular weight as being an iso-15:0 3-hydroxy fatty acid. Moreover, the 'sequential' NOE between the C_2H_2 (2.23 p.p.m.) of the 3-hydroxy fatty acid and the amide proton of G^1 unambiguously characterized the amide bond link between the fatty acid and the peptidic fragments. Finally, the PAX 3 structure was fully corroborated by MS-MS fragmentation (Figure 3).

Altogether, these data suggest the presence of the iso-15:0 3-hydroxy fatty acid linked to the cyclopeptidic part at the G^1 residue to yield a lysine-rich cyclolipopeptide with a 5-residue macrolactame ring (Figure 4). The configurations of the α-carbons of the amino acids as well as that of the C_3 of the iso-15:0 3 hydroxy acid were not determined.

The PAX 1, PAX 2 and PAX 4, ^{1}H NMR spectra in DMSO (dimethyl sulfoxide) were very similar to that of PAX 3. The two main changes were easily observed and characterized by the combination of ^{1}H NMR and ESI/MS data. The first one with regard to the peptidic part with the K^2R mutation, whereas the second one with regard to the length of the fatty acid. The PAX 2 (1079 Da) and PAX 4 (1093 Da) chemical structures consist of the K^2R mutation (Tables 1 and 3) with the iso-14:0 and the iso-15:0 3-hydroxy acid, respectively. In contrast, PAX 1 (1051 Da) displays a K2 residue and the iso-14:0 3-hydroxy acid.

Although the ^{1}H NMR spectrum of PAX 5 could not be obtained, its molecular weight identical to PAX 2 (1079 Da) suggested that it could be its normal isomer. However, when compared with PAX 3, the +14 Da delta mass could be explained either by one methylene group extension of the 3-hydroxy fatty acid to yield a 16:0 homolog or by a simultaneous presence of a K2R mutation (+28 Da) and a 14:0 3-hydroxy fatty acid (−14 Da). To choose between these two hypothesis, more material should be isolated to record the PAX 5 NMR spectrum.

Notice that in cyclolipopeptides there are two types of cyclizations involving the carboxylic group, one involving an amide bond and another an ester bond leading to a macrolactame or a macrolactone ring, respectively.[37]

Conclusion

This report describes the production, the purification and the characterization of a new antimicrobial family from *X. nematophila*. Their significant antifungal activity and their lack of cytotoxicity and entomotoxicity increase the potential interest of these molecules for vegetal or human health application.

METHODS

Producing organism

Xenorhabdus nematophila F1 (Ecologie Microbienne des Insectes et Interactions Hôtes-Pathogène collection) was grown on Luria-Bertani medium (LB,

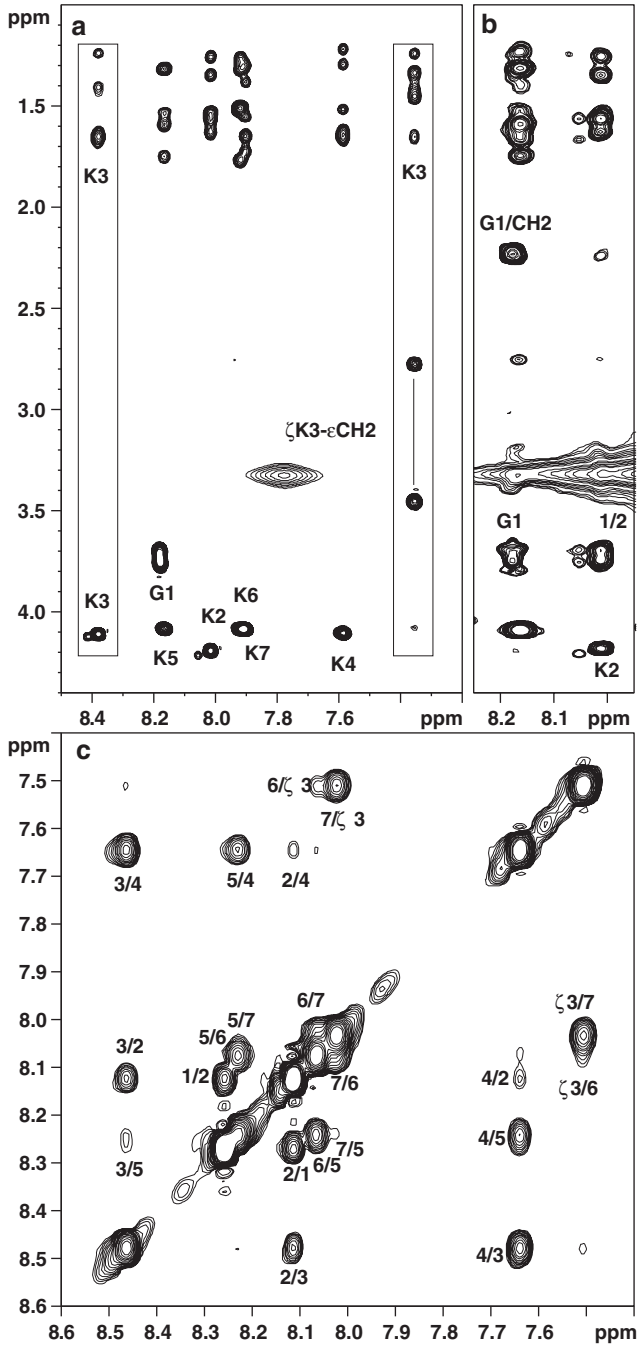

Figure 1 ^{1}H NMR data illustrating the assignment of the peptidic moiety. (**a**) Part of the TOCSY showing the different spin systems (DMSO, 305 K). ζK^{3} is for the zeta amide proton of K^{3}. The side chain spin system of K^{3} observed both from the amide and the ζK^{3} amide proton is boxed. Due to the length of the side chain the εCH$_2$ cross-peaks are of weak intensity from the amide chemical shift and not observed in this plot level. (**b**) Part of the NOESY showing the 'sequential' NOE between the αCH$_2$ of the fatty acid and the amide proton of G^{1} labeled G^{1}/CH$_2$ (DMSO-*d6*, 305 K, 250 ms of mixing time). (**c**) Part of the NOESY showing the dNN NOEs (DMSO-*d6* with 17% of water, 285 K, 250 ms of mixing time). The strong intensity NOE between HN K^{7} and ζHN K^{3} amide protons (7/ζ3) characterizes the cyclization. Notice that the dNN6–7 was not observed in pure DMSO due to the overlap of the K^{6} and K^{7} amide signals (part **a**).

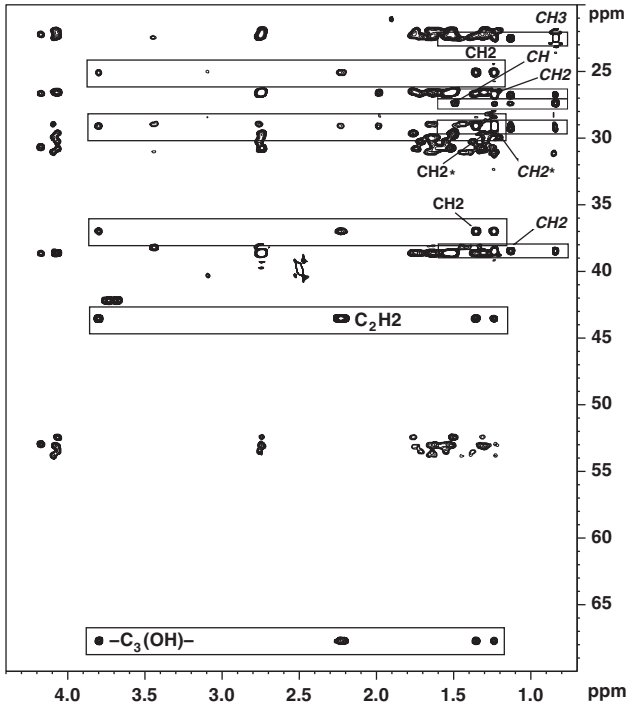

Figure 2 Part of the ^{1}H-^{13}C HSQC-TOCSY showing the spin system of the iso-15:0 3-hydroxy fatty acid. The two partial spin systems identified from the carboxyl (large rectangles) and from the methyl (small rectangles with labels in italics) groups are boxed. They share the same CH$_2$ cross-peak (twofold labeled CH$_2$*) corresponding to the overlap of several equivalent methylene groups at 1.24/28.86 p.p.m. located between the two extremities of the fatty acid. The length of the acyl chain was deduced from the molecular weight obtained by mass spectrometry.

composed of bactotryptone 10 g l^{-1}, yeast extract 5 g l^{-1} and NaCl 10 g l^{-1}) for liquid culture and on LB-agar for solid cultures. The phase status (I or II) of this strain was determined by culturing on NBTA (Nutrient agar (Difco, Detroit, MI, USA) 31 g l^{-1}, bromothymol blue 25 mg l^{-1} and 2, 3, 5-triphenyl tetrazolium chloride 1% 40 mg l^{-1}) and measuring antibacterial activity against *M. luteus*. *Xenorhabdus* exhibits two colony forms or variants when cultured *in vitro*. Modifications of the outer membrane induce differential adsorption of dyes by variants. Phase I variants absorb dyes and are blue on NBTA plates, whereas phase II colonies are red. Phases I and II of strains are indicated as suffixes (/1 and /2, respectively) attached to strain designations. This strain was maintained at 15 °C on NBTA medium.

Bacterial strains and antimicrobial agents

The following reference strains were used for the evaluation of antimicrobial activity: *P. aeruginosa* CIP 76.110, *E. coli* CIP 76.24, *Proteus vulgaris* CIP 58.60, *S. aureus* CIP 76.25, *S. epidermidis* CIP 68.21, *Bacillus cereus* ATCC 14579, *Streptococcus pneumoniae* CIP 103.566, *M. luteus* CIP 53.45 and *C. albicans* CIP 48.72 and clinical isolates (strains are indicated as suffixes H and a number) obtained from patients with infection at the University Hospital of Nîmes. Phytopathogenic fungi were obtained from Rhobio (Lyon, France). Vancomycin and polymyxin (Sigma-Aldrich, St Louis, MO, USA) were provided as standard powders by the manufacturers.

Antibacterial susceptibility testing methods

The minimal inhibitory concentration (MIC) was defined as the lowest antibiotic concentration, which yielded no visible growth. MIC was determined as recommended by the Clinical and Laboratory Standards Institute.[38] Antibiotics were tested at final concentrations (prepared from serial twofold dilutions) ranging from 100 to 0.78 mg l^{-1}. The test medium was Mueller–Hinton broth, and the inoculum was 5×10^{5} CFU ml^{-1}. The inoculated microplates were incubated at 37 °C under shaking for 18 h before reading.

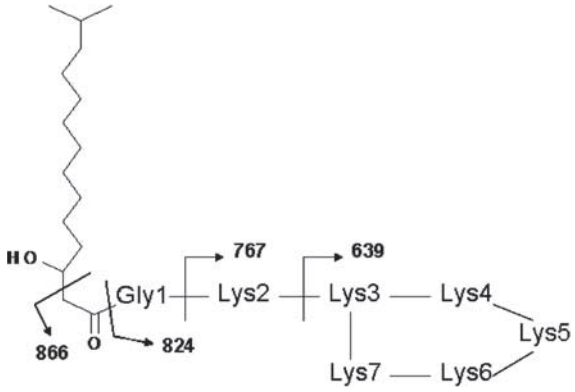

Fragment ion	
129	$[Lys^7 + H]^+$
185	$[Gly^1Lys^2 + H]^+$
257	$[Lys^7Lys^6 + H]^+$
385	$[Lys^7Lys^6Lys^5 + H]^+$
513	$[Lys^7Lys^6Lys^5Lys^4 + H]^+$
554	$[M+H]^+ - Lys^7Lys^6Lys^5Lys^4$
639	figure
641	$[Lys^7Lys^6Lys^5Lys^4Lys^3 + H]^+$
682	$[M+H]^+ - Lys^7Lys^6Lys^5$
767	figure
769	$[Lys^7Lys^6Lys^5Lys^4Lys^3Lys^2 + H]^+$
810	$[M+H]^+ - Lys^7Lys^6$
824	figure
826	$[Lys^7Lys^6Lys^5Lys^4Lys^3Lys^2Gly^1 + H]^+$
866	figure
938	$[M+H]^+ - Lys^7$
1048	$[M+H]^+ - H_2O$

Figure 3 Key fragmentations of the 1066 $[M+H]^+$ ions of PAX 3.

Antifungal susceptibility testing methods

The PAX activities were tested against the human pathogen *F. oxysporum* and against different phytopathogenic fungi by the M38-A microdilution method[39] with RPMI 1640 medium as recommended in the Clinical and Laboratory Standards Institute M23-A document.[40] The NCCLS M27-A2 broth microdilution method was used when *C. albicans* was tested.[41]

Fungal inoculi were prepared from 7-day cultures grown on potato dextrose agar and adjusted spectrophotometrically to optical densities that ranged from 0.09 to 0.17 and diluted (1:50) in RPMI 1640 broth. The density of the inoculum suspension of *C. albicans* isolate was adjusted to a density of a 0.5 McFarland standard and diluted 1:1000 in RPMI 1640 broth.[41] Microdilution trays (96 U-bottom shaped) containing 100 µl antifungal dilutions were added with 100 µl PAX solutions (final concentration ranging from 100 to 0.78 mg l^{-1} for *F. oxysporum* and *C. albicans*; 10, 20 and 40 µg ml^{-1} for other fungi). After inoculation of the trays, all microdilution trays were incubated at 30 °C in ambient air. As described in the M38-A method,[39] MICs for *F. oxysporum* were determined by visual examination at 48 h. MICs were defined as the lowest drug concentration that showed absence of growth or complete growth inhibition (100%). MICs for *C. albicans* were determined at 48 h and corresponded to 100% of growth inhibition.[41] Regarding phytopathogenic fungi, the culture absorbance was measured at 600 nm, 5 days after the beginning of the experiments. The activity results correspond to a percentage of growth inhibition $((1-Abs_{600\,nm}$ culture with PAX)/$Abs_{600\,nm}$ culture without PAX).

Cytotoxicity test

Chinese Hamster Ovary (CHO) cells were grown in RPMI medium supplemented with 5% (v/v) fetal calf serum. The cells were incubated for 24 h at 37 °C in the absence of serum and in the presence of PAX (final concentration ranging from 1000 to 7.8 mg l^{-1}).

The cytotoxicity was measured using the cell cytotoxicity Kit I (Roche Applied Sciences, Meylan, France).

Insect toxicity tests

The common cutworm, *Spodoptera littoralis*, was reared on an artificial diet[42] at 24 °C, and the wax moth, *Galleria mellonella*, was reared on pollen and wax at 28 °C. A locust, *Locusta migratoria*, was reared on grass at 28 °C. Eggs of the tobacco hornworm, *Manduca sexta*, were obtained from Monika Stengl (University of Regensburg, Regensburg, Germany). *M. sexta* larvae were reared on an artificial diet[43] at 27 °C with light-dark cycles consisting of 16 h of light and 8 h of darkness. Fifth-instar larvae of each insect species were selected and surface sterilized with 70% (v/v) ethanol before intrahemocoelic injection. The larvae were divided into groups of 12 larva, and each larva was injected with 10 µl of one of the purified PAX, corresponding to a dose of 0.1 µg per insect, or with phosphate-buffered saline. The treated larvae were incubated individually for up to 96 h, and then the number of dead insects was recorded.

A liquid hemolysis assay with sheep erythrocytes[44] was used to determine hemolytic activity of purified PAX. Cytolytic assays were performed with insect hemocytes by collecting hemolymph samples from *S. littoralis* larvae in an anticoagulant buffer.[45] Hemocytes were centrifuged, rinsed in phosphate-buffered saline to remove plasmatic factors, and resuspended in the same buffer (2×10^4 hemocytes ml^{-1}). The suspensions (10 µl) were each mixed with 10 µl of a purified PAX, corresponding to a 0.1-µg dose, deposited on a slide, and incubated for 20 min at 28 °C. Hemocytes with phosphate-buffered saline were used as a control. Cell lysis was observed with a light microscope and was recorded.

NMR and MS analysis

The NMR samples were prepared from the lyophylized lipopeptide. They were disolved in DMSO-*d6* to yield 1.0–1.5 mM solution. Chemical shifts are expressed with respect to the DMSO-*d6* residual signal set at 2.50 and 39.5 p.p.m. for ^1H and ^{13}C spectra, respectively. All NMR experiments were carried out on a Bruker Avance 600 spectrometer (Bruker Analytik GmbH, Rheinstetten, Germany) equipped with a triple resonance cryoprobe, and spectra were recorded at temperatures ranging from 295 to 310 K. Double-quantum filtered-COSY (DQF-COSY),[46,47] z-filtered total-correlated spectroscopy (z-TOCSY)[48,49] and NOESY[50] spectra were acquired in the phase-sensitive mode, using the States-TPPI method.[51] We obtained z-TOCSY spectra with a mixing time of 90 ms and NOESY spectra with mixing times of 150 and 250 ms, respectively. The ^1H-^{15}N HSQC, ^1H-^{13}C HSQC, ^1H-^{13}C HMBC, ^1H-^{13}C HSQC-TOCSY experiments[52–54] were carried out with the same sample.

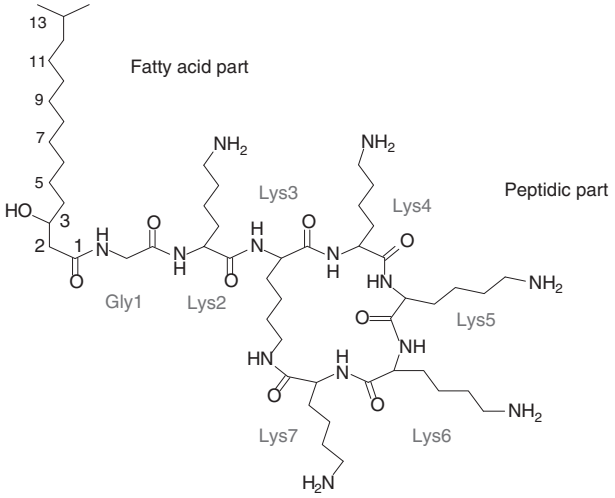

Figure 4 Chemical structure of PAX 3.

All data were processed with XWINNMR software (Bruker Analytik GmbH). The assignment of the peptidic part was achieved using the general strategy described by Wüthrich.[55] Owing to the close proximity of the K^6 and K^7 amide signals in DMSO-*d6*, the dNN_{6-7} NOE could not be observed. Thus, two other data sets were recorded with 17 and 33% of water at several temperatures ranging from 285 to 310 K. In these conditions, these two amide signals were enough separated to observe the dNN_{6-7} NOE.

The assignment of the non-peptidic part was obtained from the analysis of the homo and heteronuclear data. Owing to the overlap of ^1H resonances as well as the ^{13}C resonances of the central methylene groups of the fatty acid, giving rise to an unique HSQC cross-peak, the length of the fatty acid chain was calculated to be in agreement with the molecular weight measured by mass spectrometry. For PAX 1, 2 and 4, only ^1H-NMR data were recorded.

LC-MS was first performed to obtain the *m/z* value of the protonated PAX derivatives. ESI-LC-MS data were obtained in the positive mode on a Waters alliance LC-MS system (Waters ZQ mass detector, Waters photodiode array detector 2696, Waters alliance HPLC systems 2790). The HPLC column used was a C18 column (Waters; X-terra RP18; 5 µm; 4.6×250 mm) maintained at 35 °C. Solvents were (A) water +0.1% TFA (B) acetonitrile +0.1% TFA and the flow rate was 1 ml min^{-1}. The mobile phase composition was 80% A from 0 to 5 min, ramped to 80% B at 35 min. Samples were dissolved in solvent A (100 µl). Sample injection volume was 10 µl. UV-visible detection was by absorbance at 200–600 nm. Solvent flow to the MS was diverted to waste for the first 5 min to minimize salt build-up. PAX 3 MS-MS fragmentation data were obtained on a Waters Micromass Q-T of micro mass spectrometer.

1 Poinar, G. O. J. The presence of *Achromobacter nematophilus* in the infective stage of a *Neoaplectana sp.* (Steinernematidae: Nematoda). *Nematologica* **12,** 105–108 (1966).
2 Akhurst, R. J. Neoaplectana species: Specificity of association with bacteria of the genus *Xenorhabdus*. *Exp. Parasitol.* **55,** 258–263 (1983).
3 Herbert, E. E. & Goodrich-Blair, H. Friend and foe: the two faces of *Xenorhabdus nematophila*. *Nat. Rev. Microbiol.* **5,** 634–646 (2007).
4 Kaya, H. K. & Gaugler, R. Entomopathogenic nematodes. *Ann. Rev. Entomol.* **38,** 181–206 (1993).
5 Brown, S. E. *et al.* Txp40, a ubiquitous insecticidal toxin protein from *Xenorhabdus* and *Photorhabdus* bacteria. *Appl. Environ. Microbiol.* **72,** 1653–1662 (2006).
6 Park, Y. & Kim, Y. Eicosanoids rescue *Spodoptera exigua* infected with *Xenorhabdus nematophilus*, the symbiotic bacteria to the entomopathogenic nematode *Steinernema carpocapsae*. *J. Insect. Physiol.* **46,** 1469–1476 (2000).
7 Park, Y., Kim, Y. & Stanley, D. The bacterium *Xenorhabdus nematophila* inhibits phospholipases A2 from insect, prokaryote, and vertebrate sources. *Naturwissenschaften* **91,** 371–373 (2004).
8 Vigneux, F. *et al.* The xaxAB genes encoding a new apoptotic toxin from the insect pathogen *Xenorhabdus nematophila* are present in plant and human pathogens. *J. Biol. Chem.* **282,** 9571–9580 (2007).
9 Forst, S., Dowds, B., Boemare, N. & Stackebrandt, E. *Xenorhabdus* and *Photorhabdus spp.*: bugs that kill bugs. *Annu. Rev. Microbiol.* **51,** 47–72 (1997).
10 Webster, J. M., Chen, G., Hu, K. & Li, J. Bacterial metabolites. In *Entomopathogenic Nematology* (ed. Gangler, R.) 99–114 (CABI Publishing, New York, 2002).
11 Boemare, N. E., Boyer-Giglio, M. H., Thaler, J. O., Akhurst, R. J. & Brehelin, M. Lysogeny and bacteriocinogeny in *Xenorhabdus nematophilus* and other *Xenorhabdus spp.* *Appl. Environ. Microbiol.* **58,** 3032–3037 (1992).
12 McInerney, B. V. *et al.* Biologically active metabolites from *Xenorhabdus spp.*, Part 1. Dithiolopyrrolone derivatives with antibiotic activity. *J. Nat. Prod.* **54,** 774–784 (1991).
13 McInerney, B. V., Taylor, W. C., Lacey, M. J., Akhurst, R. J. & Gregson, R. P. Biologically active metabolites from *Xenorhabdus spp.*, Part 2. Benzopyran-1-one derivatives with gastroprotective activity. *J. Nat. Prod.* **54,** 785–795 (1991).
14 Li, J., Chen, G., Webster, J. M. & Czyzewska, E. Antimicrobial metabolites from a bacterial symbiont. *J. Nat. Prod.* **58,** 1081–1086 (1995).
15 Li, J., Chen, G. & Webster, J. M. Nematophin, a novel antimicrobial substance produced by *Xenorhabdus nematophilus* (*Enterobactereaceae*). *Can. J. Microbiol.* **43,** 770–773 (1997).
16 Webster, J. M., Chen, G., Hu, K. & Li, J. Bacterial metabolites. *Entomopathogenic Nematology* 99–114 (2002).
17 Ji, D. *et al.* Identification of an antibacterial compound, benzylideneacetone, from *Xenorhabdus nematophila* against major plant-pathogenic bacteria. *FEMS Microbiol. Lett.* **239,** 241–248 (2004).
18 Thaler, J. O., Baghdiguian, S. & Boemare, N. Purification and characterization of xenorhabdicin, a phage tail-like bacteriocin, from the lysogenic strain F1 of *Xenorhabdus nematophilus*. *Appl. Environ. Microbiol.* **61,** 2049–2052 (1995).
19 Lang, G., Kalvelage, T., Peters, A., Wiese, J. & Imhoff, J. F. Linear and cyclic peptides from the entomopathogenic bacterium *Xenorhabdus nematophilus*. *J. Nat. Prod.* **71,** 1074–1077 (2008).
20 Akhurst, R. J. Morphological and functional dimorphism in *Xenorhabdus* spp., bacteria symbiotically associated with the insect pathogenic nematodes *Neoplectana* and *Heterorhabditis*. *J. Gen. Microbiol.* **121,** 303–309 (1980).
21 Boemare, N. E. & Akhurst, R. J. Biochemical and physiological characterization of colony form variants in *Xenorhabdus* spp. (*Enterobacteriaceae*). *J. Gen. Microbiol.* **134,** 751–761 (1988).
22 De Lucca, A. J. & Walsh, T. J. Antifungal peptides: novel therapeutic compounds against emerging pathogens. *Antimicrob. Agents Chemother.* **43,** 1–11 (1999).
23 Fiechter, A. Biosurfactants: moving towards industrial application. *Trends Biotechnol.* **10,** 208–217 (1992).
24 Raaijmakers, J. M., de Bruijn, I. & de Kock, M. J. Cyclic lipopeptide production by plant-associated *Pseudomonas* spp.: diversity, activity, biosynthesis, and regulation. *Mol. Plant. Microbe Interact.* **19,** 699–710 (2006).
25 Jeu, L. & Fung, H. B. Daptomycin: a cyclic lipopeptide antimicrobial agent. *Clin. Ther.* **26,** 1728–1757 (2004).
26 Evans, M. E., Feola, D. J. & Rapp, R. P. Polymyxin B sulfate and colistin: old antibiotics for emerging multiresistant Gram-negative bacteria. *Ann. Pharmacother.* **33,** 960–967 (1999).
27 Sauermann, R., Rothenburger, M., Graninger, W. & Joukhadar, C. Daptomycin: a review 4 years after first approval. *Pharmacology* **81,** 79–91 (2008).
28 Danner, R. L. *et al.* Purification, toxicity, and antiendotoxin activity of polymyxin B nonapeptide. *Antimicrob. Agents Chemother.* **33,** 1428–1434 (1989).
29 Denning, D. W. Echinocandins: a new class of antifungal. *J. Antimicrob. Chemother.* **49,** 889–891 (2002).
30 Weis, F., Beiras-Fernandez, A. & Schelling, G. Daptomycin, a lipopeptide antibiotic in clinical practice. *Curr. Opin. Investig. Drugs* **9,** 879–884 (2008).
31 Denning, D. W. Echinocandin antifungal drugs. *Lancet* **362,** 1142–1152 (2003).
32 Nelson, P. E., Dignami, M. C. & Anaissie, E. J. Taxonomy, biology, and clinical aspects of *Fusarium* species. *Clin. Microbiol. Rev.* **7,** 479–504 (1994).
33 Boutati, E. I. & Anaissie, E. J. *Fusarium*, a significant emerging pathogen in patients with hematologic malignancy: ten years' experience at a cancer center and implications for management. *Blood* **90,** 999–1008 (1997).
34 Hennequin, C. *et al.* Invasive *Fusarium* infections: a retrospective survey of 31 cases. The French Groupe d'Etudes des Mycoses Opportunistes. *J. Med. Vet. Mycol.* **35,** 107–114 (1997).
35 Morrison, V. A., Haake, R. J. & Weisdorf, D. J. The spectrum of non-*Candida* fungal infections following bone marrow transplantation. *Medicine* **72,** 78–89 (1993).
36 Guarro, J. & Gene, J. *Fusarium* infections. Criteria for the identification of the responsible species. *Mycoses* **35,** 109–114 (1992).
37 Pfeffer, S., Hohne, W., Branner, S., Wilson, K. & Betzel, C. X-Ray structure of the antibiotic bacitracin A. *FEBS Lett.* **285,** 115–119 (1991).
38 National Committee for Clinical Laboratory Standards. *Methods for Dilution Antimicrobial Susceptibility Tests for Bacteria that Grow Aerobically*, 6th edn, Approved Standard M07-A6. (NCCLS, Villanova, PA, USA, 2003).
39 National Committee for Clinical Laboratory Standards. *Reference Method for Broth Dilution Antifungal Susceptibility Testing of Filamentous Fungi*. Approved standard. NCCLS document M38-A. (Clinical and Laboratory Standards Institute, Villanova, PA, 2002).
40 National Committee for Clinical Laboratory Standards. *Development of In Vitro Susceptibility Testing Criteria and Quality Control Parameters*. Approved guideline, 2nd edn. NCCLS document M23-A2 (Clinical and Laboratory Standards Institute, Villanova, PA, 2001).
41 National Committee for Clinical Laboratory Standards. *Reference Method for Broth Dilution Antifungal Susceptibility Testing of Yeasts*. Approved standard, 2nd edn.

NCCLS document M27-A2 (Clinical and Laboratory Standards Institute, Villanova, PA, 2002).
42 Poitout, S. & Bues, R. Elevage de plusieurs espèces de Lépidoptères *Noctuidae* sur milieu artificiel riche et sur milieu artificiel simplifié. *Ann. Zool. Ecol. Anim.* **2,** 79–91 (1970).
43 Ahmad, I. M., Waldbauer, G. P. & Friedman, S. A defined artificial diet for the larvae of *Manduca sexta*. *Entomol. Exp. Appl.* **53,** 189–191 (1989).
44 Rowe, G. E. & Welch, R. A. Assays of hemolytic toxins. *Methods Enzymol.* **235,** 657–667 (1994).
45 Anggraeni, T. & Ratcliffe, N. A. Studies on cell-cell cooperation during phagocytosis by purified haemocyte populations of the wax moth, *Galleria mellonella*. *J. Insect. Physiol.* **37,** 453–460 (1991).
46 Rance, M. *et al.* Improved spectral resolution in cosy ^{1}H NMR spectra of proteins via double quantum filtering. *Biochem. Biophys. Res. Commun.* **117,** 479–485 (1983).
47 Derome, A. E. & Williamson, M. P. 2D homonuclear shift correlation phase sensitive using TPPI with double quantum filter phase cycle. *J. Magn. Reson.* **88,** 177–185 (1990).
48 Bax, A. & Davis, G. D. Practical aspects of two-dimensional treansverse NOE spectroscopy. *J. Magn. Reson.* **65,** 355–360 (1985).
49 Rance, M. Improved techniques for homonuclear rotating-frame and isotropic mixing experiments. *J. Magn. Reson.* **74,** 557–564 (1987).
50 Macura, S., Huang, Y., Sutter, D. & Ernst, R. R. Two-dimensional chemical exchange and cross-relaxation spectroscopy of coupled nuclear spins. *J. Magn. Reson.* **43,** 259–281 (1981).
51 Marion, D., Ikura, M., Tschudin, R. & Bax, A. Rapid recording of 2D NMR-spectra without phase cycling-application to the study of hydrogen-exchange in proteins. *J. Magn. Reson.* **85,** 393–399 (1989).
52 Bodenhausen, G. & Ruben, D. J. Natural abundance nitrogen-15 NMR by enhanced heteronuclear spectroscopy. *Chem. Phys. Lett.* **69,** 185–189 (1980).
53 Bax, A. & Summers, M. F. ^{1}H and ^{13}C assignments from sensitivity-enhanced detection of heteronuclear multiple-bond connectivity by 2D multiple quantum NMR. *J. Am. Chem. Soc.* **108,** 2093–2094 (1986).
54 Bax, A. & Marion, D. Improved resolution and sensitivity in ^{1}H-detected heteronuclear multiple-bond correlation spectroscopy. *J. Magn. Reson.* **78,** 186–191 (1988).
55 Wüthrich, K. *NMR of Proteins and Nucleic Acids* (John Wiley & Sons, New York, 1986).

The Journal of Antibiotics (2009) 62, 303–308

www.nature.com/ja

ORIGINAL ARTICLE

In vitro and in vivo antitrypanosomal activities of three peptide antibiotics: leucinostatin A and B, alamethicin I and tsushimycin

Aki Ishiyama, Kazuhiko Otoguro, Masahito Iwatsuki, Miyuki Namatame, Aki Nishihara, Kenichi Nonaka, Yuta Kinoshita, Yoko Takahashi, Rokuro Masuma, Kazuro Shiomi, Haruki Yamada and Satoshi Ōmura

In the course of our screening for antitrypanosomal compounds from soil microorganisms, as well as from the antibiotics library of the Kitasato Institute for Life Sciences, we found three peptide antibiotics, leucinostatin (A and B), alamethicin I and tsushimycin, which exhibited potent or moderate antitrypanosomal activity. We report here the *in vitro* and *in vivo* antitrypanosomal properties and cytotoxicities of leucinostatin A and B, alamethicin I and tsushimycin compared with suramin. We also discuss their possible mode of action. This is the first report of *in vitro* and *in vivo* trypanocidal activity of leucinostatin A and B, alamethicin I and tsushimycin.
The Journal of Antibiotics (2009) **62,** 303–308; doi:10.1038/ja.2009.32; published online 1 May 2009

Keywords: antitrypanosomal peptide antibiotics; HAT; *in vitro*; *in vivo*; screening; *T. b. rhodesiense*; *Trypanosoma brucei brucei*

INTRODUCTION

Human African trypanosomiasis (HAT), also known as Sleeping Sickness, is recognized as one of the world's most neglected diseases and causes significant and widespread mortality and morbidity in sub-Saharan Africa. Two sub-species of trypanosomes, *Trypanosoma brucei rhodesiense* (found in eastern and southern Africa) and *T. b. gambiense* (found in west and central Africa) infect humans and wild animals, as well as domestic animals, such as pigs and dogs. Another sub-species, *T. b. brucei*, infect cattle, causing Nagana disease, which devastates livestock production and causes massive economic losses.

The trypanosome parasites are transmitted through the bite of blood-sucking tsetse flies (*Glossina* spp.). Transmission of *T. b. gambiense* is mostly human-to-human, whereas wild animals and humans both act as reservoir hosts for *T. b. rhodesiense*. During a bite from an infected tsetse, parasites are introduced into the blood-stream in which they multiply and then pass into the lymph system. This represents the early stage of HAT, during which the patient may suffer from fever, headaches, joint pains or itchiness. The second, or late, stage is more critical, because of parasites crossing the blood–brain barrier and invading the central nervous system. This results in loss of sensation, neuropathy, sleeping disorder, coma and ultimately death. *T. b. rhodesiense* infection is acute, lasting from a few weeks to several months, whereas *T. b. gambiense* infection is chronic, persisting for several years, during which times patients may be asymptomatic. In the absence of effective diagnosis and treatment, both forms cause death in humans, the former much more rapidly.

Accurate statistics for HAT are lacking, as many cases are not reported. The World Health Organization estimated that, in 2000, the disease affected some 300 000 Africans, a figure far in excess of the 27 000 cases reportedly diagnosed and treated that year. By 2005, surveillance had been reinforced, case reporting improved and was held to be more accurate, with the number of new cases actually reported falling substantially. Between 1998 and 2004, the figure for cases of both forms of the disease combined was estimated to have fallen from 37 991 to 17 616, reducing further to 10 769 in 2007. The estimated number of actual cases of infection is currently 50 000–70 000.[1,2]

Currently, the drugs pentamidine and suramin are used in the early stage of *T. b. gambiense* and *T. b. rhodesiense* infections, and melarsoprol is used in the late stage, whereas eflornithine is only used in the late stage of *T. b. gambiense* infections. These drugs are old and highly unsatisfactory, as they cannot be given orally and can be dangerous because of their severe toxicity. Melarsoprol is particularly hazardous, with 5–10% of patients dying because of toxic side effects.[3] Suramin, discovered in 1921, which is still commonly used for treatment of early-stage *T. b. rhodesiense*, provokes undesirable side effects in the urinary tract and causes major allergic reactions. Pentamidine, routinely used for treatment of early-stage Gambiense sleeping sickness was introduced in 1941 and, despite a few undesirable effects, it is generally well tolerated by patients. However, drug resistance in trypanosomes is increasing and treatment failures are becoming more common.[4,5] Therefore, there is an urgent need for new antitrypanosomal drugs

Research Center for Tropical Diseases, Center for Basic Research, Kitasato Institute for Life Sciences and Graduate School of Infectious Control Sciences, Kitasato University, Tokyo, Japan
Correspondence: Dr K Otoguro, Research Center for Tropical Diseases, Center for Basic Research, Kitasato Institute for Life Sciences and Graduate School of Infectious Control Sciences, Kitasato University, 5-9-1 Shirokane, Minato-ku, Tokyo 108-8641, Japan.
E-mail: otoguro@lisci.kitasato-u.ac.jp
Received 13 March 2009; revised 30 March 2009; accepted 1 April 2009; published online 1 May 2009

that are more effective and safer, especially those that have novel structures and mechanisms of action.

During our program to screen soil microorganisms and compounds from the antibiotic library of the Kitasato Institute for Life Sciences to discover antitrypanosomal substances, we earlier reported that various microbial metabolites exhibit potent antitrypanosomal properties.[6,7] We have discovered a further three peptide antibiotics, leucinostatin A and B (produced by soil fungi, *Paecilomyces* sp.) and alamethicin I and tsushimycin (from the antibiotic library) (Figure 1), which show potent or moderate antitrypanosomal properties. We report here the *in vitro* and *in vivo* antitrypanosomal activities and cytotoxicities of these peptide antibiotics, as compared with the widely used trypanocidal drug suramin.

Leucinostatins, isolated from cultured broth of *Paecilomyces* spp., were discovered to possess antitrypanosomal properties, although the structure–activity relationship of antitrypanosomal compounds remains unknown.[8]

The present observations are the first reports of *in vitro* and *in vivo* antitrypanosomal activities of leucinostatin A and B, alamethicin I and tsushimycin.

MATERIALS AND METHODS

Chemicals

Leucinostatin A and B were isolated from a culture broth of *Paecilomyces* sp., FKI-3045 at the Kitasato Institute for Life Sciences. Alamethicin I and tsushimycin were obtained from the antibiotics library of the Kitasato Institute for Life Sciences.

Suramin was provided by Professor R Brun (Swiss Tropical Institute, Basel, Switzerland). Iscove's modified Dulbecco's medium (with L-glutamine and HEPES, without $NaHCO_3$), minimum essential medium (MEM) with Earle's salts, MEM non-essential amino acids solution and penicillin–streptomycin solution were obtained from Gibco Laboratories Life Technologies (Grand Island, NY, USA). Fetal bovine serum was obtained from Sigma-Aldrich Inc (St Louis, MO, USA) and horse serum was obtained from Gibco Laboratories Life Technologies. Alamar Blue reagent was obtained from Sigma-Aldrich Inc.. Other chemicals were commercially available and all of analytical grade.

Taxonomic studies of FKI-3045

Fungal strain FKI-3045 was isolated from soil collected in Ishigaki Island, Okinawa, Japan. The micro-morphological characteristics of samples were observed under a Vanox-S AH-2 microscope (Olympus, Tokyo, Japan) and the ITS1 sequence of the strain FKI-3045 was deposited at the DNA Data Bank of Japan, with accession number AB480689. From the results of general characteristics,[9] the total length of the ITS1 and BLAST search,[10] the producing strain FKI-3045 was identified as a strain of *Paecilomyces* sp.

Fermentation, isolation and identification of leucinostatins

A loopful of spores of *Paecilomyces* sp. FKI-3045 was inoculated into 100 ml of seed medium consisting of 2.0% glucose, 0.2% yeast extract, 0.5% Polypepton (Wako Pure Chemical Industries, Osaka, Japan), 0.05%·$MgSO_4$ $7H_2O$, 0.1% KH_2PO_4 and 0.1% agar (adjusted to pH 6.0 before sterilization) in a 500-ml Erlenmeyer flask. The inoculated tube was incubated in a rotary shaker (210 r.p.m.) at 27 °C for 3 days. The seed culture (1 ml) was transferred to 500-ml Erlenmeyer flasks (total 93 flasks) containing 100 ml of production medium consisting of 1.0% glucose, 2.0% soluble starch, 2.0% soybean oil,

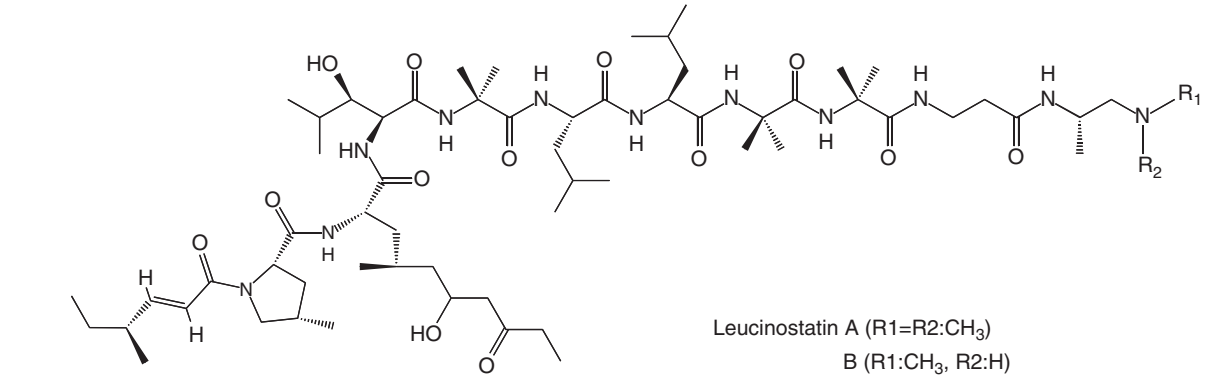

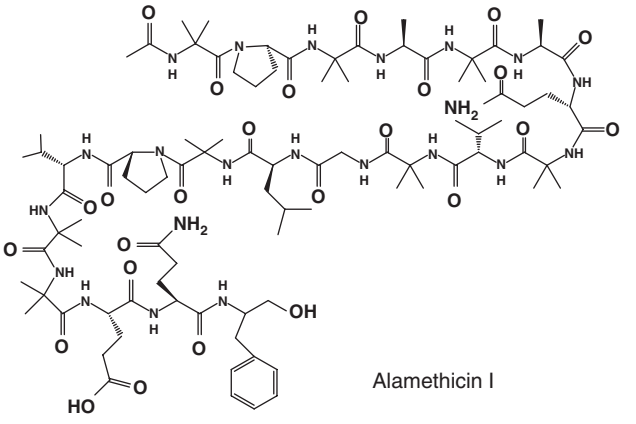

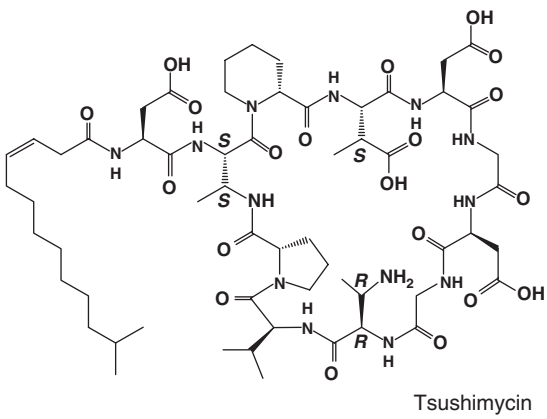

Figure 1 Structures of leucinostatin A and B, alamethicin I and tsushimycin.

1.0% Pharmamedia (Traders Protein, Lubbock, TX, USA), 0.5% meat extract, 0.1% $MgSO_4 \cdot 7H_2O$, 5.0×10^{-4}% $FeSO_4 \cdot 7H_2O$, 5.0×10^{-4}% $MgCl_2 \cdot 4H_2O$, 5.0×10^{-4}% $CuSO_4 \cdot 5H_2O$ and 5.0×10^{-4}% $CoCl_2 \cdot 6H_2O$ and 0.3% $CaCO_3$ (adjusted to pH 6.0 before sterilization), and the fermentation was carried out on a rotary shaker (210 r.p.m.) at 27 °C for 3 days, followed by stasis at 27 °C for 6 days.

The 9-day-old culture broth (9.3 l) was extracted with EtOH, followed by filtration. The fitrate was extracted with EtOAc. The EtOAc extract (12.1 g) was applied to a Diaion HP20 column (100ϕ×120 mm, Nippon Rensui Co., Tokyo, Japan). After washing with 50 and 60% acetone aq soln (3 l each), the active materials were eluted with 80% acetone aq soln. The material (10.2 g) was applied to an octadecylsilyl (ODS) column (35ϕ×200 mm, Senshu Scientific Co., Tokyo, Japan). After washing with 20 and 40% CH_3CN/0.1% HCOOH aq soln (400 ml each), the active materials were eluted with 60% CH_3CN/0.1% HCOOH aq soln. The material (66.8 mg) was purified by HPLC on a Xbridge phenylhexyl column (10ϕ×250 mm, Waters Co., Tokyo, Japan) with 60% CH_3CN/10 mM NH_4OAc aq soln (pH 10) at 2.5 ml min^{-1} detected at UV 210 nm. Each active fraction at the retention times of 22 and 26 min was concentrated *in vacuo* to dryness to afford leucinostatins B (6.9 mg) and A (9.8 mg) as white powders, respectively.

The ^1H NMR spectra of leucinostatins indicated α-proton signals of amino acid residues at δ_H 4.0–5.5 p.p.m. and singlet methyl signals of aminoisobutylic acid residues at δ_H 1.5–1.6 p.p.m. The ^{13}C NMR spectra indicated α-carbon signals of amino acid residues at δ_C 50–60 p.p.m. and amide carbonyl carbons at δ_C 175.5–189 p.p.m. Leucinostatins A and B were identified by protonated ion peak (*m/z*, $[M+H]^+$ 1218.6 ans 1024.6) and fragment ion peaks (A: *m/z*, 997.7, 784.6, 655.5, 631.1, 570.4, 546.0, 457,4, 435.3, 344.3, 259.2 and 222.2, B: *m/z*, 983.5, 770.3, 641.1, 556.3, 546.2, 443.0, 329.9, 222.0 and 111.9) observed in electrospray ionization tandem mass spectrometry (ESI-MS) analysis, respectively.

Trypanosomes

Bloodstream forms of parasite used were *T. b. brucei* strain GUTat 3.1, *T. b. rhodesiense* strain STIB900 and *T. b. brucei* strain S427, as described earlier.[6,7]

Animals

Female CD1 mice (ICR), 20–25 g, were obtained from Charles River Japan Inc. (Kanagawa, Japan). Animals were placed in groups of four per cage, kept in a room under negative pressure with flow of 0.1–0.2 m sec^{-1}. The animal room was held at a temperature of 25 ± 2 °C and 60 ± 10% relative humidity. Animals were maintained on a diet of CE-2 (Clea Japan Inc., Tokyo, Japan) and water *ad libitum*.

In vitro assay

In vitro antitrypanosomal activities for *T. b. brucei* strain GUTat 3.1 and *T. b. rhodesiense* strain STIB900 has been described earlier.[6] In brief, 95 µl of parasites suspension was incubated with 5 µl of drug solution for 72 h and Alamar Blue was used for parasites survival determination to calculate IC_{50} values.

Cytotoxicity assay against MRC-5 cells was carried out as described earlier.[11]

In vivo assay

In vivo antitrypanosomal activities for *T. b. brucei* strain S427 and *T. b. rhodesiense* strain STIB900 were described earlier.[7] In brief, female ICR mice were infected i.p. with parasites prepared from cryostabilate and drug treatment was carried out for 4 consecutive days. Efficacy of drug was determined by parasitaemia levels and the mean of survival days (MSD), compared with the untreated control group.

RESULTS

Table 1 shows *in vitro* antitrypanosomal activities of leucinostatin A and B, alamethicin I, tsushimycin and suramin. Leucinostatin A and B showed the most potent activity against both strains GUTat 3.1 and STIB900, with IC_{50} values ranging from 3.4–8.3 ng ml^{-1}. Leucinostatins show approximately 200-fold higher activity than suramin against the GUTat 3.1 strain. In the case of STIB900, they showed 12- to 15-fold higher values than suramin. Alamethicin I also showed potent impact against the GUTat 3.1 strain, with an IC_{50} value of 170 ng ml^{-1}, some 9.3-fold lower value than suramin. Although tsushimycin showed the lowest IC_{50} value of the three, it was still similar to that of suramin. The antitrypanosomal activity on strain STIB900 of both alamethicin I and tsushimycin was lower than that of suramin.

Evaluation of cytotoxicities of the peptides against MRC-5 cells is also shown in Table 1. The IC_{50} values ranged between 2550–> 100 000 ng ml^{-1}. As a means to evaluate both antitrypanosomal activity and cytotoxicity, we introduced a selectivity index (SI), which is obtained by dividing IC_{50} of cytotoxicity by IC_{50} of antitrypanosomal activity. The SI of compounds tested is shown in Table 1. All three peptides had a higher SI than suramin in the case of strain GUTat 3.1/MRC-5, whereas in the case of STIB900 they were lower than suramin.

Table 2 shows *in vivo* antitrypanosomal activity, using the *T. b. brucei* S427 acute mouse model with leucinostatin A and B, alamethicin I, tsushimycin and suramin. Leucinostatin B showed curative effect at a dose of 1.0 mg kg^{-1}×4, the same curative dosage as for suramin. Tsushimycin also showed a curative effect at a dose of 50 mg kg^{-1}×4. Alamethicin I did not achieve cure at a dose of 3.0 mg kg^{-1}×4, but extended the MSD, animals surviving approximately threefold longer than the untreated controls. Leucinostatin A and B did not show *in vivo* antitrypanosomal activity at a dose of 0.3 mg kg^{-1}×4. The LD_{50} of leucinostatin A is reported to be 1.8 mg kg^{-1} i.p.,[12] therefore we tried 0.3 mg kg^{-1} i.p. ×4 to try and avoid any toxic symptoms during treatment. Leucinostatin B showed toxicity at a dose of 2.5 mg kg^{-1} ×2 i.p.; however, treated mice withstood the toxicity and the infection was completely cured (data not shown). We also carried out *in vivo* evaluation using the *T. b. rhodesiense* strain STIB900 acute model with leucinostatin B (Table 3). Leucinostatin B showed 20% cure activity, extending MSD by >28 days at the 1.0 mg kg^{-1} ×4 dosage. Suramin did not show curative activity, though it did cause extended MSD (by 25 days) using a dose of 1.0 mg kg^{-1} ×4. At the 10 mg kg^{-1} ×4 dosage level with suramin, a 50% curative rate was observed, with an extension of MSD by >39.3 days.

DISCUSSION

With regard to the commonly used therapeutic drugs, the mode of action of suramin and pentamidine remains unknown, whereas that of melarsoprol is poorly characterized.[3]

Table 1 *In vitro* antitrypanosomal activity and cytotoxicity of leucinostatin A and B, alamethicin I, tsushimycin and drugs used to treat Human African Trypanosomiasis

	IC_{50} (ng ml^{-1})				
	Antitrypanosomal activity			*Selectivity index (SI)*	
Compound	*GUTat 3.1*	*STIB900*	*Cytotoxicity MRC-5*	*M/T.b.b.*	*M/T.b.r.*
Leucinostatin A	7.8	3.4	2550	326.9	750.0
Leucinostatin B	8.3	4.4	3110	374.7	706.8
Alamethicin I	170	380	62 500	367.6	164.5
Tsushimycin	1090	2490	>100 000	>91.7	>40.1
Suramin	1580	52	>100 000	>63	>1923

Table 2 ***In vivo*** **antitrypanosomal activity of leucinostatin A and B, alamethicin I, tsushimycin, pentamidine and suramin in** ***T. b. brucei*** **S427 mouse model**

Compound	*Dosage (mg kg^{-1})*	*Route*	*No. of mice cured/no. of mice infected*	*Mean survival days (MSD)*	*Control MSD*
Leucinostatin A	0.3×4	i.p.	0/4	5.5	5.5
Leucinostatin B	1.0×4	i.p.	4/4	>30	5.5
	0.3×4	i.p.	0/4	6.75	6.0
Alamethicin I	3.0×4	i.p.	0/4	15	4.5
Tsushimycin	50.0×4	i.p.	4/4	>30	4.4
Suramin	1.0×4	i.p.	4/4	>30	5.5

Table 3 ***In vivo*** **antitrypanosomal activity of leucinostatin B, pentamidine and suramin in** ***T. b. rhodesience*** **STIB900 mouse model**

Compound	*Dosage (mg kg^{-1})*	*Route*	*No. of mice cured/no. of mice infected*	*Treated MSD*	*Control MSD*
Leucinostatin B	1.0×4	i.p.	1/4	>28	11.3
	0.3×4	i.p.	0/4	13	11.3
Suramin	10.0×4	i.p.	2/4	>39.3	12.5
	1.0×4	i.p.	0/4	25	8.5

Leucinostatins,[13–15] alamethicin I[16,17] and tsushimycin[18] are lipophilic peptide antibiotics produced as microbial metabolites. These antibiotics showed potent and moderately antitrypanosomal activity both *in vitro* and *in vivo*. Significantly, these three peptide antibiotics exhibited different characteristics compared with suramin with respect to sensitivity against strain GUTat 3.1 and strain STIB900. Consequently, the mode of action of the three might be different to that of suramin.

Leucinostatin acts on gram-positive bacteria,[13,14] as an uncoupler in mitochondria,[14,19–21] inhibitor of mitochondrial ATP synthesis,[22] weak ionophore and immunosuppressant,[23] blocker of virus glycoprotein expression[24] and as a nematicide.[25]

Although the bloodstream form of *T. brucei* has no oxidative phosphorylation,[26] *T. brucei* mitochondrial ATP synthetase has been isolated and characterized.[27] Brown *et al.*[28] reported that ATP synthetase is responsible for the maintenance of membrane potential in blood-stream form trypanosomes, showing that RNAi knockdown of the α and β subunits of the F_1 portion of ATP synthetase caused a slowdown in cell growth. It is therefore possible that leucinostatin A and B might be specific against *T. brucei* ATP synthetase.

Ishiguro *et al.*[29] reported that leucinostatin might act on membrane phospholipids. When leucinostatin A acts as an ionophore, mono- (H^+ and $^{86}Rb^+$) and divalent ($^{45}Ca^{2+}$ and $^{65}Zn^{2+}$) cations were transported across both mouse thymocyte and artificial membrane and it increases intracellular calcium and decreases intracellular pH in the mouse thymocyte.[23] *T. brucei* bloodstream-form parasites exposed to A-23187 (calcium ionophore) show gradual cell swelling, eventually forming a spherical appearance that was completed within 45 min.[30] Ruben *et al.* reported that intracellular calcium was increased approximately threefold by the addition of 4Br-A23187 (calcium ionophore) and intracellular calcium was superinduced with the proton ionophore FCCP, the K^+/H^+ exchanger nigericin, and also intracellular pH was decreased.[31] They also reported that amphiphilic peptide and amine caused Ca^{2+} influx across the plasma membrane, but did not disrupt membrane integrity.[32]

Ca^{2+} is a major signal transduction molecule in several organisms, including protozoan parasites.[33] Acidocalcisomes are the main Ca^{2+} storage compartment in trypanosomatids and apicomplexan parasites, as well as an energy store for Ca^{2+} signaling and intracellular pH homeostasis.[34] We had already found that leucinostatin A possesses antimalarial properties.[35] There is thus an expectation that leucinostatins act as ionophores and disrupt parasite homeostasis resulting in antiparasite impact, but there might be an as yet unknown mode of action, including mitochondrial ATP synthesis inhibition, because leucinostatins show highly potent antiparasite activity both *in vitro* and *in vivo*.

Alamethicin I is reported to have mostly anti-gram-positive bacterial activity,[36] act as an uncoupler of oxidative phosphorylation in rat mitochondria[37] and possess hemolytic activity.[38] The mode of action of alamethicin is considered to be through its effect on biomembrane systems by ion channel formation in lipid-membranes bilayers.[17,39,40] It was reported that alamethicin seems to form ionic channels on chromaffin cells, which are permeable to Ca^{2+}, Mn^{2+} and Ni^{2+}.[41] Dathe *et al.*[42] reported that alamethicin induces catecholamine secretion from chromaffin cells and enhanced metabolic activity in endothelial cells. They showed that catecholamine secretion from bovine adrenal chromaffin cell was enhanced by alamethi cin dose-dependently in Ca^{2+}-containing medium, whereas there was no effect using Ca^{2+}-free medium. They suggested a peptide-mediated Ca^{2+} entry into the cells. Alamethicin I might also act as an ionophore.

Tsushimycin, isolated from the culture broth of a *Streptomyces* strain, is related to the amphomycin–glumamycin group of antibiotics.[18,43] The mode of action of tsushimycin is reportedly through inhibition of the formation of dolichyl phosphate mannose, dolichyl phosphate glucose and dolichyl pyrophosphate *N*-acetylglucosamine, using particulate enzyme preparation from pig aorta.[44] The related antibiotic, amphomycin, is reported to show *in vivo* antitrypanosomal activity against *T. b. gambiense*- and *T. b. rhodesiense*-infected mice.[45] Furthermore, amphomycin showed inhibition of trypanosomal dolichol phosphate mannose synthase that gives mannose from dolichol phosphate mannose to synthesize the glycosylphosphatidylinositol anchor under the cell-free system.[46] Tsushimycin may also inhibit *T. brucei* in the same manner as amphomycin. Study of the crystallized

tsushimycin suggested that bioactive tsushimycin is most likely to involve Ca^{2+} ions that may interact with bacteria cell membranes at their fatty-acid side chain.[43]

The mode of action of the three antibiotics reported here is mainly expected to be via interaction with the membrane-lipid layer of trypanosomes.

It has been reported that antimicrobial peptides, such as defensins, cathelicidins[47] and some cathelicidin families[48] showed antitrypanosomal activity against both the bloodstream form and procyclic form of *T. brucei*. Especially, protegrin-1, a cathelicidin-class peptide showed *in vivo* survival elongation effect with daily treatment of 5 mg kg^{-1} i.p., treated parasites showing significant morphological change.[47] The mode of action was described as disruption of cell wall/membrane integrity because of cationic and amphipathic characteristics. On the basis of cationic and amphipathic antibacterial peptides, Gonzalez-Reyet *et al.*[49] reported that vasoactive intestinal polypeptide and the structurally related pituitary adenylate cyclase-activating polypeptide have antitrypanosomal activity, specifically against the bloodstream form of parasites and that these peptides enter into and accumulate in the parasite cytosol.

Antimicrobial peptides have been classified into four groups on the basis of their structure (β-sheet, α-helical, extended and loop) and cationic and amphipathic characters.[50] We showed that antitrypanosomal activity of the peptide antibiotics discussed have cationic and lipophilic character in the structure (Figure 1) and also these antibiotics have any of the β-sheet, α-helical or loop conformations.[17,43,51] Therefore, these peptides might act more selectively on *T. brucei* than mammalian cells, in spite of their toxicity. In the case of leucinostatin A, it has been reported that leucinostatin A-loaded nanospheres show anti-*Candida albicans* activity both *in vitro* and *in vivo*, but with drastic reduction of toxicity.[52]

The above results reveal that leucinostatin A and B, alamethicin I and tsushimycin are promising lead compounds for a new type of antitrypanosomal activity. Further investigation of the antitrypanosomal potential of these peptide antibiotics is in progress.

ACKNOWLEDGEMENTS

This work was supported, in part, by funds from the Drugs for Neglected Diseases initiative (DND*i*), and a grant for All Kitasato Project Study (AKPS). We are grateful to Dr Y Yabu, the Nagoya City University, Professor R Brun and Dr M Kaiser, the Swiss Tropical Institute, Professor T Kinoshita, the Research Institute for Microbial Diseases, Osaka University and Professor S Croft, Dr Eric Chatelain, Dr J-R Ioset, Dr C Brünger and Miss F Hirabayashi, DND*i*, for valuable discussions. We also thank Miss H Sekiguchi, Mr T Furusawa, Miss M Niitsuma and Miss J Hashida (Kitasato university) for her technical assistance throughout this work.

1 http://www.dndi.org/.
2 http://www.who.int/mediacentre/factsheets/fs259/en/.

3 Fairlamb, A. H. Chemotherapy of human African trypanosomiasis: current and future prospects. *Trends Parasitol.* **19,** 488–494 (2003).
4 Matovu, E., Seebeck, T., Enyaru, J. C. K. & Kaminsky, R. Drug resistance *in Trypanosoma brucei spp.*, the causative agents of Sleeping Sickness in man and Nagana in cattle. *Microbes Infect.* **3,** 763–770 (2001).
5 Brun, R., Schumacher, R., Schmid, C., Kunz, C. & Burri, C. The phenomenon of treatment failures in Human African Trypanosomiasis. *Trop. Med. Int. Health* **6,** 906–914 (2001).
6 Otoguro, K. *et al.* Selective and potent *in vitro* antitrypanosomal activities of 10 microbial metabolites. *J. Antibiot.* **61,** 372–378 (2008).
7 Ishiyama, A. *et al. In vitro* and *in vivo* antitrypanosomal activities of two microbial metabolites, KS-505a and Alazopeptin. *J. Antibiot.* **61,** 627–632 (2008).
8 Shaw, I. M. & Taylor, A. The chemistry of peptides related to metabolites of *Trichoderma* spp. 2. An improved method of characterization of peptides of 2-methylalanine. *Can. J. Chem.* **64,** 164–173 (1986).
9 von Arx, J. A. The genera of fungi sporulating in pure culture. 3rd edn., p. 263, *J. Cramer. Vaduz.* (1981).
10 Altschul, S. F., Gish, W., Miller, W., Myers, E. W. & Lipman, D. J. Basic local alignment search tool. *J. Mol. Biol.* **215,** 403–410 (1990).
11 Otoguro, K. *et al.* Potent antimalarial activities of the polyether antibiotic, X-206. *J. Antibiot.* **54,** 658–663 (2001).
12 Mikami, Y. *et al.* Leucinostatins, peptide mycotoxins produced by *Paecilomyces lilacinus* and their possible roles in fungal infection. *Zbl. Bakt. Hyg.* **257,** 275–283 (1984).
13 Arai, T., Mikami, Y., Fukushima, K., Utsumi, T. & Yazawa, K. A new antibiotic, leucinostatin, derived from *Penicillium lilacinum. J. Antibiot.* **26,** 157–161 (1973).
14 Fukushima, K. & Arai, T. Studies on peptide antibiotics, leucinostatins I. Separation, physico-chemical properties and biological activities of leucinostatin A and B. *J. Antibiot.* **36,** 1606–1612 (1983).
15 Fukushima, K. & Arai, T. Studies on peptide antibiotics, leucinostatins II. The structures of leucinostatin A and B. *J. Antibiot.* **36,** 1613–1630 (1983).
16 Pandey, R. C., Cook, Jr J. C. & Rinehart, Jr K. L. High resolution and field desorption mass spectrometry studies and revised structures of alamethicins I and II. *J. Am. Chem. Soc.* **99,** 8469–8483 (1977).
17 Leitgeb, B., Szekeres, A., Manczinger, L., Vágvölgyi, C. & Kredics, L. The history of alamerhicin: a review of the most extensively studied peptaibol. *Chem. Biodivers.* **4,** 1027–1051 (2007).
18 Shoji, J., Kozuki, S., Okamoto, S. & Sakazaki, R. Studes on tsushimycin. I. Isolation and characterization of an acidic acylpeptide containing a new fatty acid. *J. Antibiot.* **21,** 439–443 (1968).
19 Lardy, H., Reed, P. & Lin, C. H. Antibiotic inhibitors of mitochondrial ATP synthesis. *Fed. Proc.* **34,** 1707–1710 (1975).
20 Reed, P. W. & Lardy, H. A. Uncoupling and specific inhibition of phosphoryl transfer reactions in mitochondria by the antibiotic A20668. *J. Biol. Chem.* **250,** 3704–3708 (1975).
21 Mori, Y., Suzuki, M., Fukushima, K. & Arai, T. Structure of leucinostatin B, an uncoupler on mitochondria. *J. Antibiot.* **36,** 1084–1086 (1983).
22 Shima, A., Fukushima, K., Arai, T. & Terada, H. Dual inhibitory effects of the peptide antibiotics leucinostatin in oxidative phosphorylation in mitochondria. *Cell Struct. Funct.* **15,** 53–58 (1990).
23 Csermely, P. *et al.* The nonapeptide leucinostatin A acts as s weak ionophore and as an immunosuppressant on T lymphocytes. *Biochim. Biophys. Acta.* **1221,** 125–132 (1994).
24 Muroi, M. *et al.* Novel blockade of cell surface expression of virus glycoprotein's by leucinostatin *A. J. Antibot.* **49,** 119–1126 (1996).
25 Park, J. O. *et al.* Production of leucinostatins and nematicidal activity of Australian isolates of *Paecilomyces lilacinus* (Thom) Samson. *Lett. Appl. Microbiol.* **38,** 271–276 (2004).
26 Kita, K., Nihei, C. & Tomitsuka, E. Parasite mitochondria as drug target: diversity and dynamic change during the life cycle. *Curr. Med. Chem.* **23,** 2535–2548 (2003).
27 Williams, N., Choi, S. Y., Ruyechan, W. T. & Frank, P. H. The mitochondrial ATP synthase of *Trypanosma brucei*: Developmental regulation through the life cycle. *Arch. Biochem. Biophys.* **288,** 509–515 (1991).
28 Brown, S. V., Hosking, O., Li, J. & Wiliams, N. ATP synthase is responsible for maintaining mitochondrial membrane potential in bloodstream form *Trypanosoma brucei. Eukaryotic Cell* **5,** 45–53 (2006).
29 Ishiguro, K. & Arai, T. Action of the peptide antibiotic Leucinostatin. *AAC* **9,** 893–898 (1976).
30 Bowles, D. J. & Voorheis, H. P. Release of the surface coat from the plasma membrane of intact bloodstream forms of *Trypanosoma brucei* requires Ca^{2+}. *FEBS Lett.* **139,** 17–21 (1982).
31 Ruben, L., Hutchinson, A. & Moehlman, J. Calcium homeostasis in *Trypanosoma brucei. J. Biol. Chem.* **266,** 24351–24358 (1991).
32 Ruben, L., Akins, C. D., Haghighat, N. G. & Xue, L. Calcium influx in *Trypanosoma brucei* can be induced by amphiphilic peptides and amines. *Mol. Biochem. Parasitol.* **81,** 191–200 (1996).
33 Moreno, S. & Docampo, R. Calcium regulation in protozoan parasites. *Curr. Opin. Microbiol.* **6,** 359–364 (2003).
34 Docampo, R., Souza, W., Miranda, K., Rohloff, P. & Moreno, S. Acidocalcisomes-conserved from bacteria to man. *Nat. Rev. Microbiol.* **3,** 251–261 (2005).
35 Otoguro, K. *et al. In vitro* antimalarial activities of microbial metabolites. *J. Antibiot.* **56,** 322–324 (2003).
36 Meyer, P. & Reusser, F. A polypeptide antibacterial agent isolated from *Trichoderma viride. Experientica* **23,** 85–86 (1967).
37 Mathew, M. K., Nagaraj, R. & Balaram, P. Alamethicin and synthetic peptide fragments as uncouplers of mitochondrial oxidative phosphorylation. Effect of chain length and charge. *BBRC* **98,** 548–555 (1981).
38 Irmscher, G. & Jung, G. The hemolytic properties of the membrane modifying peptide antibiotics, alamethicin, suzukacillin and trichotoxin. *Eur. J. Biochem.* **80,** 165–174 (1977).
39 Mueller, P. & Rudin, D. O. Action potentials induced in biomolecular lipid membranes. *Nature* **217,** 713–719 (1968).
40 Woolley, G. A. Channel-forming activity of alamethicin: Effects of covalent tethering. *Chem. Biodivers.* **4,** 1323–1337 (2007).
41 Fonteriz, R. I., López, M. G., Garcia-Sancho, J. & Garca, A. G. Alamethicin channel permeation by Ca^{2+}, Mn^{2+} and Ni^{2+} in bovine chromaffin cells. *FEBS Lett.* **283,** 89–92 (1991).

42 Dathe, M. *et al*. Proline at position 14 of alamethicin is essential for hemolytic activity, catecholamine secretion from chromaffin cells and enhanced metabolic activity in endothelial cells. *Biochim. Biophys. Acta.* **1370,** 175–183 (1998).
43 Bunkóczi, G., Vértesy, L. & Sheldric, G. M. Structure of the lipopeptide antibiotic tsushimycin. *Acta. Crystallogr. D Biol. Crystallogr.* **61,** 1160–1164 (2005).
44 Elbein, A. D. The effect of tsushimycin on the synthesis of lipid-linked saccharides in aorta. *Biochem. J.* **193,** 477–484 (1981).
45 Packchanian, A. Chemotherapy of African sleeping sickness. II. Chemotherapy of experimental *Trypanosoma gambiense* and *Trypanosoma rhodesiense* infections in mice (*Mus musculus*) with a new antibiotic, amphomycin. *Antibiot. Chemother.* **6,** 684–691 (1956).
46 Menon, A. K., Mayor, S. & Schwarz, R. T. Biosynthesis of glycosyl-phoshatidylinositol lipids in *Trypanosoma brucei*: involvement of mannosyl-phosphoryldolichol as the mannose donor. *EMBO J.* **9,** 4249–4258 (1990).
47 McGwire, B. S., Olson, C. L., Tack, B. F. & Engman, D. M. Killing of African trypanosomes by antimicrobial peptides. *JID* **188,** 146–152 (2003).
48 Haines, L. R., Hancock, R. & Pearson, T. W. Cationic antimicrobial peptides killing of African trypanosomes and *Sodalis glossinidius*, a bacterial symbiont of the insect vector of sleeping sickness. *Vector Borne Zoonotic Dis.* **3,** 175–186 (2003).
49 Gonzalez-Rey, E., Chorny, A. & Delgado, M. VIP: An agent with license to kill infective parasites. *Ann. NY Acad. Sci.* **1070,** 303–308 (2006).
50 Powers, J. P. & Hancock, R. The relationship between peptide structure and antibacterial activity. *Peptides* **24,** 1681–1691 (2003).
51 Cerrini, S., Lamba, D., Scatturin, A. & Ughetto, G. The crystal and molecular structure of the alpha-helical nonapeptide antibiotic leucinostatin A. *Biopolymers* **28,** 409–420 (1989).
52 Ricci, M. *et al*. Leucinostatin-A loaded nanospheres: characterization and *in vivo* toxicity and efficacy evaluation. *Int. J. Pharm.* **275,** 61–72 (2004).

The Journal of Antibiotics (2009) 62, 309–313

www.nature.com/ja

ORIGINAL ARTICLE

Role of *nsdA* in negative regulation of antibiotic production and morphological differentiation in *Streptomyces bingchengensis*

Xiang-Jing Wang[1], Suo-Lian Guo[1], Wan-Qian Guo[2], Di Xi[1] and Wen-Sheng Xiang[1]

To investigate the function of *nsdA* in *Streptomyces bingchengensis*, it was cloned and sequenced, which presented an 89.89% identity with that of *S. coelicolor*. The λRED-mediated PCR-targeting technique was used to create *nsdA* replacement in the *S. bingchengensis*_226541 chromosome. The *nsdA* disruption mutant, BC29, was obtained, which produced more pigment and spores than did the ancestral strain. HPLC analysis revealed that the disruption of *nsdA* efficiently increased milbemycin A_4 production and nanchangmycin production by 1.5-fold and 9-fold, respectively. Complementation of the *nsdA* mutation restored the phenotype and antibiotic production. These results showed that *nsdA* negatively affected sporulation and antibiotic production in *S. bingchengensis*.
The Journal of Antibiotics (2009) **62,** 309–313; doi:10.1038/ja.2009.33; published online 15 May 2009

Keywords: antibiotic production; *nsdA*; sporulation; *Streptomyces bingchengensis*

INTRODUCTION

Streptomyces have attracted great interest because of their well-known ability to produce a great variety of antibiotics and other secondary metabolites.[1] Secondary metabolism is a very complex regulatory network.[2] Pathway-specific regulatory genes, such as *actII-orf4*, *redD*, *cdaR* and *mmyR*, are at the bottom of the regulatory network, each controlling one antibiotic biosynthetic pathway.[3] Global regulators, such as *bldA*,[4] *bldB*,[5] *bldD*[6] and *bldG*,[7] perform the highest level regulation and affect both morphological and physiological differentiation.[8,9] At intermediate levels in the regulatory cascades, many regulatory genes, such as *afsB*,[10] *abaA*,[11] *absB*,[12] *afsK-afsR*[13,14] and *tcrA*,[15] and two-component systems, such as *afsQ1-afsQ2*,[16] *absA1-absA2*,[17,18] *cutS-cutR*[19] and *phoR-phoP*,[20] have been identified, which regulate the synthesis of two or more antibiotics. *absA1-absA2*, *cutS-cutR*, *phoR-phoP*, *tcrA* and some pathway-specific repressors regulate antibiotic production in a negative manner, as mutations in these genes resulted in the overproduction of the corresponding antibiotic(s). Global regulators may also play a negative role, as in the case of the A-factor receptor protein, ArpA, in *Streptomyces griseus*. When A-factor is absent, ArpA binds to the *adpA* promoter and represses the expression of AdpA, which is an activator of a regulon that consists of operons involved in mycelial differentiation and antibiotic production. The *arpA*-null mutants produced more streptomycin and formed aerial hyphae earlier than the wild-type strain did.[21–23] Recent microarray data have indicated a cross-regulation among disparate antibiotic biosynthetic pathways and even some backregulation from cluster-situated regulators to a "higher level" pleiotropic regulatory gene.[24] These studies showed that regulating antibiotic biosynthesis and mycelial differentiation is important for understanding the factors affecting antibiotic yield.

Among the many regulatory genes, *nsdA* was able to negatively control sporulation and antibiotic production, which was first found in *Streptomyces coelicolor* A3(2) in 2006.[25] Subsequent studies showed that *nsdA* is widely existent and conserved in *Streptomyces*, such as *S. hygroscopicus* 10～22, *S. spiecies* FR-008, *S. lividans* ZX64, *S. aureofaciens* 211, *S. albus* JA3453, *S. hygroscopicus* 5008, *S. avermitilis* NRRL8165 and *S. coelicolor* M145.[26] The disruption of chromosomal *nsdA* resulted in the overproduction of spores and three of four known *S. coelicolor* antibiotics of different chemical types.[26] It suggested that *nsdA* might have some general effects on antibiotic production. However, the function of *nsdA* was less investigated.

The S. bingchengensis used in this study was isolated from soil samples collected from Harbin, China. As a novel strain, *S. bingchengensis* produces at least two kinds of antibiotics, the polyether nanchangmycin and macrolide compound milbemycins, A_3 and A_4, (Figure 1). In addition, it also generates new milbemycins, β_{13}, β_{14}, α_{28}, α_{29} α_{30}, and two new seco-milbemycins.[27–29] The mixture of milbemycins A_3 and A_4 was marketed as an acaricide for the control of mites in 1990.[30] Subsequently, in animal health fields, 5-oxime derivatives of milbemycins, A_3 and A_4, were found to be highly effective as anthelmintics and were marketed. However, nanchangmycin is an antibiotic that affects cation transport, and is effective in

[1]School of Life Science, Northeast Agricultural University, Harbin, China and [2]State Key Laboratory of Uraban Resource and Environment, Harbin Institute of Technology, Harbin, China
Correspondence: Professor W-S Xiang, School of Life Science, Northeast Agricultural University, Harbin 150030, China.
E-mail: xiangwensheng@yahoo.com.cn
Received 22 December 2008; revised 8 April 2009; accepted 14 April 2009; published online 15 May 2009

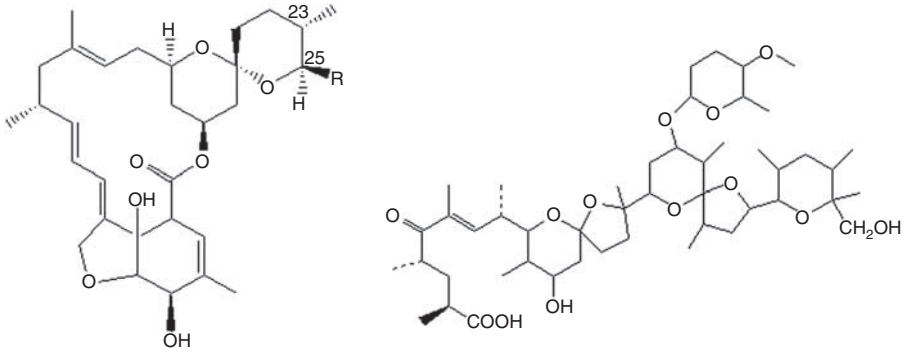

milbemycin A3, R=methyl
milbemycin A4, R=ethyl

Nangchangmycin

Figure 1 The structures of milbemycins, A3 and A4, and nanchangmycin.

treating coccidiosis in chickens.[31] The identification of new genes that regulate antibiotic biosynthesis and mycelial differentiation is important for understanding the factors affecting antibiotic yield. In this study, we report the identification of a new gene, *nsdA*, negatively affecting both processes. In light of our results, we propose a novel view of improving the output of milbemycins and nanchangmycin in *S. bingchengensis*.

MATERIALS AND METHODS

Microorganisms, cloning vectors and cultivation

For routine subcloning, *Eschericha coli* DH5α was cultivated and transformed according to the method of Sambrook *et al*.[32] ET12567 was used to propagate unmethylated DNA for introduction into *Streptomyces bingchengensis*_226541 by transformation or conjugation. *E. coli* BW25113/pIJ790 (gifts from Professor Andrew Hesketh) was the host for λRED-mediated PCR-targeting mutagenesis. pIJ773 was used as the template for the amplification of a disruption cassette containing the apramycin resistance gene, *aac(3)IV,* and the RK2 origin of transfer (*oriT*), flanked by recognition sites for FLP recombinase.[33] *E. coli–Streptomyces* shuttle plasmid, pHZ1358 (provided by Dr Yinghua Zheng), was used to construct the *nsdA* gene-replacement vector. pIJ8600, which integrated into the *S. bingchengensis*_226541 chromosome by site-specific recombination at the bacteriophage ΦC31 attachment site, *attB*,[34,35] was used to introduce single copies of genes into the *S. bingchengensis*_226541 chromosome.

S. bingchengensis was isolated from soil samples collected in Harbin, China. *S. bingchengensis* has been stored at the China General Microbiology Culture Collection Center (accession no.: CGMCC1734), and the 16S rDNA sequence was determined (accession no.: DQ449953 in National Center for Biological Information). Several *Streptomyces* media were used. MS agar[36] was used to make spore suspensions and for plating-out conjugations with *E. coli* ET12567 containing the RP4 derivative, pUZ8002.[37] R2YE was used for protoplast transformation.[36] Yeast extract–malt extract was a liquid medium.[36] All *Streptomyces* cultivations were carried out at 30 °C.

Genetic procedures

Standard genetic procedures with *E. coli* and *in vitro* DNA manipulations were carried out as described by Sambrook *et al*.[32] Recombinant DNA manipulations in the *Streptomyces* species and isolation of genomic DNA were performed as described by Kieser *et al*.[36] DNA restriction and modifying enzymes were used as recommended by the manufacturers (BRL, Carlsbad, CA, USA and Takara Biotechnology Ltd Company, Dalian, China). DNA fragments were purified from agarose gels with the Geneclean kit II (BIO101, Beijing, China).

DNA sequencing and analysis

Primers were designed by using the data obtained from the *S. coelicolor* and *S. avermitilis* genome sequences.[25] Total DNA was isolated from *S. bingchengensis*_226541,[36] and a DNA fragment containing a coding region for the *nsdA* was amplified with *nsdA* R (5′-CCTCGGCGAAGATGTCCTCC-3′) and *nsdA* L (5′-TCTCCGTCGAGGACCTGGGC-3′) primers. The amplified fragment was ligated into a pMD18-T vector to obtain the recombinant plasmid, pBC106. Then, *nsdA* was subcloned into the *Bgl*II site of an *E. coli–Streptomyces* shuttle plasmid, pHZ1358, to obtain pBC118, with *nsdA* 2L (5′-TCGAGATCTG TACGCGGGGATC-3′, wherein underlined letters indicate restriction sites) and *nsdA* 2R (5′-GCATGCCTGCAGATCTACGATC-3′). Thereafter, pBC118 was used as a template for the following PCR mutagenesis experiments. Subclone sequencing was performed by Takara Biotechnology Ltd Company. DNA and deduced protein sequences were analyzed using publicly available programs at the following websites: http://www.ncbi.nlm.nih.gov/blast/, http://watson.nih.go.jp/~jun/cgi-bin/frameplot-3.0b.pl and http://motif.genome.jp/.

nsdA replacement and verification

The *nsdA* gene replacement vector was constructed by λRED-mediated PCR-targeting mutagenesis.[33,38] Two PCR primers, BC-*nsdA*-F and BC-*nsdA*-R, corresponding to the regions upstream and downstream of the *nsdA* coding region (underlined), respectively, were used to amplify *aac(3)*IV+*ori*T from pIJ773.

BC-*nsdA*-F: 5′-CCGCCGCGGCTTCCTCGGCACCTCGCTCGCGCTCTCC GCATTCCGGGGATCCGTCGACC-3′

BC-*nsdA*-R: 5′-GCGAAGGTGTCCTCGGCCATCCGCACGGCCCGCTTG CACTGTAGGCTGGAGCTGCTTC-3′

The amplified fragment was used to replace the *nsdA* in pBC118. The resulting plasmid, named pBC929, was verified by PCR and restriction analysis, and then passed through the non-methylating *E. coli* ET12567/pUZ8002 before reintroduction into *S. bingchengensis*_226541 by conjugation. The gene mutant was verified by PCR analysis.

In the complementation experiments, the intact *nsdA* fragments were amplified by the primers, P3 (5′-GAAGATCTCCTCGTTACCTCCATCAC-3′, where underlined letters indicate restriction sites) and P4 (5′-GAAGATCT TCTGCACGCTGTCGGCCT-3′), and then inserted into the *Bam*HI site of pIJ8600 to give pJC3. The resulting vectors were introduced into the *nsdA* disruption mutant.

Fermentation and analysis of antibiotic production

The seed for preculture was spores. The medium for sporulation contained sucrose 4.0 g, yeast extract 2.0 g, malt extract 5.0 g and skimmed milk powder 1.0 g in 1 l water. The pH was adjusted to 7.0 with 1 M NaOH, 20 g of agar was added and this mixture was sterilized at 121 °C for 30 min. The spore suspension was prepared from agar plates incubated at 28 °C for 7–8 days.

A spore suspension of the culture of *S. bingchengensis,* 1.0 ml, was transferred to a 250-ml Erlenmeyer flask that contained 25 ml of the seed medium comprising sucrose 0.25 g, polypeptone 0.1 g and K_2HPO_4 1.25 mg. The

inoculated flasks were incubated at 28 °C for 42 h on a rotary shaker at 250 r.p.m. Then, 8.0 ml of the culture was transferred into 1-l Erlenmeyer flasks containing 100 ml of the fermentation medium consisting of sucrose 8.0%, soybean powder 1.0%, yeast extract 0.2%, meat extract 0.1%, $CaCO_3$ 0.3%, K_2HPO_4 0.03%, $MgSO_4{\cdot}7H_2O$ 0.1% and $FeSO_4{\cdot}7H_2O$ 0.005%. The medium pH was 7.2 before sterilization. Fermentation was carried out at 28 °C for 8 days on a rotary shaker at 250 r.p.m.[27,28,29]

To analyze milbemycin A4 and nanchangmycin titer, the samples were collected from fermentation flasks and processed for milbemycin extraction by mixing one volume of the whole culture with five volumes of ethanol and sonicated at room temperature for 30 min. The samples were centrifuged at 3250 *g* for 10 min and the supernatant was analyzed by HPLC using a 5-μl particle size NOVA-PAK (Waters, Milford, MA, USA) column (3.9×150 mm) eluted at a flow rate of 1.5 ml min^{-1} with a 15-min linear gradient from 0 to 90% (V/V) of phase B. Phase A was MeCN-H_2O-MeOH (350:50:100, V/V/V) and phase B was MeOH. Chromatography was performed with a SHIMADZU LC-2010CHT HPLC system (Shimadzu Corporation, Kyoto, Japan) and detection was at 242 nm. As standard for antibiotic titer determination, a sample of milbemycin A4 (100 μg ml^{-1}) and nanchangmycin (200 μg ml^{-1}) was used. The peak positions for milbemycin A4 and nanchangmycin were determined compared with those for the standard compounds.

RESULTS

DNA sequencing and analysis

The nucleotide sequence of the 1.5-kb DNA fragment was amplified by PCR. Sequence analysis showed that the 1485-bp DNA fragment encoded a 494-amino-acid protein (GenBank EU779992), which shared 89.89% identity in the nucleotide sequence and 97.82% similarity at the amino-acid level compared with those of *S. coelicolor* (Table 1).

Replacement of *nsdA* gene

To understand the function of *nsdA*, the gene replacement vector, pBC929, was constructed using λRED-mediated PCR-targeting mutagenesis,[33] and then conjugated into *S. bingchengensis*_226541. The mutant strains were selected using apramycin and thiostrepton. Seven apramycin-resistant and thiostrepton-resistant (Am^RTsr^R) strains (named BC19) were obtained from conjugation plates, indicating the single cross-over events. Three apramycin-resistant and thiostrepton-sensitive (Am^RTsr^S) strains (named BC29) were obtained from conjugation plates, implying the loss of the plasmid by a second homologous recombination. Gene replacement events were confirmed by PCR using the *nsdA*2L-*nsdA*2R primers with genomic DNA from *S. bingchengensis*_226541 and gene disruptants. The expected 1.5-kb *nsdA* fragment was amplified from the *S. bingchengensis*_226541 genome by PCR. The PCR products from the double-cross-over recombination mutant, BC29, were larger than those from the ancestral strain by about 0.5 kb in size. However, the single-cross-over recombination mutant, BC19, has both 1.5- and 2-kb gene fragments. These results showed that the *nsdA* was replaced precisely by an *oriT+aac(3)* IV in the homologous double-cross-over recombination mutant.

Phenotype of *nsdA* disruption mutant

The *nsdA* disruption mutant, BC29, was different from the ancestral strain in the rate and extent of sporulation. When cultured on an MS medium, the mutant BC29 began to produce a yellow pigment at 36 h, which was about 24 h earlier than that by *S. bingchengensis*_226541. The *nsdA* disruption mutant, BC29, gave rise to abundant gray spores grown for 72 h, whereas the ancestral strain produced white aerial hyphae at this time. Both pigment amounts and eventual sporulation levels in the mutant BC29 seemed to be greater than those of the ancestral strain (Figure 2). When we plated out diluted spores harvested from colonies on the MS medium grown for 10 days and counted the colony, BC29 spore suspensions reproducibly formed about twice as many colonies as did *S. bingchengensis*_226541.

All the phenotypic changes of the *nsdA* disruption mutant, BC29, were complemented by introducing pJC3, excluding potential polar effects on adjacent genes or an additional mutation in BC29 as alternative explanations. These results suggested that *nsdA* played a negative role in *S. bingchengensis*_226541 morphological differentiation.

Enhanced production of two antibiotics in *nsdA* disruption mutant

HPLC assays on the *nsdA* disruption mutant, BC29, revealed that disruption of *nsdA* remarkably increased antibiotic production. Milbemycin A_4 production increased from 670 to 1005 μg ml^{-1}, whereas nanchangmycin production improved from 230 to 2070 μg ml^{-1}. The yield of milbemycin A_4 and nanchangmycin increased by 1.5- and 9-fold, respectively (Figure 3). The change of milbemycin and nanchangmycin production was reversed to the ancestral level by the introduction of *nsdA* back into BC29 (data not shown), excluding potential polar effects on adjacent genes as an explanation. It inferred that *nsdA* had repressed the production of milbemycins and nanchangmycin by *S. bingchengensis*_226541.

DISCUSSION

In this paper, *nsdA* in *S. bingchengensis*_226541 was identified, which encoded a 483-amino-acid protein that shared a 97.82% sequence identity with the NsdA of *S. coelicolor*. Blast searching indicated that there was an ortholog with sequence identity over 80% to each of these NsdA ortholog proteins in *Streptomyces*. NsdA contained a conserved domain, DUF921, which was defined as a *Streptomyces* protein domain of unknown function. Proteins containing the

Table 1 Comparison of *nsdA* homologous genes of different *Streptomyces*

	GenBank accession numbers	*Length of gene/protein (bp/amino acid)*	*Similarity with* nsdA *of* S. bingchengensis_226541	
			Amino acid	*Nucleotide*
Streptomyces bingchengensis_226541	EU779992	1450/494	100%	100%
S. avermitilis MA-4680	SAV2652	1476/491	83.93%	83.33%
S. lividans ZX64	DQ478681	1503/500	97.82%	89.77%
S. qingfengmyceticus A553	DQ478680	1503/500	75.00%	76.13%
S. coelicolor M145	EU779992	1450/483	97.82%	89.89%
S. hygroscopicus 5008	DQ478679	1527/508	86.11%	84.15%
S. albus JA3453	DQ478678	1473/490	81.94%	82.06%
S. spiecies FR-008	DQ478677	1485/494	71.23%	79.39%

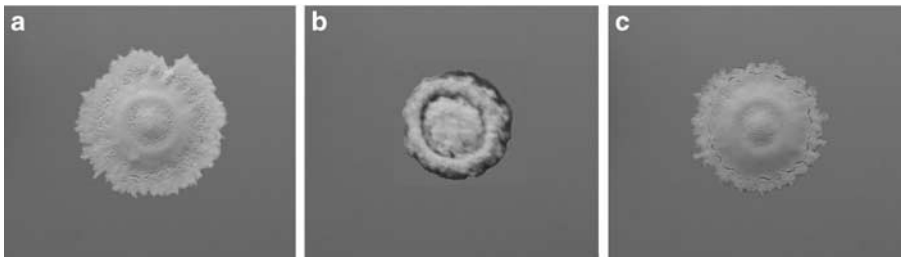

Figure 2 (**a**–**c**) The effect of *nsdA* disruption on morphological differentiation grown for 72 h. (**a**) *S. bingchengensis*_226541: ancestral strain; (**b**) BC29: *nsdA* disruption mutant in which *nsdA* was replaced by an *oriT+aac(3)IV* cassette; (**c**) BC29 complemented by pJC3 (a pIJ8600-derived plasmid containing *nsdA*).

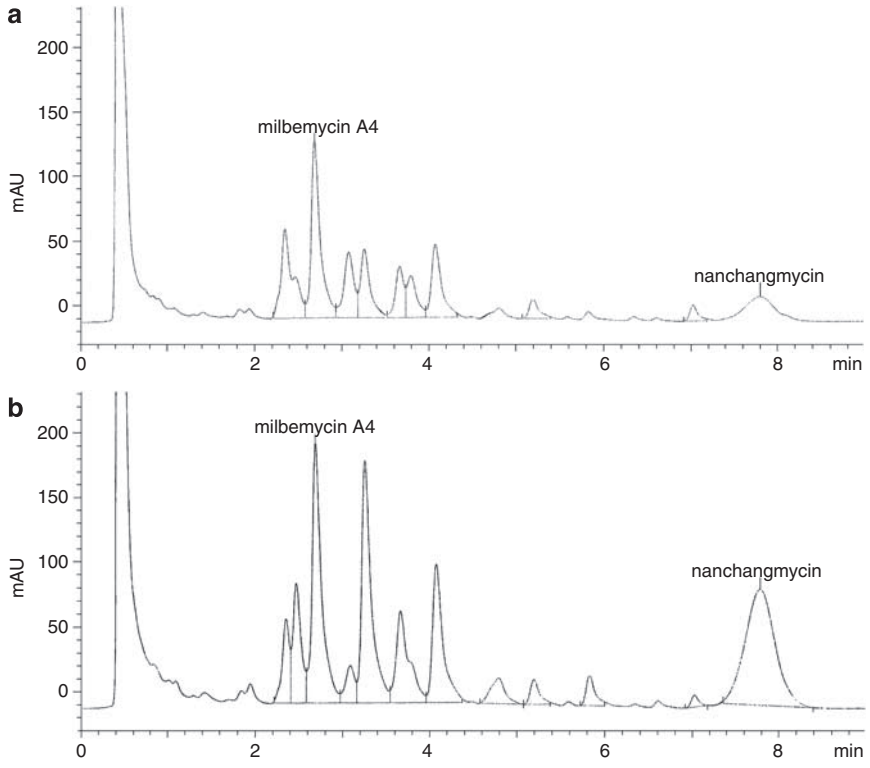

Figure 3 HPLC analysis of milbemycin A_4 and nanchangmycin in (**a**) ancestral strain *Streptomyces bingchengensis*_226541 and (**b**) *nsdA* disruption mutant, BC29.

DUF921 domain included several putative regulatory proteins from *S. coelicolor* and *S. griseus*.[39] A search in the superfamily server also revealed that NsdA and other homologous proteins in *Streptomyces* had tetratricopeptide repeat-like repeats,[40] which mediated protein–protein interactions.[41] We are currently using an *E. coli* two-hybrid system to seek NsdA-interacting proteins. The disruption of the *SCO4114* homologous gene, which had earlier been shown to prevent premature sporulation septation of *S. griseus*, had no obvious phenotypic effects on *S. bingchengensis* (data not shown). Possibly, there are differences in the manner deployed in the two species.

nsdA negatively affects both antibiotic biosynthesis and mycelial differentiation. The repressing effect was obvious even when the *nsdA* gene was disrupted. Gene disruption mutant, BC29, showed abundant gray spores in contrast to the white phenotype of the ancestral strain, and markedly increased the yield of milbemycin A_4 and nanchangmycin. In view of the fact that the structures of milbemycin A_4 and nanchangmycin are quite unlike each other, this result suggested that *nsdA* might have some general effects on secondary metabolism. As the disruption of chromosomal *nsdA* resulted in higher productions of Act, CDA, Mmy and spores in *S. coelicolor*, *actII-orf4* mRNA was increased in an *nsdA* mutant, suggesting that the negative effect of *nsdA* on Act biosynthesis was exerted at the level of transcription of the pathway-specific activator gene.[25,42] Although the genomic library of *S. bingchengensis* is under way, the new transcription factors, including pathway-specific regulators of milbemycin A_4 and nanchangmycin biosynthesis cluster, will be identified, which may be correlated with *nsdA*, suppressing antibiotic production. The elucidation of correlations between *nsdA* and its corresponding factors could be helpful in enhancing antibiotic yield.

ACKNOWLEDGEMENTS

We are very grateful to Professor Andrew Hesketh (John Innes Centre, Norwich, UK) and Dr Yinghua Zheng (State Key Laboratory of Agricultural Microbiology, Huazhong Agricultural University, China) for their gifts and

helpful suggestions. This study was supported by the National Key Technology R&D Program (no. 2006BAD31B02), the Program for New Century Excellent Talents in University, the Outstanding Youth Foundation of Heilongjiang Province (no. JC200706) and the China Postdoctoral Science Foundation-funded project (no. 20070410274).

1 Baltz, R. H. Renaissance in antibacterial discovery from actinomycetes. *Curr. Opin. Phamacol.* **8,** 557–563 (2008).
2 Bibb, M. J. Regulation of secondary metabolism in *Streptomycetes*. *Curr. Opin. Microbiol.* **8,** 208–215 (2005).
3 Bibb, M. The regulation of antibiotic production in *Streptomyces coelicolor* A3(2). *Microbiology* **142,** 1335–1344 (1996).
4 Fernández-Moreno, M. A., Caballero, J. L., Hopwood, D. A. & Malpartida, F. The act cluster contains regulatory and antibiotic export genes, direct targets for translational control by the *bldA* tRNA gene of *Streptomyces*. *Cell* **66,** 769–780 (1991).
5 Eccleston, M., Ali, R. A., Seyler, R., Westpheling, J. & Nodwell, J. Structural and genetic analysis of the BldB protein of *Streptomyces coelicolor*. *J. Bacteriol.* **184,** 4270–4276 (2002).
6 Elliot, M., Damji, F., Passantino, R., Chater, K. & Leskiw, B. The *bldD* gene of *Streptomyces coelicolor* A3(2): a regulatory gene involved in morphogenesis and antibiotic production. *J. Bacteriol.* **180,** 1549–1555 (1998).
7 Bignell, D. R., Warawa, J. L., Strap, J. L., Chater, K. F. & Leskiw, B. K. Study of the *bldG* locus suggests that an anti-anti-sigma factor and an anti-sigma factor may be involved in *Streptomyces coelicolor* antibiotic production and sporulation. *Microbiology* **146,** 2161–2173 (2000).
8 Chater, K. F. Genetics of differentiation in *Streptomyces*. *Annu. Rev. Microbiol.* **47,** 685–713 (1993).
9 Chater, K. F. Regulation of sporulation in *Streptomyces coelicolor* A3(2): a checkpoint multiplex? *Curr. Opin. Microbiol.* **4,** 667–673 (2001).
10 Horinouchi, S., Hara, O. & Beppu, T. Cloning of a pleiotropic gene that positively controls biosynthesis of A-factor, actinorhodin, and prodigiosin in *Streptomyces coelicolor* A3(2) and *Streptomyces lividans*. *J. Bacteriol.* **155,** 1238–1248 (1983).
11 Fernández-Moreno, M. A. *et al*. *abaA*, a new pleiotropic regulatory locus for antibiotic production in *Streptomyces coelicolor*. *J. Bacteriol.* **174,** 2958–2967 (1992).
12 Champness, W., Riggle, P., Adamidis, T. & Vandervere, P. Identification of *Streptomyces coelicolor* genes involved in regulation of antibiotic synthesis. *Gene* **115,** 55–60 (1992).
13 Horinouchi, S. & Beppu, T. Regulation of secondary metabolism and cell differentiation in *Streptomyces*: A-factor as a microbial hormone and the AfsR protein as a component of a two-component regulatory system. *Gene* **115,** 167–172 (1992).
14 Matsumoto, A., Hong, S. K., Ishizuka, H., Horinouchi, S. & Beppu, T. Phosphorylation of the AfsR protein involved in secondary metabolism in *Streptomyces* species by a eukaryotic-type protein kinase. *Gene* **146,** 47–56 (1994).
15 Liu, J. M. & Yang, K. Q. Functional analyses of TcrA-a TPRcontaining regulatory protein in *Streptomyces coelicolor* A3(2). *Acta Microbiol. Sin.* **46,** 33–37 (2006).
16 Ishizuka, H., Horinouchi, S., Kieser, H. M., Hopwood, D. A. & Beppu, T. A putative two-component regulatory system involved in secondary metabolism in *Streptomyces spp*. *J. Bacteriol.* **174,** 7585–7594 (1992).
17 Anderson, T. B., Brian, P. & Champness, W. C. Genetic and transcriptional analysis of *absA*, an antibiotic gene cluster-linked two-component system that regulates multiple antibiotics in *Streptomyces coelicolor*. *Mol. Microbiol.* **39,** 553–566 (2001).
18 Ryding, N. J., Anderson, T. B. & Champness, W. C. Regulation of the *Streptomyces coelicolor* calcium-dependent antibiotic by *absA*, encoding a cluster-linked two-component system. *J. Bacteriol.* **184,** 794–805 (2002).
19 Chang, H. M., Chen, M. Y., Shieh, Y. T., Bibb, M. J. & Chen, C. W. The *cutRS* signal transduction system of *Streptomyces lividans* represses the biosynthesis of the polyketide antibiotic actinorhodin. *Mol. Microbiol.* **21,** 1075–1085 (1996).
20 Sola-Landa, A., Moura, R. S. & Martin, J. F. The two-component PhoR-PhoP system controls both primary metabolism and secondary metabolite biosynthesis in *Streptomyces lividans*. *Proc. Natl Acad. Sci. USA* **100,** 6133–6138 (2003).
21 Onaka, H. *et al*. Cloning and characterization of the A-factor receptor gene from *Streptomyces griseus*. *J. Bacteriol.* **177,** 6083–6092 (1995).
22 Ohnishi, Y., Yamazaki, H., Kato, J. Y., Tomono, A. & Horinouchi, S. AdpA, a central transcriptional regulator in the A-factor regulatory cascade that leads to morphological development and secondary metabolism in *Streptomyces griseus*. *Biosci. Biotechnol. Biochem.* **69,** 431–439 (2005).
23 Tomono, A., Tsai, Y., Ohnishi, Y. & Horinouchi, S. Three chymotrypsin genes are members of the AdpA regulon in the A-factor regulatory cascade in *Streptomyces griseus*. *J. Bacteriol.* **187,** 6341–6353 (2005).
24 Huang, J. Q. *et al*. Cross regulation among disparate antibiotic biosynthetic pathways of *Streptomyces coelicolor*. *Mol. Microbiol.* **58,** 1276–1287 (2005).
25 Li, W. C. *et al*. Identification of a gene negatively affecting antibiotic production and morphological differentiation in *Streptomyces coelicolor* A3(2). *J. Bacteriol.* **188,** 8368–8375 (2006).
26 Yu, Z., Wang, Q., Deng, Z. X. & Tao, M. F. Activation of silent antibiotic synthesis in *Streptomyces lividans* by disruption of a negative regulator *nsdA*, a gene conserved in *Streptomyces*. *Chin. J. Biotechnol.* **22,** 751–762 (2006).
27 Xiang, W. S., Wang, J. D., Wang, X. J. & Zhang, J. Two new â-class milbemycins from *Streptomyces bingchenggensis*: fermentation, isolation, structure elucidation and biological properties. *J. Antibiot.* **60,** 351–356 (2007).
28 Xiang, W. S., Wang, J. D., Wang, X. J., Zhang, J. & Wang, Z. Further new milbemycin antibiotics from *Streptomyces bingchenggensis*. *J. Antibiot.* **60,** 608–613 (2007).
29 Xiang, W. S., Wang, J. D., Fan, H. M., Wang, X. J. & Zhang, J. New seco-milbemycins from *Streptomyces bingchenggensis*: fermentation, isolation and structure elucidation. *J. Antibiot.* **61** (1), 27–32 (2008).
30 Ide, J. *et al*. Milbemycin: discovery and development. *Annu. Rep. Sankyo Res. Lab.* **45,** 1–98 (1993).
31 Liu, T. *et al*. Identification of NanE as the thioesterase for polyether chain release in nanchangmycin biosynthesis. *Chem. Biol.* **13** (9), 945–955 (2006).
32 Sambrook, J., Fritsch, E. F. & Maniatis, T. *Molecular Cloning: A Laboratory Manual* 2nd ed. Cold Spring Harbor Laboratory Press: New York (1989).
33 Gust, B., Challis, G. L., Fowler, K., Kieser, T. & Chater, K. F. PCR-targeted *Streptomyces* gene replacement identifies a protein domain needed for biosynthesis of the sesquiterpene soil odor geosmin. *Proc. Natl Acad. Sci. USA* **100,** 1541–1546 (2003).
34 Sun, J., Kelemen, G. H., Fernandez-Abalos, J. M. & Bibb, M. J. Green fluorescent protein as a reporter for spatial and temporal gene expression in *Streptomyces coelicolor* A3(2). *Microbiology* **145,** 2221–2227 (1999).
35 Kuhstoss, S. & Rao, R. N. Analysis of the integration function of the streptomycete bacteriophage ΦC31. *J. Mol. Biol.* **222,** 897–908 (1991).
36 Kieser, T., Bibb, M. J., Buttner, M. J., Chater, K. F. & Hopwood, D. A. *Practical Streptomyces Genetics* 2nd ed. The John Innes Foundation: Norwich (2000).
37 Flett, F., Mersinias, V. & Smith, C. P. High efficiency intergeneric conjugal transfer of plasmid DNA from *Escherichia coli* to methyl DNA restricting *Streptomycetes*. *FEMS Microbiol. Lett.* **155,** 223–229 (1997).
38 Gust, B., Kieser, T. & Chater, K. F. *PCR Targeting System in Streptomyces coelicolor A3 (2),* The John Innes Foundation: UK, (2002).
39 Marchler-Bauer, A. *et al*. CDD: a curated Entrez database of conserved domain alignments. *Nucleic Acids Res.* **31,** 383–387 (2003).
40 Zhang, L., Li, W. C., Zhao, C. H., Chater, K. F. & Tao, M. F. NsdB, a TPR-like-domain-containing protein negatively affecting production of antibiotic s in *Streptomyce coelicolor* A3(2). *Acta Microbiol. Sin.* **47,** 849–854 (2007).
41 D'Andrea, L. D. & Regan, L. TPR proteins: the versatile helix. *Trends Biochem. Sci.* **28,** 655–662 (2003).
42 Uguru, G. C. *et al*. Transcriptional activation of the pathway-specific regulator of the actinorhodin biosynthetic genes in *Streptomyces coelicolor*. *Mol. Microbiol.* **58,** 131–150 (2005).

The Journal of Antibiotics (2009) 62, 315–318

www.nature.com/ja

ORIGINAL ARTICLE

A cell-based screening system for detection of inhibitors toward mycobacterial cell wall core

Peng Gao, Yan Guan, Danqing Song and Chunling Xiao

Mycobacterium tuberculosis **and nonpathogenic bacteria,** ***Corynebacterium glutamicum,*** **possess a common and unusual cell wall architecture. A cell-based screening system was designed to identify novel compounds interacting with the synthesis, assembly or regulation of the** ***M. tuberculosis*** **cell wall.** ***C. glutamicum*** **was tested in a paired medium assay in 96-well plates with natural product extracts and pure chemical compounds in the presence and absence of the osmotic stabilizer, sorbitol and some ions. Growth was visually examined over a 12-h period and detected with a microplate reader for absorbance at 544 nm. Screening hits from the osmotic stabilizer rescue were then examined by mycolic acid analysis to confirm the effect on cell wall integrity.**
The Journal of Antibiotics (2009) **62,** 315–318; doi:10.1038/ja.2009.34; published online 15 May 2009

Keywords: cell wall core; *Corynebacterium glutamicum*; *Mycobacterium tuberculosis*; mycolic acid; screening system

INTRODUCTION

The cell wall is crucial for the survival of *Mycobacterium tuberculosis*. Enzymes related to the process of biosynthesis, assembly and regulation of cell wall are particularly good molecular targets, because there are no homologs in the mammalian system.[1] *M. tuberculosis* and nonpathogenic bacteria, *Corynebacterium glutamicum,* share a common and unusual cell wall architecture.[2] The cell wall core consists of a peptidoglycan layer and a lipid mycolic acid layer that are connected by the polysaccharide, arabinogalactan.[1] The *C. glutamicum* is a more convenient and representative test strain than are mycobacteria because of its short growth cycle, its nonpathogenicity and similar cell wall architecture to *M. tuberculosis*. *M. smegmatis* has been preferred in the past as the screening organism, as it is a species related to *M. tuberculosis*. However, the mutant of key cell wall biosynthetic enzymes cannot be conducted and therefore this organism is not a reliable screening organism.[2–5]

Inhibition of the key enzymes involved in the synthesis, assembly or regulation of the *M. tuberculosis* cell wall results in cell disruption and death of *M. tuberculosis* and *M. smegmatis*. However, in the case of the *C. glutamicum* inhibition of cell wall, biosynthetic enzymes result in slow growth and not in cell death.[2] The addition of an osmotic stabilizer can protect the cell from cell wall disruption.[2,6] Arabinofuranosyltransferase, coded by *AftB*, is involved in the terminal step of cell wall arabinan biosynthesis, which catalyzes the linkage of the last arabinose to arabinogalactan. In the mutant strain with the *aftB* mutant gene, mycolic acid cannot link with arabinogalactan and the mutant grows slower than does the wild type. The addition of sorbitol almost completely restores the growth of this mutant.[5]

To confirm the interaction between screening hits and cell wall targets and to differentiate these effects from other possibilities related to rescue from osmotic pressure lysis, we developed a simple method to analyze the change of cell wall. Although electron microscopy can show morphological changes better than the optical microscope, the electron micrograph is not compatible with high-throughput screening (HTS).[7] As mycolic acid is the outer layer of the cell wall,[5] mycolic acid analysis by TLC could show the change in cell wall and be conducted by HTS. In this report, we have successfully established an HTS system, using *C. glutamicum* as the test strain. Two of the inhibitors identified through screening were confirmed by mycolic acid analysis.

MATERIALS AND METHODS

Bacterial strains, growth conditions and antibiotics

Corynebacterium glutamicum ATCC 13032 (the wild-type strain, referred to simply as *C. glutamicum*) was purchased from the China Center of Industrial Culture Collection (CICC, Beijing, China), and was cultured in BHI (3.7% brain–heart infusion (Difco, Sparks, MD, USA)) and BHIS (3.7% brain–heart infusion, 10.92% sorbitol, 1% NaCl and 0.05% $MgSO_4$) at 30 °C. The mutant strain, *C. glutamicum* Δ*aftB*, was provided by Dr L Eggeling.[5] *M. smegmatis mc²155* was purchased from the China General Microbiological Culture Collection Center (CGMCC, Beijing, China), and was grown in medium no. 54 (1% tryptone, 0.5% malt extract, 0.5% yeast extract, 0.5% casein acid hydrolysate (Sigma, St Louis, MO, USA), 0.2% beef extract, 0.2% glycerol, 0.005% Tween 80 and 0.1% $MgSO_4$ $7H_2O$, pH 7.2) at 37 °C. Solid growth medium was prepared by the addition of 1.5% agar to the liquid medium.

The antibiotics used in this study are cephalothin, ethambutol (EMB), isoniazid, vancomycin, streptomycin, levofloxacin, rifampicin, actinomycin D,

Institute of Medicinal Biotechnology, Chinese Academy of Medical Sciences, Peking Union Medical College, Beijing, China
Correspondence: Professor CL Xiao, Key Lab, Institute of Medicinal Biotechnology, Chinese Academy of Medical Sciences, Peking Union Medical College, Tiantanxili 1, Chongwen District, Beijing 100050, China.
E-mail: xiaoimb@gmail.com
Received 6 January 2009; revised 14 April 2009; accepted 17 April 2009; published online 15 May 2009

lincomycin, tetracycline and D-cycloserine. All of them were purchased from National Institute for the Control of Pharmaceutical and Biological Products (Beijing, China) and dissolved in sterile water or DMSO, sterilized by filtration and diluted with sterile water.

Preparation of cells

Bacterial stock cultures were streaked on BHI agar plates and incubated overnight at 30 °C. A single colony from the plate was used to inoculate BHI, and was incubated for 12 h with shaking at 200 r.p.m. at 30 °C. When the cell density reached 4.5–5.5 OD at 600 nm, the culture was diluted to 3 OD at 600 nm and was stored at 4 °C as seed culture for screening. The growth curve and the inhibition of EMB-treated control were measured to obtain the optimal inoculum concentration and culture period.

Screening protocol

The screen was developed as a 96-well plate test. Except for the blank control, 180 µl of *C. glutamicum* culture (the medium with 0.3% inoculum from the seed culture) and 20 µl of test samples or controls to the final volume 200 µl were added to each well. Each plate contained 80 wells as the sample group, with 1 µg ml^{-1} of test compounds, and the remaining 16 wells were the control group, which included four wells with 1‰ DMSO (regular growth control), four wells with 180 µl BHI/BHIS medium and 1‰ DMSO (blank control), four wells with 1 µg ml^{-1} rifampicin (negative control) and four wells with 1 µg ml^{-1} EMB (positive control). The OD at 544 nm was measured after the plates were incubated at 12 h at 30 °C. The inhibition rate can be calculated as follows: Inhibition (%)=(OD of regular growth control−OD of sample)/(OD of regular growth control−OD of blank control)×100%.

The inhibition difference (Δinhibition) between the BHI medium and the BHIS medium was calculated as the screening factor.

$$\Delta\text{inhibition} = I_{\text{BHI}} - I_{\text{BHIS}}$$

I_{BHI}, the inhibition of samples/controls in BHI medium; I_{BHIS}, the inhibition of samples/controls in BHIS medium.

In the screening system, 1 µg ml^{-1} EMB and rifampicin were used as controls to monitor the reproducibility of the screen. When the Δinhibition of the EMB-treated sample was larger than 50% and the Δinhibition of rifampicin was smaller than 5%, the results were considered to be reliable.

Application of the screening system to known antibiotics and HTS assay

Different antibiotics with diverse targets were tested against *C. glutamicum* according to the screening protocol. The final concentration of known antibiotics and samples was 1 µg ml^{-1}. The screen was validated using the Δinhibition of positive and negative antibiotics with a known mode of action.

After screening the compound library and natural product extracts, the positive samples were added to the culture at the appropriate concentration to characterize the mycolic acid in methanol extracts of lysates.

The mycolic acid analysis

Corynebacterium glutamicum were harvested at an absorbance of 10–15 OD at 600 nm. The cultivation of *C. glutamicum* Δ*aftB* and wild type treated with positive samples required two precultures. First, a 5-ml BHIS culture was grown for 8 h, which was then inoculated with 50 ml BHIS and cultured for 15 h. It was then used to inoculate a 100 ml BHIS culture and grown to an absorbance of 1 OD at 600 nm. Each culture was harvested after reaching an absorbance of 3 OD at 600 nm.[2,5]

The cells were harvested, washed and freeze dried. The cells (100 mg) were extracted by adding 2 ml of methanol–toluene–oil of vitriol, 30:15:1 (v/v), for 18 h at 75 °C. After being cooled to room temperature, they were extracted by 2 ml petroleum ether. The supernatants were then injected into a NH_4HCO_3 column and washed with petroleum ether (2 ml), and the extract was centrifuged (3000 r.p.m., 10 min). After centrifugation, the clear supernatants were again dried and re-suspended in petroleum ether (100 µl). An aliquot (10 µl) from each strain was subjected to TLC using silica gel plates (5735 silica gel $60F_{254}$; Merck, Darmstadt, Germany), developed in petroleum ether/acetone (95:5, v/v) and charred using 10% sulphuric acid in ethanol at 100 °C to reveal corynomycolic acid methyl esters.[5,8]

MIC testing

In vitro activity (MICs) was determined by inoculating 5×10^5 cells per ml of *M. smegmatis* into medium no. 54 in 96-well plates. The final volume in each well was 100 µl. The MIC was defined as the minimum concentration resulting in a cell density less than 0.01 OD at 600 nm,[9] which corresponded to no visible growth, after incubating for 48 h at 37 °C.

RESULTS

Screening conditions

Inoculum concentrations. The sensitivity of the screen is dependent on the OD of the culture at the beginning. The growth curve of *C. glutamicum* (Figure 1a) shows that inoculum concentrations lower than 1% of the seed culture are optimal for observing significant differences between the density at stationary phase and the starting culture density. It was found that 12 h is sufficient for the growth period. In the BHI medium, 0.3% seed culture presented the most significant Δinhibition of *C. glutamicum* (Figure 1b). However, in the

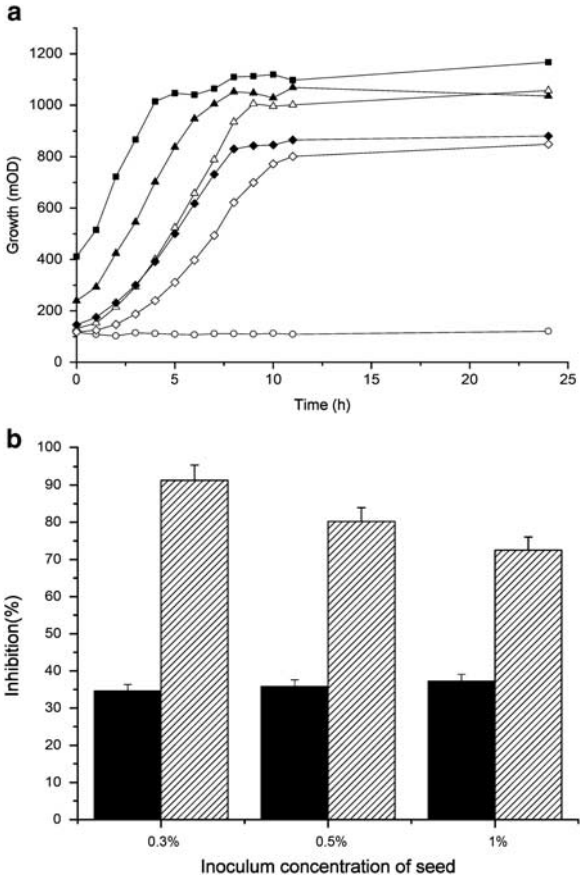

Figure 1 Growth curves of *C. glutamicum* in BHI medium and the inhibition by EMB of *C. glutamicum* grown in BHI and BHIS media, starting with different concentrations of seed inocula. The absorbance was detected with microplate reader at 544 nm. (**a**) Growth of *C. glutamicum* with different inoculum concentrations of seed: 5% (■), 1% (▲), 0.5% (△), 0.3% (◆), 0.1% (◇) and blank (○). (**b**) Effect of EMB at a concentration of 1 µg ml^{-1} on the growth of *C. glutamicum* in BHI and BHIS media started with different seed inocula concentrations. The black bar is the inhibition of *C. glutamicum* in the BHIS medium; the diagonal bar is that in the BHI medium.

Table 1 The inhibition of different target antibiotics to *Corynebacterium glutamicum* in both of the media

Antibiotics	*ΔInhibition (%)*[a]
Cephalothin	17.5 ± 2.23
EMB	56.5 ± 5.71
Isoniazid	—
Vancomycin	4.4 ± 1.33
Streptomycin	5.1 ± 1.02
Levofloxacin	4.9 ± 1.56
Rifampicin	2.0 ± 0.88
Actinomycin D	1.2 ± 0.80
Lincomycin	−0.5 ± 0.22
Tetracycline	2.7 ± 0.53
D-Cycloserine	13 ± 3.01[b]

Abbreviation: EMB, ethambutol.
[a]The Δinhibition test with compounds at 1 μg ml^{-1}.
[b]D-Cycloserine was tested at 10 μg ml^{-1}; —, without any inhibition.

BHIS medium, changing the inoculum concentration did not produce a measurable change of inhibition.

Selection of control drug concentrations: 1 μg ml^{-1} of EMB showed a large Δinhibition of 56.5 ± 5.71; higher concentrations of EMB, 10 and 100 μg ml^{-1}, yielded lower Δinhibitions of 22.8 ± 2.13 and 9 ± 0.87, respectively. These results obtained in the BHIS medium show that *C. glutamicum* cannot grow at higher EMB concentrations and no differential growth can be measured. Thus, 1 μg ml^{-1} was chosen as the concentration of compounds to be tested in the HTS assay.

Application of the screening system to known antibiotics

Using the method described in the screening protocol, we tested the inhibition of known antibiotics in *C. glutamicum*. According to the results (Table 1), two conclusions were reached. The results obtained with EMB, D-cycloserine and negative controls showed that the screening system was reliable. D-Cycloserine inhibited the growth of *C. glutamicum* at 10 μg ml^{-1}, and the inhibition (%) in the BHI medium was 55 ± 5.0. In the case of D-cycloserine, the activity against *C. glutamicum* was different from its activity against *M. tuberculosis* and *M. smegmatis* (MICs are 25 and 75 μg ml^{-1}, respectively). Streptomycin and tetracycline, which target the 30S subunit of the bacterial ribosome, and lincomycin, which targets the 50S subunit of the bacterial ribosome, showed a similar activity against *C. glutamicum* when tested in both media. Rifampicin and actinomycin D, which target the initial step of RNA synthesis and DNA replication, respectively, were negative in the screen and served as negative controls. Levofloxacin, which targets DNA gyrase subunit A, was also negative in the screen.

Some differences between *Corynebacterium* and *Mycobacterium* were noted. Cephalothin, which does not inhibit the growth of mycobacteria, was growth inhibitory in the assay, whereas isoniazid, which targets tuberculosis cell wall, did not have an effect on *Corynebacterium*.

Comparing the Δinhibition among the selected antibiotics, we chose 10% as the cutoff criteria for selecting positive samples. At the same time, the inhibition in the BHI medium showed larger than 50%.

The utilization of the screening system and further validation

The assay was used to screen a compound library with 1680 compounds. Fifteen compounds with mycobacteria inhibitory activity were found, and the hit rate was 0.9%.

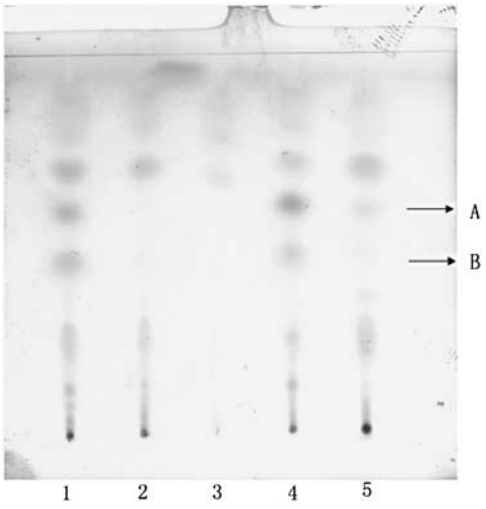

Figure 2 The TLC pattern of whole-cell mycolic acids in methanol lysates of *C. glutamicum*. The samples extracted from (1) *C. glutamicum* wild type; (2) *C. glutamicum* Δ*aftB*; (3) the control of EMB; (4) *C. glutamicum* wild type treated with compound 2008551; and (5) *C. glutamicum* wild type treated with compound 2009461. The spots: (A) α-mycolates, R_f=0.6; (B) keto-mycolates, R_f=0.45.

To confirm the interaction of the positive samples with the cell wall, we chose two of the hits and analyzed their effect on the cell wall mycolic acid content. We compared the mycolic acid in methanol extracts of lysates from wild type treated with screening hits with the mycolic acid present in the cell walls of the wild-type strain treated with EMB or the cell wall of the Δ*aftB* mutant, which is deficient of mycolic acid. EMB is known to target the assembly of arabinogalactan.[7] The cell wall of mutant and EMB-treated wild-type organisms lacks α-mycolates and/or keto-mycolates (Figure 2). A similar pattern, that is, a loss of mycolic acids, was noted in one of the hit compound (compound 2009461 but not compound 2008551)-treated cell walls, suggesting that the components of cell wall may be the target for at least one of the hits, and showing that screen could be reliable to find cell wall inhibitors. The compound, 2009461 (Figure 3a), is erythromycin A 11, 12-cyclic carbonate, which is mainly known to target protein biosynthesis, whereas our study indicates that it has an effect on cell wall biosynthesis (Figure 3b). The inhibition of *C. glutamicum* in BHI and BHIS media by EMB, rifampicin and a screening sample, 2009461, indicates that because compound 200946 has other effects, BHIS medium could not complement the growth of *C. glutamicum* treated with compound 2009461 as well, as was seen with EMB. The MICs obtained with compound 2009461 and EMB against *M. smegmatis* were 0.4 and 0.8 μg ml^{-1}, respectively. The specific enzyme targets of the hits are still being determined.

DISCUSSION

In this study, we established a screening system on the basis of differential growth rates of *C. glutamicum* in two growth media. Through this screening system, we could identify hits targeting the synthesis, assembly or regulation of cell wall core biosynthesis, which is dependent on unknown key enzymes. The screening system incorporated the ability to exclude false-positive hits that have clouded other molecular-based screening systems. Being a cell-based system, the screen has the advantage of identifying only those compounds that are active in whole cells.

Furthermore, although *C. glutamicum* and *M. tuberculosis* have a common cell wall architecture, there are differences between them.

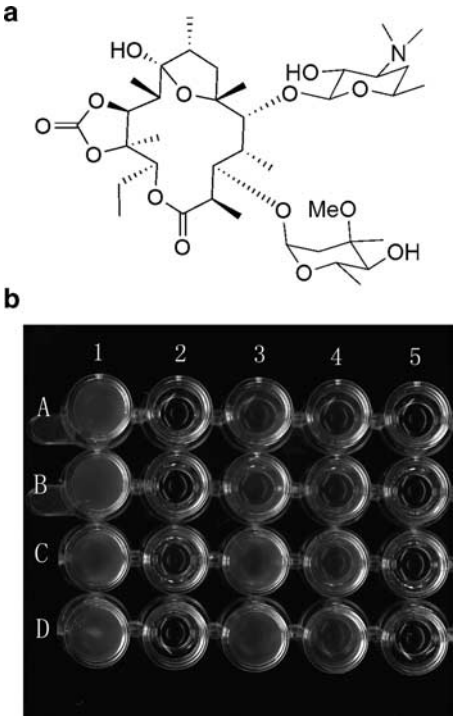

Figure 3 The structure of 2009461 and the inhibition of *C. glutamicum* by EMB, 2009461 and rifampicin grown in BHI and BHIS media. (**a**) The structure of 2009461, which is erythromycin A 11, 12-cyclic carbonate. (**b**) The compounds were all used at 1 μg ml^{-1}. Lines A and B: BHI medium; lines C and D: BHIS medium. (1) *C. glutamicum* grown with 20 μl of 1% DMSO; (2) blank medium with 20 μl of 1% DMSO; (3) growth system with 20 μl EMB; (4) growth system with 20 μl 2009461; and (5) growth system with 20 μl rifampicin.

C. glutamicum is more sensitive to antibiotics than is tuberculosis. Therefore, we needed to test the antimycobacterial activity of positive samples using *M. smegmatis* and *M. tuberculosis*. Isoniazid is a prodrug,[10] and the BLAST analysis indicated that *C. glutamicum* does not have the KatG gene, which has been proposed to activate isoniazid. Nonetheless, we choose *C. glutamicum* as the test strain because of its short growth period and the convenience for further study in mutant organisms that are available, such as *embAB*,[4] *aftA*[2] and *aftB*,[5] which are unavailable in *M. smegmatis*.

It was noted that during screening, when the Δinhibition was smaller than 10% and the inhibition was larger than 90%, the samples should be diluted to 1/10 of the former concentration and re-tested. If the results after being diluted are larger than 10%, they could be positive samples.

In addition, the compounds identified from this screening system may target any key enzymes related to the cell wall. The specific target still needed further experimentation. Compounds that target proteins related to protecting the cell from osmotic pressure may also be identified as positive. These hits were eliminated by an analysis of mycolic acid in methanol extracts. Further verification of hits will be essential using mutant construction and enzyme expression.

ACKNOWLEDGEMENTS

We thank L Eggeling for providing the mutant strain. This research was supported by National Natural Science Foundation of China (NSFC), and the project number is 30873186.

1 Barryl, C. E., Crick, D. C. & McNeil, M. R. Targeting the formation of the cell wall core of *M. tuberculosis*. *Infect. Disord. Drug Targets* **7,** 182–202 (2007).
2 Alderwick, L. J., Seidel, M., Sahm, H., Besra, G. S. & Eggeling, L. Identification of a novel Arabinofuranosyltransferase (AftA) involved in cell wall Arabinan biosynthesis in *Mycobacterium tuberculosis*. *J. Biol. Chem.* **281,** 15653–15661 (2006).
3 Berg, S., Kaur, D., Jackson, M. & Brennan, P. J. The glycosyltransferases of mycobacterium tuberculosis; roles in the synthesis of arabinogalactan, lipoarabinomannan, and other glycoconjugates. *Glycobiology* **17,** 35–56R (2007).
4 Alderwick, L. J. *et al.* Deletion of Cg-emb in corynebacterianeae leads to a novel truncated cell wall arabinogalactan, whereas inactivation of Cg-ubiA results in an arabinan-deficient mutant with a cell wall galactan core. *J. Biol. Chem.* **280,** 32362–32371 (2005).
5 Seidel, M. *et al.* Identification of a novel arabinofuranosyltransferase AftB involved in a terminal step of cell wall arabinan biosynthesis in Corynebacterianeae, such as *Corynebacterium glutamicum* and *Mycobacterium tuberculosis*. *J. Biol. Chem.* **282,** 14729–14740 (2007).
6 Frost, D. J., Brandt, K. D., Cugier, D. & Goldman, R. A whole-cell *Candida albicans* assay for the detection of inhibitors towards fungal cell wall synthesis and assembly. *J. Antibiot.* **48,** 306–310 (1995).
7 Radmacher, E. *et al.* Ethambutol, a cell wall inhibitor of *Mycobacterium tuberculosis*, elicits L-glutamate efflux of *Corynebacterium glutamicum*. *Microbiology* **151,** 1359–1368 (2005).
8 Minnikin, D. E., Minnikin, S. M., Parlett, J. H., Goodfellow, M. & Maqnusson, M. Mycolic acid patterns of some species of Mycobacterium. *Arch. Microbiol.* **259,** 446–460 (1985).
9 Sun, D., Cohen, S., Mani, N., Murphy, C. & Rothstein, D. M. A pathway-specific cell based screening system to detect bacterial cell wall inhibitors. *J. Antibiot.* **55,** 279–287 (2002).
10 Zhang, Y. & Amzel, L. M. Tuberculosis drug targets. *Curr. Drug Targets* **3,** 131–154 (2002).

The Journal of Antibiotics (2009) 62, 319–323

www.nature.com/ja

ORIGINAL ARTICLE

A profile of drug resistance genes and integrons in *E. coli* causing surgical wound infections in the Faisalabad region of Pakistan

Muhammad Azeem Saeed, Abdul Haque, Aamir Ali, Mashkoor Mohsin, Saira Bashir, Ayesha Tariq, Amna Afzal, Tayyaba Iftikhar and Yasra Sarwar

Escherichia coli **are one of the leading causes of infection in wounds. Emerging multiple drug resistance among *E. coli* poses a serious challenge to antimicrobial therapy for wounds. This study was conducted to ascertain a baseline profile of antimicrobial resistance in *E. coli* isolates infecting surgical wounds. A total of 64 pus samples from hospitalized patients were screened and 29 (45.3%) were found to have *E. coli,* which were identified biochemically and confirmed by molecular methods. Using the disc diffusion method, antimicrobial resistance was observed toward tetracycline (100%), cefradine (100%), nalidixic acid (93.1%), ampicillin (86.2%), gentamicin (86.2%), cefixime (82.8%), ceftriaxone (82.8%), aztreonam (82.8%), ciprofloxacin (75.9%), streptomycin (72.4%), cefoperazone (65.5%), chloramphenicol (58.6%) and amikacin (58.6%). In an effort to find relevant genes, 11 different genes were targeted by PCR. Among these, the mutated *gyrA* gene was found to be the most prevalent (82.8%), followed by the *TEM* (72.4%), *catP* (68.9%), *catA1* (68.9%), *tetB* (62.1%), *blt* (58.6%), $bla_{CTX-M-15}$ (27.6%), bla_{TEM} (20.7%), bla_{OXA} (17.2%), *tetA* (17.2%) and *aadA1* (13.8%) genes. The presence of integrons was also studied among these isolates. The prevalence of class 1 integrons was the highest (44.8%), followed by class 2 (27.6%). Three (10.3%) isolates carried both class 1 and class 2 integrons (first report from *E. coli* infecting wounds). The high incidence of integrons points toward their facilitation for carriage of antimicrobial resistance genes; however, in nearly 37% isolates, no integrons were detected, indicating the significance of alternative mechanisms of gene transfer. Another salient finding was that all isolates were multidrug-resistant *E. coli.***
The Journal of Antibiotics (2009) **62,** 319–323; doi:10.1038/ja.2009.37; published online 15 May 2009

Keywords: drug resistance; *E. coli*; genetic elements; wounds

INTRODUCTION

Wounds may be community acquired or related to surgery. Medical practitioners combating wound infections often face a serious problem created by the presence of bacteria that are resistant to multiple antimicrobial drugs. Antimicrobial drug resistance complicates wound healing, lengthens the postoperative course and increases treatment costs. According to a report by the Center for Disease Control (CDC) in 1996, *E. coli* is the fourth most common pathogen implicated in surgical wound infections.[1] However, depending on many socioeconomic factors, the prevalence and antimicrobial resistance patterns of *E. coli* also vary in wound specimens isolated from different regions around the globe.[2] Multidrug-resistant (MDR) strains of *E. coli* pose a big challenge for the selection of antimicrobial drugs during treatment course. Plenty of economic and health losses occur every year because of all kinds of infections caused by extra-intestinal *E. coli*, which include wound infections, neonatal meningitis, complicated urinary tract infections, spontaneous peritonitis, pneumonia, etc. In the United States alone, the total estimated cost associated with surgical wound infections is 1.2–4.0 billion dollars per year, with an estimated *E. coli*-associated share of 94–252 million dollars per annum.[1]

It has been established that the spread of drug-resistance genes through horizontal routes has been a primary force in the swift evolution of resistance to a wide range of distinct drugs among various bacterial species.[3] In addition to cross-resistance among antimicrobial drugs, there may be multiple genes conferring resistance to a single antimicrobial drug, and it may not be possible to explore all of them in a single study. Therefore, the results of phenotypic drug resistance (disc diffusion tests) and the molecular detection of respective genes may not always tally.[3,4] Among the acquired mechanisms of resistance, the transfer of resistance determinants borne on plasmids, bacteriophages, transposons and particularly integrons is of utmost importance. Depending on the nature of the integrase, five classes of integrons have been documented to date, but three of them

Health Biotechnology Division, National Institute for Biotechnology and Genetic Engineering, Faisalabad, Pakistan
Correspondence: Dr A Haque, Health Biotechnology Division, National Institute for Biotechnology and Genetic Engineering, PO Box 577, Jhang Road, Faisalabad 38000, Pakistan.
E-mails: ahaq_nibge@yahoo.com or abdulhaque@nibge.org
Received 17 February 2009; revised 22 April 2009; accepted 23 April 2009; published online 15 May 2009

(particularly class 1) have clinical and epidemiological significance regarding antimicrobial resistance in human isolates.[3] A critique of earlier studies revealed that *E. coli* readily transfer their mobile genetic elements to other *E. coli* and to strains of different genera, which could worsen the situation.[5]

In most developing countries, there is lack of information on the antimicrobial resistance patterns of *E. coli* infecting wounds. An extensive research work is needed to elucidate an overall profile of these wound-infecting *E. coli* in order to make an effective treatment strategy. The main objective of this study was to establish a baseline antimicrobial resistance profile of *E. coli* infecting wounds isolated from the local population.

MATERIALS AND METHODS

Isolation and biochemical identification of *E. coli*

Pus swabs were aseptically collected from wounds of 64 patients of all age groups and both sexes, admitted to the local hospitals of Faisalabad, Pakistan from January 2008 to April 2008. Each specimen was collected before an antiseptic application on the wound, using a sterile cotton swab, avoiding any contamination with the commensals of the skin. These specimens were transported to the laboratory in sterile conditions soon after collection. The specimens were streaked on MacConkey agar plates and incubated overnight at 37 °C for the isolation of *E. coli*. Only a single isolate was processed from an individual patient. The isolates were subcultured on the same media for obtaining isolated colonies. For biochemical identification, these colonies were inoculated into triple sugar iron (TSI) agar slants in each case and results were interpreted according to the manufacturer's guidelines.

DNA extraction

Total genomic DNA from *E. coli* isolates was extracted from the overnight culture at 37 °C in tryptic soy broth (TSB) using the phenol–chloroform method.[6] The integrity of DNA samples was checked by electrophoresis on 1% agarose gel, and purity was determined by the ratio of A260/A280 spectrophotometrically. DNA samples were quantified with a fluorometer (DyNA Quant 200, Hoefer, Inc., Silver Spring, MD, USA).

PCR for confirmation of *E. coli*

The PCR was carried out for the confirmation of *E. coli* isolates by targeting the *uidA* gene for β-glucronidase using primers described earlier (Table 1). Each 100 µl of the PCR reaction mixture contained, in addition to 20 ng of template DNA, 1.5 mM of $MgCl_2$, 18 µM of each dNTP, 0.8 µM of each primer and 5 U of *Taq* polymerase. The thermal cycler conditions were as follows: 94 °C for 5 min (initial denaturation), followed by 30 cycles of 94 °C for 1 min, 50 °C for 1 min, 72 °C for 1 min and a final extension of 72 °C for 7 min.

Antimicrobial susceptibility testing

E. coli isolates confirmed by PCR were tested for their phenotypic susceptibility to seven major antimicrobial groups by the disc diffusion method, using discs of 13 representative antimicrobial drugs (Table 2). These antimicrobial drugs are currently in routine use for the treatment of different kinds of wounds in Pakistan. However, nalidixic acid was included only for comparison with ciprofloxacin. The results were interpreted following the guidelines of the Clinical and Laboratory Standards Institute (CLSI).[7]

PCR for detection of integrons

Class 1, 2 and 3 integrons (*intI1, intI2* and *intI3* genes, respectively) were targeted by PCR using earlier reported primer sets (Table 1). The thermal cycler conditions for *intI1* and *intI2* were as follows: 96 °C for 30 s, 55 °C for 1 min and 70 °C for 3 min, followed by 25 cycles of 96 °C for 15 s, 55 °C for 30 s and 70 °C for 3 min. PCR for *intI3* was performed at 94 °C for 5 min, followed by 30 cycles of 94 °C for 2 min, 57 °C for 1 min and 72 °C for 1.5 min. A final extension at 72 °C for 7 min was performed at the end of each PCR.

For confirmation of the isolates carrying both class 1 and class 2 integrons, a multiplex PCR targeting both *intI1* and *intI2* genes simultaneously was also performed under the same thermal cycler conditions. Each 100 µl of the PCR mixture for multiplex PCR contained, in addition to 20 ng of DNA, 1.5 mM of $MgCl_2$, 70 µM of each dNTP, 1.0 µM of each primer and 10 U of *Taq* polymerase.

Restriction analyses of integrons

To confirm the amplified products of class 1 and class 2 integrons, restriction endonucleases having their target sites in the amplified sequences of *intI1* (AB365868) and *intI2* (AJ001816) gene fragments from the nucleotide sequence database (GenBank) were selected. Endonucleases, *Nsb*I and *Eco*521, were used to restrict the amplified products of class 1 integrons, whereas class 2 integron amplicons were restricted with *Nsb*I only. Each 30 µl of the restriction mixture contained 1 µl (10 U) of enzyme, 8 µl of PCR-amplified product, 3 µl of enzyme buffer and 18 µl of double-distilled water. Restriction mixtures were incubated at 37 °C for 45 min and electrophoresed on 2% agarose gel.

PCR for antimicrobial resistance genes

The PCR was performed for the detection of 12 different antimicrobial resistance genes, using primer sets mentioned in Table 1. As no proper data are available regarding drug resistance genes from Pakistan, the studied genes were selected on the basis of their high prevalence worldwide to confer resistance against the used antimicrobial drugs in different *E. coli* isolates. PCR reaction mixture conditions were the same as those mentioned earlier for the *uidA* gene. Thermal cycler conditions for *TEM*, bla_{TEM}, bla_{OXA}, *catP*, $bla_{CTX-M-15}$, *catA*, *tetB* and *blt* genes were as follows: 94 °C for 5 min, followed by 30 cycles of 94 °C for 1 min, 51 °C for 1 min and 72 °C for 1 min. PCR for the *gyrA* gene was conducted at 94 °C for 5 min, followed by 30 cycles of 94 °C for 1 min, 60 °C for 1 min and 72 °C for 1 min. The conditions for amplification of the *aadA1* and *aac(3)-I* genes were 94 °C for 5 min, followed by 30 cycles of 94 °C for 30 s, 50 °C for 30 s and 72 °C for 1 min, whereas for the *tetA* gene, the conditions were 94 °C for 5 min, followed by 30 cycles of 94 °C for 30 s, 53 °C for 30 s and 72 °C for 1.5 min. A final extension for 7 min at 72 °C was performed at the end of each PCR. The amplified products were separated by electrophoresis on 2% agarose gels and photographed by UV transilluminator.

RESULTS

Biochemical and molecular detection of *E. coli* isolates

Of the 64 pus samples, 29 (45.3%) isolates were biochemically identified as *E. coli* in TSI agar slants. All these (29) isolates were confirmed as *E. coli* by PCR for the *uidA* gene.

PCR and restriction analyses of integrons

Class 1 integrons were the most prevalent, being found in 13 (44.8%) isolates. Class 2 integrons were detected in eight (27.6%) isolates, whereas all isolates were negative for class 3 integrons. Three (10.3%) isolates were found to be carrying both class 1 and class 2 integrons, as confirmed by multiplex PCR also (Figure 1). Restriction of amplification products of the *intI1* and *intI2* genes generated the bands of expected sizes.

Antimicrobial resistance profile

For the sake of results interpretation, all isolates with intermediate susceptibility were regarded as resistant.[5] The overall phenotypic and molecular drug resistance profile has been summarized in Table 2. By the disc diffusion method, all 29 (100%) isolates showed resistance to at least three antimicrobial drugs belonging to structurally different antimicrobial groups; hence, all the isolates were considered as MDR. There were 28 (96.6%) isolates that showed resistance to at least five drugs. A total of 22 (75.9%) isolates were resistant to a minimum of 10 drugs and six (20.7%) of the strains were found resistant to all drugs used.

Regarding β-lactam drugs, twenty-five (86.2%) isolates were found resistant to ampicillin by the disc diffusion method. Three

Table 1 Primer sets used in PCR

Genes	*Primer sequences (5′–3′)*	*Amplicon size (bp)*	*References*
uidA	ATCACCGTGGTGACGCATGTCGC CACCACGATGCCATGTTCATCTGC	486	Heininger *et al.*[23]
TEM	GCACGAGTGGGTTACATCGA GGTCCTCCGATCGTTGTCAG	311	Carlson *et al.*[24]
bla_{TEM}	ATGAGTATTCAACTTTCCGTGT TTACCAATGCTTAATCAGTGACG	876	Chu *et al.* [25]
bla_{OXA}	ATGAAAAACACAATACATATCAACTTCGC GTGTGTTTAGAATGGTGATCGCATT	820	Peirano *et al.*[26]
gyrA	TACCGTCATAGTTATCCACGA GTACTTTACGCCATGAACGT	342	Molbak *et al.*[27]
catP	CCTGCCACTCATCGCAGT CACCGTTGATATATCCC	623	Guerra *et al.*[28]
catA1	CGCCTGATGAATGCTCATCCG CCTGCCACTCATCGCAGTAC	457	Molbak *et al.*[27]
tetA	GTAATTCTGAGCACTGTCGC CTGCCTGGACAACATTGCTT	956	Guardabassi *et al.*[20]
tetB	CTCAGTATTCCAAGCCTTTG CTAAGCACTTGTCTCCTGTT	416	Guardabassi *et al.*[20]
blt	CCCCTATTTGTTTATTTTTC GACAGTTACCAATGCTTAAT	962	Yan *et al.*[29]
$bla_{CTX-M-15}$	AGAATAAGGAATCCCATGGTT ACCGTCGGTGACGATTTTAG	875	Mendonca *et al.*[30]
aadA1	TGATTTGCTGGTTACGGTGAC CGCTATGTTCTCTTGCTTTTG	284	Van *et al.*[18]
aac(3)-I	ACCTACTCCCAACATCAGCC ATATAGATCTCACTACGCGC	157	Van *et al.*[18]
intI1	ATCATCGTCGTAGAGACGTCGG GTCAAGGTTCTGGACCAGTTGC	892	Rosser *et al.*[31]
intI2	GCAAATGAAGTGCAACGC ACACGCTTGCTAACGATG	467	Rosser *et al.*[31]
intI3	GCAGGGTGTGGACAGATACG ACAGACCGAGAAGGCTTATG	760	Senda *et al.*[32]

Table 2 Antimicrobial resistance profile of 29 isolates by disc diffusion and PCR

Group isolates	*Drug discs*	*Resistant* n *(%)*	*Genes*	*Positive* n *(%)*
Tetracylins	Tetracycline	29 (100.0)	*tetB*	18 (62.1)
			tetA	5 (17.2)
Quinolones	Nalidixic acid	27 (93.1)		
	Ciprofloxacin	22 (75.9)	*gyrA*	24 (82.8)
Aminoglycosides	Gentamicin	25 (86.2)	*aac(3)-I*	0 (0)
	Streptomycin	21 (72.4)	*aadA1*	4 (13.8)
	Amikacin	17 (58.6)		
Phenicol derivatives	Chloramphenicol	17 (58.6)	*catA*	20 (68.9)
			catP	20 (68.9)
Cephalosporins	Cefradine	29 (100.0)	*blt*	17 (58.6)
	Cefixime	24 (82.4)	$bla_{CTX-M-15}$	8 (27.6)
	Ceftriaxone	24 (82.4)		
	Cefoperazone	19 (65.5)		
Penicillins	Ampicillin	25 (86.2)	*TEM*	21 (72.4)
			*bla*TEM	5 (17.2)
			bla_{OXA}	5 (17.2)
Monobactam	Aztreonam	24 (82.4)		

major genes responsible for conferring resistance to ampicillin were amplified: *TEM* in 21 (72.4%), bla_{TEM} in 6 (20.7%) and bla_{OXA} in 5 (17.2%) isolates. All isolates positive for bla_{TEM} were also found positive for the *TEM* gene. Among cephalosporins, 29 (100%), 24 (82.8%), 24 (82.8%) and 19 (65.5%) isolates showed resistance to cefradine, cefixime, ceftriaxone and cefoperazone, respectively. The related antimicrobial resistance genes, *blt* and $bla_{CTX-M-15}$, were found in 17 (58.6%) and eight (27.6%) isolates, respectively. The majority of isolates, 24 (82.8%), were resistant to monobactam (aztreonam).

Tetracycline resistance was observed in all 29 (100%) isolates; the relevant resistance gene, *tetB*, was detected in 18 (62.1%) isolates, followed by *tetA* in five (17.2%) isolates. One of the isolates was observed to have both *tetA* and *tetB* genes.

Chloramphenicol resistance was found in 15 (62.5%), whereas chloramphenicol genes, *catP* and *catA*, were detected in 20 (68.9%) isolates each; 17 (58.6%) isolates carried both of these genes.

A total of 27 (93.1%) isolates showed phenotypic resistance to nalidixic acid and 22 (75.9%) to ciprofloxacin. A total of 24 (82.4%) isolates were found to have a respective mutated *gyrA* gene.

In vitro resistance to aminoglycosides (gentamicin, streptomycin and amikacin) was found in 25 (86.2%), 21 (72.4%) and 17 (58.6%) isolates, respectively. The gene, *aadA1*, responsible for imparting resistance against streptomycin, was found only in four (13.8%) isolates; however, none of the isolates was found positive for the *aac(3)-I* gene specific to gentamicin.

In most isolates, a unique pattern of resistance genes was observed. However, three combinations were found in more than one isolate.

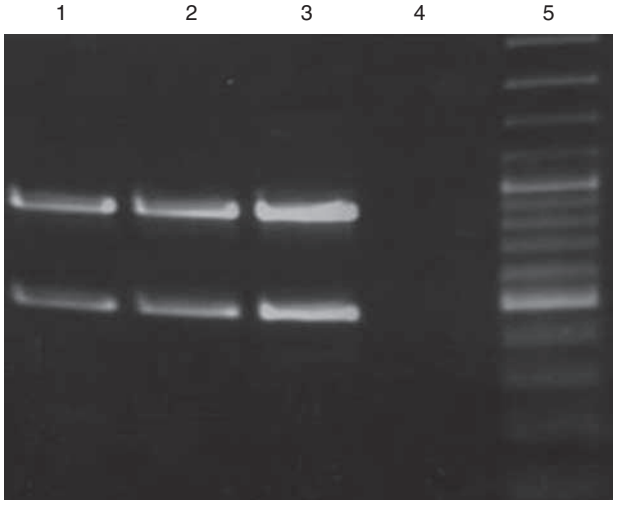

Figure 1 Multiplex PCR for integrons. Lane 1, 2 and 3: *intI1* (upper band=892 bp) and *intI2* (lower band=467 bp) in three different isolates; Lane 4: negative control PCR (PCR mix without template DNA); Lane 5: molecular weight marker (Fermentas SM0323; showing bands of 3000, 2000, 1500, 1200, 1031, 900, 800, 700, 600, 500, 400, 300, 200 and 100 bp).

These were *TEM*, *tetB*, *capP*, *catA* and *blt* in eight (27.6%) isolates, *TEM*, *capP*, *catA* and *blt* in four (13.8%) and *TEM*, *tetB*, *capP* and *catA* in two (6.9%) isolates.

DISCUSSION

Advancements to control wound infections have been hampered by the rapid emergence of antimicrobial resistance among bacterial population. However, there is a paucity of information with regard to antimicrobial resistance determinants in *E. coli* isolated from human wound infections, especially in developing countries. There are only few reports from Pakistan regarding antimicrobial resistance determinants in clinical isolates of *E. coli* at a molecular scale.[8,9] There is no report that specifically deals with wound infections. This study was executed to analyze antimicrobial resistance of local *E. coli* isolates infecting surgical wounds, both at phenotypic and molecular levels.

One of the main mechanisms of drug resistance is gene transfer through integrons that are able to capture, integrate and express gene cassettes encoding antimicrobial resistance in clinical *E. coli* isolates.[3] In our study, class 1 and 2 integrons were found in 44.8 and 27.6% isolates, respectively, whereas none of the isolates harbored class 3 integrons. Interestingly, 10.3% of the isolates were found to harbor both class 1 and 2 integrons. The simultaneous occurrence of two types of integrons in one *E. coli* isolate was significant, because it is relatively rare in clinical *E. coli* isolates.[10–12] To our knowledge, it is the first time in the world that two types of integrons have been amplified simultaneously in wound-infecting *E. coli.* This highlights the increasing sophistication in the armory of these pathogens. The prevalence of integrons is relatively high as compared with some earlier reports,[10,11] yet is comparable with a report from the United States.[13] This high level of occurrence of integrons (62.6%) highlights the threat of MDR.[14]

All our isolates showed resistance to at least three drugs, belonging to structurally different antimicrobial groups; hence, by definition, all the isolates could be classified as MDR.

We used ampicillin as representative of penicillins and found a high incidence of resistance (86.2%) in our isolates (Table 2). It is in accordance with observations made by other researchers.[15] There were 20.7% isolates resistant to ampicillin by the disc diffusion method, but were negative for the three most common genes involved in resistance against ampicillin (*TEM*, bla_{TEM} and bla_{OXA} genes). The drug resistance in these isolates may be related to several other genes that were not included in this study.

In β-lactams, cephalosporins constitute another major group. We used four drugs representing different generations of cephalosporins: cefradine (1st generation), cefixime and cefoperazone (2nd generation) and ceftriaxone (3rd generation). Interestingly, cefoperazone, not ceftriaxone, was the most effective drug (Table 2). However, the high sensitivity to cefoperazone (34.5%) is not in line with some earlier reports.[15]

Fluoroquinolones are perhaps the most important synthetic antimicrobial drugs used in clinical practice. Although there are several mechanisms for the development of resistance, mutation in the *gyrA* gene is the most common.[16] The high occurrence of ciprofloxacin resistance (75.9%) in our isolates is in accordance with some other reports from Asia,[15,17] but it is in contrast to a report from Vietnam.[18] As expected, the incidence of resistance to nalidixic acid, which is a simple quinolone, was higher (93.1%) and in agreement with some earlier reports.[4]

Aminoglycosides are an important group of bactericidal drugs that are very effective against Gram-negative bacteria. We used amikacin, streptomycin and gentamicin as representatives of this group. Amikacin was the most effective drug, as 41.4% isolates were sensitive to it. These results are in accordance with earlier reports from Pakistan and India.[15,19] The resistance to gentamicin (86.2%) and streptomycin (72.4%) was found to be relatively high as compared with some earlier reports.[4,15,19]

Tetracycline has been a widely used antimicrobial drug, but all of our isolates showed resistance to it. Similar results have been reported earlier from Vietnam.[18] Twenty-two (75.9%) isolates were positive for either one or both of the *tetA* and *tetB* genes. However, we found neither of these genes in 24.1% isolates. This may be due to some other resistance phenomenon not studied in this work such as efflux pumps.[20]

Chloramphenicol is a broad-spectrum bacteriostatic, inhibitor of protein synthesis that has utility in human clinical practice. Surprisingly, it was relatively the most effective drug (with 41.4% sensitivity) besides amikacin in our study. Similar results were documented previously,[21] but Anguzu reported 100% resistance against chloramphenicol in Uganda.[2] This difference may be due to geographical disparity. However, it is interesting that five (17.2%) isolates were having *catP* or *catA* genes, although they were sensitive to chloramphenicol by disc diffusion method. This indicates that genes may be silenced in these isolates due to many factors, including the reduced use of chloramphenicol in clinical practice because of its toxic effects.[22]

We analyzed the data for the presence of multiple gene cassettes, which may indicate wholesome horizontal transfer of drug resistance. But generally speaking, this was not the case. In most isolates, a unique pattern of resistance genes was observed. However, three combinations encompassing 14 isolates were detected in more than one isolate. Details have been given in the Results section.

We conclude that MDR is very frequent in wound-infecting *E. coli.* In developing countries, the careless use of antimicrobial drugs by clinicians and easy access without prescription are the main factors. To date, very little work has been carried out on the antimicrobial

resistance profile of *E. coli* infecting wounds at the molecular level, and more inputs are needed so that clinicians can be better equipped to cope with these infections.

1 Russo, T. A. & Johnson, J. R. Medical and economic impact of extraintestinal infections due to *Escherichia coli*: focus on an increasingly important endemic problem. *Microbes. Infect.* **5,** 449–456 (2003).
2 Anguzu, J. R. & Olila, D. Drug sensitivity patterns of bacterial isolates from septic post-operative wounds in a regional referral hospital in Uganda. *Afr. Health. Sci.* **7,** 148–154 (2007).
3 Rowe-Magnus, D. A. & Mazel, D. The role of integrons in antibiotic resistance gene capture. *Int. J. Med. Microbiol.* **292,** 115–125 (2002).
4 Srinivasan, V. *et al.* Characterization of antimicrobial resistance patterns and class 1 integrons in *Escherichia coli* O26 isolated from humans and animals. *Int. J. Antimicrob. Agents.* **29,** 254–262 (2007).
5 Zhao, S. *et al.* Antimicrobial susceptibility and molecular characterization of avian pathogenic *Escherichia coli* isolates. *Vet. Microbiol.* **107,** 215–224 (2005).
6 Sambrook, J., Fritsch, E. F. & Maniatis, T. *Molecular cloning: A laboratory manual* (Cold Spring Harbor Laboratory Press, New York, 1989).
7 National Committe for Clinical Laboratory Standards. *Performance standards for antimicrobial susceptibility testing.* Fourth informational supplement. Document M100-S14 (NCCLS: Wayne, PA, 2004).
8 Shanahan, P. M., Karamat, K. A., Thomson, C. J. & Amyes, S. G. Characterization of multi-drug resistant *Salmonella typhi* isolated from Pakistan. *Epidemiol. Infect.* **124,** 9–16 (2000).
9 Hawkey, P. M. Prevalence and clonality of extended-spectrum beta-lactamases in Asia. *Clin. Microbiol. Infect.* **14** (Suppl 1), 159–165 (2008).
10 Reyes, A. *et al.* Prevalence and types of class 1 integrons in aminoglycoside-resistant Enterobacteriaceae from several Chilean hospitals. *J. Antimicrob. Chemother.* **51,** 317–321 (2003).
11 Yu, H. S. *et al.* Changes in gene cassettes of class 1 integrons among *Escherichia coli* isolates from urine specimens collected in Korea during the last two decades. *J. Clin. Microbiol.* **41,** 5429–5433 (2003).
12 Mathai, E., Grape, M. & Kronvall, G. Integrons and multidrug resistance among *Escherichia coli* causing community-acquired urinary tract infection in southern India. *APMIS.* **112,** 159–164 (2004).
13 Solberg, O. D., Ajiboye, R. M. & Riley, L. W. Origin of class 1 and 2 integrons and gene cassettes in a population-based sample of uropathogenic *Escherichia coli*. *J. Clin. Microbiol.* **44,** 1347–1351 (2006).
14 Skurnik, D. *et al.* Integron-associated antibiotic resistance and phylogenetic grouping of *Escherichia coli* isolates from healthy subjects free of recent antibiotic exposure. *Antimicrob. Agents. Chemother.* **49,** 3062–3065 (2005).
15 Nagoba, B. S. *et al.* A simple and effective approach for the treatment of chronic wound infections caused by multiple antibiotic resistant *Escherichia coli*. *J. Hosp. Infect.* **69,** 177–180 (2008).
16 Piatti, G., Mannini, A., Balistreri, M. & Schito, A. M. Virulence factors in urinary *Escherichia coli* strains: phylogenetic background and quinolone and fluoroquinolone resistance. *J. Clin. Microbiol.* **46,** 480–487 (2008).
17 Mehrgan, H. & Rahbar, M. Prevalence of extended-spectrum beta-lactamase-producing *Escherichia coli* in a tertiary care hospital in Tehran, Iran. *Int. J. Antimicrob. Agents.* **31,** 147–151 (2008).
18 Van, T. T., Chin, J., Chapman, T., Tran, L. T. & Coloe, P. J. Safety of raw meat and shellfish in Vietnam: an analysis of *Escherichia coli* isolations for antibiotic resistance and virulence genes. *Int. J. Food. Microbiol.* **124,** 217–223 (2008).
19 Jabeen, K., Zafar, A. & Hasan, R. Frequency and sensitivity pattern of extended spectrum beta lactamase producing isolates in a tertiary care hospital laboratory of Pakistan. *J. Pak. Med. Assoc.* **55,** 436–439 (2005).
20 Guardabassi, L., Dijkshoorn, L., Collard, J. M., Olsen, J. E. & Dalsgaard, A. Distribution and *in-vitro* transfer of tetracycline resistance determinants in clinical and aquatic Acinetobacter strains. *J. Med. Microbiol.* **49,** 929–936 (2000).
21 Srinivasan, V., Nguyen, L. T., Headrick, S. I., Murinda, S. E. & Oliver, S. P. Antimicrobial resistance patterns of Shiga toxin-producing *Escherichia coli* O157:H7 and O157:H7- from different origins. *Microb. Drug. Resist.* **13,** 44–51 (2007).
22 Enne, V. I., Delsol, A. A., Roe, J. M. & Bennett, P. M. Evidence of antibiotic resistance gene silencing in *Escherichia coli*. *Antimicrob. Agents. Chemother.* **50,** 3003–3010 (2006).
23 Heininger, A. *et al.* PCR and blood culture for detection of *Escherichia coli* bacteremia in rats. *J. Clin. Microbiol.* **37,** 2479–2482 (1999).
24 Carlson, S. A. *et al.* Detection of multiresistant *Salmonella typhimurium* DT104 using multiplex and fluorogenic PCR. *Mol. Cell. Probes.* **13,** 213–222 (1999).
25 Chu, C. *et al.* Large drug resistance virulence plasmids of clinical isolates of *Salmonella enterica* serovar Choleraesuis. *Antimicrob. Agents. Chemother.* **45,** 2299–2303 (2001).
26 Peirano, G., Agerso, Y., Aarestrup, F. M. & dos Prazeres Rodrigues, D. Occurrence of integrons and resistance genes among sulphonamide-resistant *Shigella* spp. from Brazil. *J. Antimicrob. Chemother.* **55,** 301–305 (2005).
27 Molbak, K. *et al.* An outbreak of multidrug-resistant, quinolone-resistant *Salmonella enterica* serotype typhimurium DT104. *N. Engl. J. Med.* **341,** 1420–1425 (1999).
28 Guerra, B., Soto, S. M., Arguelles, J. M. & Mendoza, M. C. Multidrug resistance is mediated by large plasmids carrying a class 1 integron in the emergent *Salmonella enterica* serotype [4,5,12:i:-]. *Antimicrob. Agents. Chemother.* **45,** 1305–1308 (2001).
29 Yan, J. J. *et al.* Dissemination of CTX-M-3 and CMY-2 beta-lactamases among clinical isolates of *Escherichia coli* in southern Taiwan. *J. Clin. Microbiol.* **38,** 4320–4325 (2000).
30 Mendonca, N., Leitao, J., Manageiro, V., Ferreira, E. & Canica, M. Spread of extended-spectrum beta-lactamase CTX-M-producing *Escherichia coli* clinical isolates in community and nosocomial environments in Portugal. *Antimicrob. Agents. Chemother.* **51,** 1946–1955 (2007).
31 Rosser, S. J. & Young, H. K. Identification and characterization of class 1 integrons in bacteria from an aquatic environment. *J. Antimicrob. Chemother.* **44,** 11–18 (1999).
32 Senda, K. *et al.* PCR detection of metallo-beta-lactamase gene (blaIMP) in Gram-negative rods resistant to broad-spectrum beta-lactams. *J. Clin Microbiol.* **34,** 2909–2913 (1996).

The Journal of Antibiotics (2009) 62, 325–332

www.nature.com/ja

ORIGINAL ARTICLE

Identification of the biosynthetic gene cluster of A-500359s in *Streptomyces griseus* SANK60196

Masanori Funabashi[1], Koichi Nonaka[1], Chieko Yada[1], Masahiko Hosobuchi[1], Nobuhisa Masuda[2], Tomoyuki Shibata[3] and Steven G Van Lanen[4]

A-500359s, produced by *Streptomyces griseus* SANK60196, are inhibitors of bacterial phospho-*N*-acetylmuramyl-pentapeptide translocase. They are composed of three distinct moieties: a 5′-carbamoyl uridine, an unsaturated hexuronic acid and an aminocaprolactam. Two contiguous cosmids covering a 65-kb region of DNA and encoding 38 open reading frames (ORFs) putatively involved in the biosynthesis of A-500359s were identified. Reverse transcriptase PCR showed that most of the 38 ORFs are highly expressed during A-500359s production, but mutants that do not produce A-500359s did not express these same ORFs. Furthermore, *orf21*, encoding a putative aminoglycoside 3′-phosphotransferase, was heterologously expressed in *Escherichia coli* and *Streptomyces albus*, yielding strains having selective resistance against A-500359B, suggesting that ORF21 phosphorylates the unsaturated hexuronic acid as a mechanism of self-resistance to A-500359s. In total, the data suggest that the cloned region is involved in the resistance, regulation and biosynthesis of A-500359s.
The Journal of Antibiotics (2009) **62,** 325–332; doi:10.1038/ja.2009.38; published online 29 May 2009

Keywords: A-500359s; biosynthetic gene cluster; resistance gene; RT-PCR; *Streptomyces griseus*

INTRODUCTION

Nucleoside antibiotics are a structurally diverse group of secondary metabolites with a broad range of biological activities, such as antibacterial, antifungal, antiviral, insecticidal, immunostimulative, immunosuppressive and antitumor activities. For example, blasticidin S[1] and mildiomycin,[2] peptidyl nucleoside antibiotics containing cytosine-derived bases, are cytotoxic to fungi by virtue of binding to the 50S ribosomal subunit. Polyoxins and nikkomycins, peptidyl nucleoside antibiotics, also exhibit antifungal activity, but in this case by the inhibition of chitin synthase,[3] and have been commercialized in the United States and Japan for agricultural application. There are a large number of uracil-containing nucleoside antibiotics that have antibacterial activities, such as mureidomycins, pacidamycins, napsamycins, liposidomycins, caprazamycins, muramycins and capuramycins.[4] Interestingly, they all inhibit bacterial phospho-*N*-acetylmuramyl-pentapeptide translocase (translocase I), which is an enzyme that catalyzes the first step in the lipid cycle of peptidoglycan biosynthesis: the transfer of phospho-*N*-acetylmuramic acid-pentapeptide to undecaprenyl phosphate to generate undecaprenyl-diphospho-*N*-acetylmuramic acid-pentapeptide, also known as lipid intermediate I. As peptidoglycan has an essential role in the vitality of bacteria, and the biosynthesis of peptidoglycan is a proven target for many antibiotics, including β-lactams, vancomycin and bacitracin, translocase I represents a valid target for the discovery and development of new antibacterial agents.

Nucleoside antibiotics not only possess potent and desirable biological activities but also are endowed with unique structural features, suggesting the occurrence of novel or unusual enzymatic transformations during their biosynthesis. To date, six complete biosynthetic gene clusters for nucleoside antibiotics have been cloned and reported: nikkomycin and polyoxin, peptidyl nucleoside antibiotics containing a uracil- or 4-formyl-imidazolin-2-one base;[5,6] puromycin, an adenine-containing aminonucleoside antibiotic;[7] streptothricins, peptidyl guanidine nucleoside antibiotics;[8] and blasticidin S[9] and toyocamycin, pyrrolopyrimidine nucleoside antibiotics.[10] Furthermore, two enzymes involved in mildiomycin biosynthesis have been functionally characterized.[11] However, there have been no reports on the cloning and characterization of a biosynthetic gene cluster for nucleoside antibiotics that target translocase I. Given that deciphering the mechanism of assembly of nucleoside antibiotics inhibiting translocase I will ultimately facilitate applications to promote the molecular diversity of natural and unnatural nucleoside antibiotics and also to enhance the

[1]Bioengineering Research Group I, Process Technology Research Laboratories, Pharmaceutical Technology Division, Daiichi Sankyo Co. Ltd, Fukushima, Japan; [2]Group IV, Biological Research Laboratories IV, Research and Development Division, Daiichi Sankyo Co. Ltd, Tokyo, Japan; [3]Group V, Exploratory Research Laboratories I, Research and Development Division, Daiichi Sankyo Co. Ltd, Tokyo, Japan and [4]Department of Pharmaceutical Sciences, College of Pharmacy, University of Kentucky, College of Pharmacy, Lexington, KY, USA
Correspondence: Dr K Nonaka, Process Technology Research Laboratories, Daiichi Sankyo Co. Ltd, Aza-ohtsurugi, Shimokawa, Izumi-machi, Iwaki-shi, Fukushima 971-8183, Japan.
E-mail: nonaka.koichi.k2@daiichisankyo.co.jp
Received 15 January 2009; revised 26 April 2009; accepted 7 May 2009; published online 29 May 2009

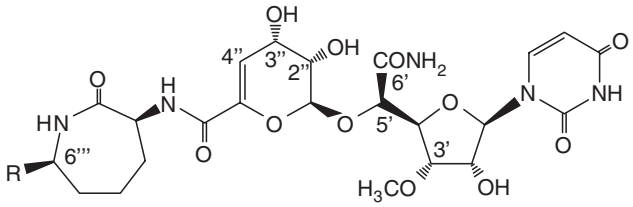

A-500359A: R = CH_3
A-500359B: R = H

Figure 1 The structure of the two main capuramycin-related metabolites isolated from *S. griseus* SANK60196.

production of desired nucleoside antibiotics, we initiated studies to identify the biosynthetic locus for model translocase I inhibitors.

A-500359s, which are capuramycin derivatives classified as a family of glycosyl nucleoside antibiotics, are produced by *Streptomyces griseus* SANK60196. They consist of three primary moieties, a 5′-carbamoyl uridine, an unsaturated hexuronic acid and an aminocaprolactam (Figure 1). The biosynthesis of A-500359s was previously analyzed using isotope-feeding experiments and was reported by Ohnuki *et al.*[12] to reveal the origin of every carbon atom, including the potential precursors of each moiety as uridine, mannose and lysine, respectively. Recently, we showed that a giant linear plasmid (SGF200) in *S. griseus* SANK60196 might be required for A-500359s biosynthesis; however, the biosynthetic gene cluster was not identified in SGF200 (unpublished data). We report here the identification of a putative gene cluster involved in the biosynthesis, regulation and resistance of A-500359s. Using reverse transcriptase PCR (RT-PCR), open reading frames (ORFs) within this gene cluster are shown to be highly expressed during A-500359s production. In addition, we show that ORF21 within this locus confers selective resistance to A-500359B. The identification of the A-500359s gene cluster now sets the stage to explore the mechanism of biosynthesis of this family of nucleoside antibiotics.

MATERIALS AND METHODS

Chemicals, strains and general recombinant DNA techniques

Escherichia coli JM109, restriction enzymes and DNA-modifying enzymes were purchased from Takara Bio (Shiga, Japan). *E. coli* XL1-Blue MR was purchased from Stratagene (La Jolla, CA, USA). Media, growth conditions and general recombinant DNA techniques for *E. coli* were described by Sambrook and Russell.[13] *Streptomyces albus* J1074 and plasmid vectors pWHM3[14] and pWHM79[15] were gifts from Professor Ben Shen, University of Wisconsin at Madison. *E. coli* MG1655 (ATCC 47076) was obtained from the American Type Culture Collection (Manassas, VA, USA).

RT-PCR analysis

A loopful of mycelia of cultured *S. griseus* SANK60196 derivatives HP, 35-4, 37-3 and 37-9 was inoculated into a test tube containing 5 ml of PM-1 medium and cultured with shaking (310 r.p.m.) at 23 °C for 3 days, as described previously.[16] Then 1 ml aliquots of each culture were transferred into a 100-ml Erlenmeyer flask containing 20 ml OM-1 medium and cultivation was continued for 7 days. The cultured mycelia were harvested from the culture broth by centrifugation (20 000×*g*, 5 min, 4 °C) and were treated overnight with RNAlater (Ambion, Austin, TX, USA) at 4 °C. Total RNA was isolated from the treated mycelia using RNAqueous (Ambion), according to the manufacturer's instructions. The isolated total RNA was treated with DNaseI to digest any contaminating genomic DNA. For RT-PCR cloning of NDP-glucose dehydratase (NGDH) in *S. griseus* SANK60196, the total RNA isolated from the mycelia of strain HP cultured for 7 days was used for cDNA synthesis using TOYOBO RT-Ace (TOYOBO, Osaka, Japan), and the desired fragment was amplified by LA-Taq with GC buffer (Takara Bio). The NGDH degenerate primer pairs used for PCR (dehy-f: 5′-CSGGSGSSGCSGGSTTCATSGG-3′/dehy-r: 5′-GGGWRCTGGYRSGGSCCGATGTTG-3′) were designed on the basis of the report by Decker *et al.*[17] RT-PCR amplification for expression analysis was carried out on a GeneAmp PCR system 9700 (Perkin-Elmer/ABI, Foster City, CA, USA) using TaKaRa One Step RNA PCR kit (AMV) (Takara Bio) and was conducted in 25 cycles. *glk*, encoding glucokinase, was used as an internal control, and unique primers (Glk-f: 5′-CGGCGGCACGAAGATC-3′/Glk-r: 5′-GCGCAGCTTGTTGCCG-3′) were designed on the basis of the highly conserved sequences, IGGTKI and IGNKLR, corresponding to the *N*- and the *C*-terminal amino-acid sequence of glucokinase in *Streptomyces coelicolor* A3(2) (NP_626383), *Streptomyces avermitilis* MA-4680 (NP_827250) and *S. griseus* IFO13350 (YP_001826889).

Genomic library construction

S. griseus SANK60196 genomic DNA was partially digested with *Sau*3AI to give 30- to 50-kb DNA fragments. These fragments were dephosphorylated with bacterial alkaline phosphatase and ligated into *Bam*HI-digested cosmid vector SuperCos1 (Stratagene), which was dephosphorylated by bacterial alkaline phosphatase after *Xba*I digestion. The ligation products were packaged with Gigapack III Gold packaging extract (Stratagene) as described by the manufacturer, and the resulting recombinant phage was used to transfect *E. coli* XL1-Blue MR. Approximately 20 000 colonies from the obtained genomic library were screened by colony hybridization using a digoxigenin (DIG)-labeled 0.55-kb fragment, including a part of the cloned putative NGDH. Hybridization was carried out using DIG easy hyb (Roche, Indianapolis, IN, USA) at 42 °C, and the resulting filter was washed under high stringency conditions (0.1× SSC including 0.1% SDS, 68 °C). Detection was performed using CDP-Star (Roche) according to the manufacturer's procedures. The resultant positive cosmids were isolated and sequenced.

DNA sequencing

Automated DNA sequencing was carried out on an ABI PRISM 3700 DNA Analyzer (Perkin-Elmer/ABI). The DNA sequence of the isolated cosmids was determined by shotgun sequencing. The cosmid DNA was sheared using a Nebulizer Kit (Invitrogen, Carlsbad, CA, USA) according to the manufacturer's procedures and the treated DNA was analyzed by agarose gel electrophoresis. The DNA fragments from 1 to 3 kb were purified using a QIAquick PCR purification kit (Qiagen, Gaithersburg, MD, USA). The recovered DNA fragments were cloned into pHSG398 (Takara Bio) and transformed into *E. coli* JM109. Approximately 400 plasmids extracted using R.E.A.L. Prep 96 (Qiagen) were sequenced and the sequence data were assembled using ATGC (Genetyx, Tokyo, Japan). Database comparison for sequence homology was performed with BLAST search tools using the National Center for Biotechnology Information (Bethesda, MD, USA). The DNA sequence has been deposited in DDBJ under the accession number AB476988.

Disruption of *tolC* in *E. coli* MG1655 for a test of resistance ability against A-500359B

An in-frame deletion of the *tolC* gene (AC_000091) in *E. coli* MG1655 was carried out using the pKO3-derived plasmid carrying an in-frame fusion of the 5′ and 3′ flanking regions of *tolC* reported previously.[18] The pKO3-derived plasmid for the deletion of *ΔtolC* was introduced into *E. coli* MG1655-competent cells by electroporation, and integrants, which contained the plasmid in the chromosome, were selected using Luria-Bertani (LB) medium containing chloramphenicol at 43 °C. One of the integrants was grown in LB liquid medium without selection pressure for 9 h and the serially diluted culture broth was plated and incubated on LB agar supplemented with 10% (wt/vol) sucrose at 30 °C for 24 h. Chloramphenicol-susceptible and sucrose-resistant colonies were isolated and subjected to PCR for the confirmation of gene deletion using the following pairs of primers I: 5′-AAGGAAAAAAGC GGCCGCTGCTAAACAGTATCGCAACCAGTC-3′ and II: 5′-CGCACGCATGT CGACTCGTATAGTGACGTTGGCGTATC-3′. The resulting clone, named

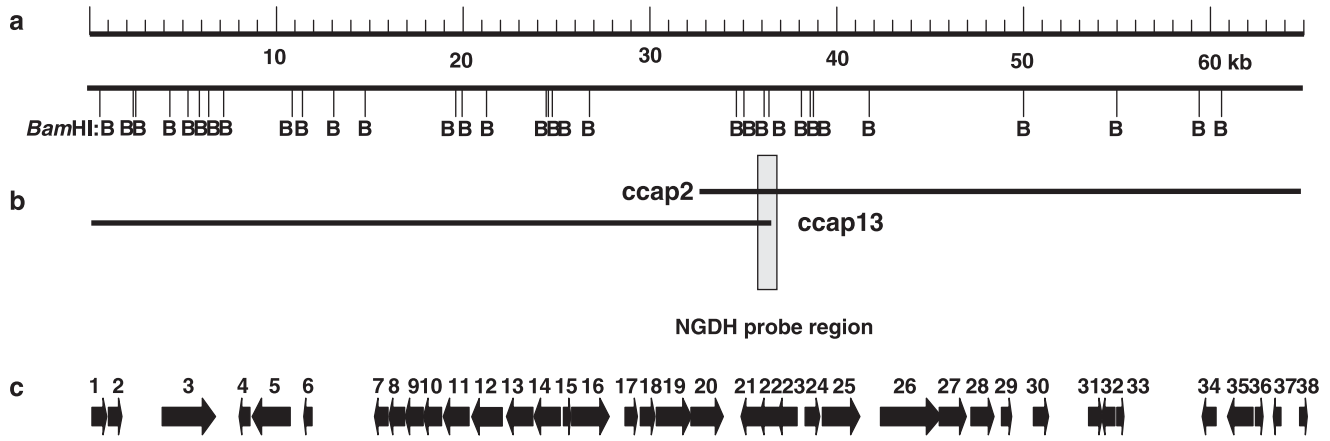

Figure 2 Restriction map of *Bam*HI and genetic organization of the A-500359s biosynthetic gene cluster. (**a**) *Bam*HI cleavage sites are illustrated. (**b**) Overlapping cosmids, ccap2 and ccap13, which contain the NGDH homolog. (**c**) Genetic organization of the fully sequenced ccap13 and ccap2 inserts encoding the A-500359s biosynthetic gene cluster.

E. coli ΔtolC, was sensitive against A-500359s and was used to test resistance against A-500359B.

Construction of *orf21* expression vector in *E. coli ΔtolC*

An *orf21* expression construct in *E. coli* was generated as follows: *orf21* was amplified using primers III: 5′-GCGA***AGCT***TGGTGGCAGCGGACGGG-3′ (the *Hin*dIII site is shown in italics and the Ser residue of LacZ in bold) and IV: 5′-GCGG*AATTC*TCAGGTTCGAGTCGCG-3′ (the *Eco*RI site is shown in italics). The resulting 1-kb amplified fragment was cloned into pSC-B using a StrataClone PCR Cloning Kit (Stratagene) to yield strata-ec-*orf21*. After sequencing to confirm PCR fidelity, the *Hin*dIII–*Eco*RI fragment was excised from strata-ec-*orf21* and introduced into pUC19 (Takara Bio) at *Hin*dIII–*Eco*RI sites to yield pUC19-*orf21*. The desired plasmid was transformed into *E. coli ΔtolC*-competent cells to confirm its resistance against A-500359B. *E. coli ΔtolC* harboring pUC19 was used as a control.

Construction of *orf21* expression vector in *Streptomyces*

An *orf21* expression vector in *Streptomyces* was constructed as follows: a 450-bp *Eco*RI–*Bam*HI fragment that harbored the *ermE** promoter from pWHM79 was ligated at *Eco*RI–*Bam*HI sites in pWHM3 to yield pWHM3-*Ep*. *orf21* was amplified using primers V: 5′-GCG*CTGCAG*GTGGCAGCGGACGGG-3′ (the *Pst*I site is shown in italics) and VI: 5′-GCG*AAGCTT*CAGGTTC-GAGTCGCG-3′ (the *Hin*dIII site is shown in italics) and the resulting 1-kb fragment was cloned into pSC-B using a StrataClone PCR Cloning Kit (Stratagene) to yield strata-st-*orf21*. After sequencing to confirm PCR fidelity, the *Pst*I–*Hin*dIII fragment was excised from strata-st-*orf21* and ligated into pWHM3-*Ep* at *Pst*I–*Hin*dIII sites to yield pWHM3-*Ep*-*orf21*. The desired plasmid was introduced into *S. albus* J1074 by polyethylene glycol-mediated protoplast transformation[19] to confirm its resistance against A-500359B. *S. albus* J1074, harboring pWHM3, was used as control.

Test of resistance to A-500359B in *Streptomyces* and *E. coli*

S. albus J1074, harboring the appropriate plasmid, was inoculated into 5 ml of Trypto Soy Broth (TSB) medium containing 50 μg ml^{-1} of thiostrepton and grown at 28 °C for 3 days. After homogenization, the culture broth was diluted with TSB medium to OD_{600}=3.0. Ten microliters of 100- and 1000-fold dilution prepared from the resulting culture broth was spotted on the ISP-2 agar containing 0, 100, 200, 500 or 1000 μg ml^{-1} of A-500359B, and the spotted plate was incubated at 27 °C for 4 days.

E. coli ΔtolC, harboring the appropriate plasmid, was inoculated into 2 ml of LB medium containing 100 μg ml^{-1} of ampicillin sodium salt and cultured at 37 °C for 1 day. The culture broth was diluted with LB medium to OD_{600}=1.0. Twenty microliters of the resulting culture broth was spotted on the LB agar containing 0, 10, 100 or 1000 μg ml^{-1} of A-500359B with 1 mM isopropyl-β-D-thiogalactopyranoside and the spotted plate was incubated at 37 °C for 1 day.

RESULTS

Identification of A-500359s biosynthetic gene cluster

Using RT-PCR, it was observed that a gene for a putative NGDH was abundantly transcribed during the production of A-500359s in a high-producing strain (strain HP). In contrast, this same gene was not expressed in a mutant strain that does not produce A-500359s. A 550-bp fragment of the NGDH gene was subsequently cloned and sequenced, and the deduced amino-acid sequence of the cloned region resembled that of other NGDHs cloned to date.

The cloned NGDH fragment was used as a probe leading to the entire A-500359s biosynthetic gene cluster. Approximately 20 000 clones from the genomic library were screened using the DIG-labeled NGDH fragment. The resulting two contiguous cosmids, named ccap2 and ccap13, were isolated and sequenced by the shotgun method. Consequently, the sequenced DNA covered approximately 65 kb, revealing 38 *orf*s (Figure 2), including *orf*22, the NGDH gene. The sequence was analyzed by a comparison with the database, and the predicted functions of 38 ORFs are summarized in Table 1.

The deduced functions of *orfs 9, 11, 12, 13*, *22* and *23* are those of 3-ketoreductase, NDP-4-keto-6-deoxy-glucose-2,3-dehydratase, UDP-glucose-4-epimerase, glycosyltransferase, UDP-glucose-4,6-dehydratase and glucose-1-phosphate thymidylyltransferase, respectively. They have been frequently identified in natural product biosynthesis containing a sugar moiety such as that observed in the structure of A-500359s. The deduced function of *orf7* is that of a non-heme, iron-dependent oxygenase. The *orf10* gene encodes a putative clavaminic synthase (also a non-heme, iron-dependent oxygenase), which is a key enzyme in clavulanic acid biosynthesis. The *orf8* gene encodes a putative truncated carbamoyltransferase, and the presumed function of *orf14* is that of a serine hydroxymethyltransferase (SHMT). Although it is well known that SHMT has an important role in amino-acid catabolism, the deduced amino-acid sequence of ORF14 is significantly different from that of SHMTs conserved in *Streptomyces*. The *orf16, -17* and *-18* genes encode a putative CO dehydrogenase large subunit, small subunit and medium subunit, respectively. The *orf21* gene encodes a putative aminoglycoside 3′-phosphotransferase, which is commonly observed as a mechanism of self-resistance and is often found in aminoglycoside-producing strains. The *orf26* and *orf27* genes were deduced to encode non-ribosomal peptide synthetase,

Table 1 Deduced function of ORFs in the A-500359s biosynthetic gene cluster

Protein	*Size*[a]	*Proposed function*	*Sequence similarity (protein, accession no., origin)*	*Identity %/ similarity %*
ORF1	>296	Unknown	Mflv_2879 (YP _001134144) *Mycobacterium gilvum* PYR-GCK	60/70
ORF2	245	Deoxyribonuclease	Mflv_2878 (YP _001134143) *Mycobacterium gilvum* PYR-GCK	58/74
ORF3	897	Endonuclease	SGR_4678 (YP_001826190) *Streptomyces griseus* NBRC 13350	46/61
ORF4	185	Terminal protein	TpgA1 (NP_828744) *Streptomyces avermitilis* MA-4680	87/95
ORF5	744	Telomere-associated protein	TapA1 (NP_828743) *Streptomyces avermitilis* MA-4680	83/86
ORF6	148	Unknown	SCO0007 (NP_624368) *Streptomyces coelicolor* A3(2)	89/92
ORF7	293	Dioxygenase	Aave_3719 (YP_972040) *Acidovorax avenae* subsp. *citrulli* AAC00-1	35/51
ORF8	302	Carbamoyl transferase	Bphy_7715 (YP_001863651) *Burkholderia phymatum* STM815	47/62
ORF9	316	3-Ketoreductase	ChlC4 (AAZ77681) *Streptomyces antibioticus*	30/48
ORF10	324	Clavaminic synthase	CAS (CAA58905) *Streptomyces clavuligerus*	57/70
ORF11	465	NDP-4-keto-6-deoxy-Glc-2,3-dehydratase	Sim20 (AAL15606) *Streptomyces antibioticus*	42/59
ORF12	313	UDP-Glc-4-epimerase	GalE3 (YP_134444) *Haloarcula marismortui* ATCC 43049	32/44
ORF13	383	Glycosyltransferase	SACE_6476 (YP_001108570) *Saccharopolyspora erythraea* NRRL 2338	25/40
ORF14	461	Serine hydroxymethyltransferase	Orf(-4) (AAN85510) *Streptomyces atroolivaceus*	41/59
ORF15	87	Pyrophosphatase	SAV_326 (NP_821500) *Streptomyces avermitilis* MA-4680	52/72
ORF16	759	Carbonmonoxide dehydrogenase	SACE_1162 (YP_001103415) *Saccharopolyspora erythraea* NRRL 2338	58/68
ORF17	168	Carbonmonoxide dehydrogenase	SACE_0536 (YP_001102808) *Saccharopolyspora erythraea* NRRL 2338	72/83
ORF18	289	Carbonmonoxide dehydrogenase	SACE_0538 (YP_001102810) *Saccharopolyspora erythraea* NRRL 2338	56/69
ORF19	606	ABC transporter	SGR_2091 (YP_001823603) *Streptomyces griseus* NBRC 13350	68/78
ORF20	649	ABC transporter	SGR_2092 (YP_001823604) *Streptomyces griseus* NBRC 13350	69/78
ORF21	334	Aminoglycoside phosphotransferase	Strop_0209 (YP_001157072) *Salinispora tropica* CNB-440	64/76
ORF22	321	UDP-Glc-4,6-dehydratase	StaB (BAC55206) *Streptomyces* sp. TP-A0274	70/80
ORF23	356	Glc-1-phosphate thymidylyltransferase	StaA (BAC55207) *Streptomyces* sp. TP-A0274	71/84
ORF24	255	Methyltransferase	MAV_4317 (YP_883454) *Mycobacterium avium* 104	44/56
ORF25	645	*C*-Methyltransferase	PctJ (BAF92592) *Streptomyces pactum*	47/63
ORF26	1087	NRPS	Npun_F2463 (YP_001865967) *Nostoc punctiforme* PCC 73102	29/48
ORF27	469	NRPS	OciB (ABI26078) *Planktothrix agardhii* NIVA-CYA 116	29/45
ORF28	402	β-Lactamase	Pjdr2DRAFT_1210 (ZP_02846103) *Paenibacillus* sp. JDR-2	44/56
ORF29	145	DNA ligase	SSAG_00834 (EDX21043) *Streptomyces* sp. Mg1	54/65
ORF30	258	ABC transporter	SSAG_06370 (EDX26579)	85/90

Table 1 Continued

Protein	*Size*[a]	*Proposed function*	*Sequence similarity (protein, accession no., origin)*	*Identity %/ similarity %*
			Streptomyces sp. Mg1	
ORF31	232	Transposase	SCP1.214 (NP_639820)	74/77
			Streptomyces coelicolor A3(2)	
ORF32	251	Transposase	SGR_6970 (YP_001828482)	94/96
			Streptomyces griseus NBRC13350	
ORF33	161	Unknown	SGR_6969 (YP_001828481)	98/100
			Streptomyces griseus NBRC13350	
ORF34	219	Endonuclease	SGR_6967 (YP_001828479)	100/100
			Streptomyces griseus NBRC13350	
ORF35	428	Transporter	SGR_6966 (YP_001828478)	99/100
			Streptomyces griseus NBRC13350	
ORF36	155	Transcriptional regulator	SGR_6965 (YP_001828477)	100/100
			Streptomyces griseus NBRC13350	
ORF37	132	Regulatory protein	SGR_6963 (YP_001828475)	100/100
			Streptomyces griseus NBRC13350	
ORF38	>182	Alkaline serine protease	SGR_6962 (YP_001828474)	100/100
			Streptomyces griseus NBRC13350	

Abbreviation: ORFs, open reading frames.
[a]Numbers are in amino acids.

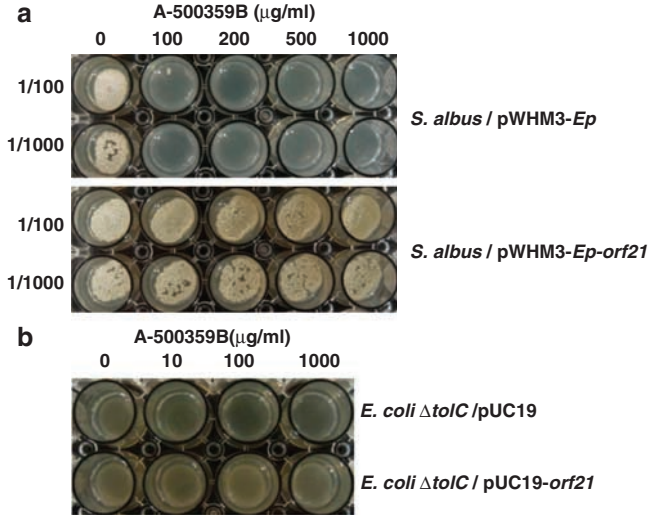

Figure 3 Overexpression of ORF21 in *S. albus* J1074 and *E. coli ΔtolC*. (**a**) *S. albus* J1074, harboring pWHM3-*Ep* and pWHM3-*Ep-orf21,* was incubated on ISP-2 agar containing 0, 100, 200, 500 and 1000 μg ml^{-1} of A-500359B. 1/100 and 1/1000 indicate the dilution ratio of cultured mycelium spotted on the agar plate. (**b**) *E. coli ΔtolC,* harboring pUC19 or pUC19-*orf21,* was incubated on LB agar containing 0, 10, 100 and 1000 μg ml^{-1} of A-500359B with 1 mM IPTG.

which catalyzes peptide bond formation, with the *orf26* gene product consisting of a condensation (C), adenylation (A) and a peptidyl-carrier protein (PCP) domain, and the *orf27* gene product consisting of a C domain. The *orf24* gene encodes a putative *S*-adenosylmethionine (SAM)-dependent methyltransferase, which is well known as a tailoring enzyme in secondary metabolite biosynthesis. The *orf25* gene product belongs to the radical SAM superfamily, which is a group of enzymes that catalyze a wide range of reactions such as protein radicals, sulfur insertion, isomerization, ring formation, oxidation, dehydrogenation and unusual methylation included in various biosyntheses of secondary metabolites.[20] In particular, the function of *orf25* was speculated to be that of *C*-methyltransferase by BLAST analysis. The deduced function of *orf28* gene is that of a β-lactamase, which is often involved in the self-resistance to β-lactam compounds. The *orf36* and *orf37* genes encode putative regulatory factors for A-500359s biosynthesis.

Functional analysis of ORF21

The *orf21* gene product, consisting of 334 amino acids, was deduced to belong to the aminoglycoside 3′-phosphotransferase family, which catalyzes the phosphorylation of aminoglycoside antibiotics and confers resistance. The gene for the aminoglycoside 3′-phosphotransferase is typically found in or near the biosynthetic gene cluster as observed for the aminoglycosides neomycin, ribostamycin, streptomycin and gentamicin, among others.[21] The 3′-hydroxy group of A-500359s is essential for translocase I inhibitory activity (unpublished data), thus consistent with ORF21 catalyzing the phosphorylation of the hexuronic acid moiety of A-500359s as a mechanism for self-resistance.

An efficient transformation system in *S. griseus* SANK60196 has not yet been developed; thus, the functional analysis of *orf21* was heterologously conducted in *S. albus* J1074 and *E. coli ΔtolC*. *S. albus* J1074 does not grow on ISP-2 agar containing more than 100 μg ml^{-1} of A-500359B. On the other hand, *E. coli* MG1655 is resistant to A-500359B at all concentrations tested. Therefore, the gene, *tolC*, encoding a multifunctional outer-membrane channel,[22] was disrupted in *E. coli* MG1655 to yield the mutant strain *E. coli ΔtolC,* which was sensitive to A-500359B and does not grow on LB agar containing 100 μg ml^{-1} of A-500359B. *S. albus* J1074 and *E. coli ΔtolC* strains were thus utilized as test organisms.

S. albus J1074, harboring pWHM3-*Ep* or pWHM3-*Ep-orf21,* was initially analyzed for resistance to A-500359B. *S. albus* J1074/pWHM3-*Ep* did not grow on a TSB agar supplemented with A-500359B. On the other hand, *S. albus* J1074/pWHM3-*Ep-orf21* acquired resistance against A-500359B and grew on ISP-2 agar at concentrations of A-500359B greater than 1000 μg ml^{-1}, as shown in Figure 3a. The *orf*21 gene was next expressed under the control of *lac* promoter in *E. coli ΔtolC*, and *E. coli ΔtolC,* harboring pUC19 or pUC19-*orf21,* was isolated and analyzed for resistance to A-500359B. *E. coli ΔtolC/*

Table 2 Primers for RT-PCR

Primers	*Sequence (5′–3′)*	*Description*
ORF1-RT-f	AAACCACCACCCGATCACG	Forward primer for *orf1*
ORF1-RT-r	AGTGGACCGTTGCGCAGG	Reverse primer for *orf1*
ORF2-RT-f	GCTCGGCAGACGCCCTGG	Forward primer for *orf2*
ORF2-RT-r	GGCGAGGTGAACAATGACG	Reverse primer for *orf2*
ORF3-RT-f	CCCAGGTCGAGCAGGAGC	Forward primer for *orf3*
ORF3-RT-r	GACCGTGCCGCAGGAACC	Reverse primer for *orf3*
ORF4-RT-f	ACGCCGCGGTGCACAAGG	Forward primer for *orf4*
ORF4-RT-r	TCGAACTCAAGGTGCTCG	Reverse primer for *orf4*
ORF5-RT-f	TGGACTGGACGCTCAAGG	Forward primer for *orf5*
ORF5-RT-r	CTCCGAGGTGCGTTTGCC	Reverse primer for *orf5*
ORF6-RT-f	CAGGCTCCGGCACGGCCC	Forward primer for *orf6*
ORF6-RT-r	CAACGTCTCGCCGGCACC	Reverse primer for *orf6*
ORF7-RT-f	CCGAGTGGGAGTTCGTCC	Forward primer for *orf7*
ORF7-RT-r	AGAGAAGGGCTTCCGCTGC	Reverse primer for *orf7*
ORF8-RT-f	CCGGAAGTCCGGCCCGACG	Forward primer for *orf8*
ORF8-RT-r	GTAGCCGGCTCAGTGCTTG	Reverse primer for *orf8*
ORF9-RT-f	GCGGAGGCCACCAACTACGC	Forward primer for *orf9*
ORF9-RT-r	GGTAGGCAGTCGTGAAGCCG	Reverse primer for *orf9*
ORF10-RT-f	GGCTATCTGCTCCTTCGAGG	Forward primer for *orf10*
ORF10-RT-r	GTCGATGATCAGCAGGTCGC	Reverse primer for *orf10*
ORF11-RT-f	ATCTGGTCCAGTACGCCGCG	Forward primer for *orf11*
ORF11-RT-r	GCCTGGACGAGGAAGTGCAG	Reverse primer for *orf11*
ORF12-RT-f	CGCTGGTGATCGACCTCTGC	Forward primer for *orf12*
ORF12-RT-r	CGACGTTGACCGTTGCAGGC	Reverse primer for *orf12*
ORF13-RT-f	ATGACCGACCAACTCATCG	Forward primer for *orf13*
ORF13-RT-r	CCAGGGTCGAGGACCGCAC	Reverse primer for *orf13*
ORF14-RT-f	GCGGAAAGCGGCCACCGC	Forward primer for *orf14*
ORF14-RT-r	GTGCTGGGAGAGTACTCC	Reverse primer for *orf14*
ORF15-RT-f	GTTCCCTGCAGCGACTCG	Forward primer for *orf15*
ORF15-RT-r	ACTCGGATTAGCCGCCG	Reverse primer for *orf15*
ORF16-RT-f	TGCTCGACGACACCCTCC	Forward primer for *orf16*
ORF16-RT-r	GATCCATGCCGATCTCGG	Reverse primer for *orf16*
ORF17-RT-f	TGCGTAAACGGCACGACG	Forward primer for *orf17*
ORF17-RT-r	TCATGTACACGCCTGGCC	Reverse primer for *orf17*
ORF18-RT-f	TGCTTGTCGACATCAACC	Forward primer for *orf18*
ORF18-RT-r	TCGGCGTGGTGCCCTCG	Reverse primer for *orf18*
ORF19-RT-f	ACGGGCACACTGGTGGCG	Forward primer for *orf19*
ORF19-RT-r	AGCCCCTGTTCGCCGACC	Reverse primer for *orf19*
ORF20-RT-f	GCTCCATGCTCGCCTACC	Forward primer for *orf20*
ORF20-RT-r	CGAGCGTCAGGCTGAAGC	Reverse primer for *orf20*
ORF21-RT-f	GCAGAAGCGTACGGTCGCG	Forward primer for *orf21*
ORF21-RT-r	GGGCTGATGCAGGGCGGTG	Reverse primer for *orf21*
ORF22-RT-f	GTCTCCGGTGGCTCCCCGGC	Forward primer for *orf22*
ORF22-RT-r	GGTGACGTGGTAGGAGCGTGC	Reverse primer for *orf22*
ORF23-RT-f	GTCCTCGCAGGAGGTTCCG	Forward primer for *orf23*
ORF23-RT-r	CGAACGGACGTGGATCGGC	Reverse primer for *orf23*
ORF24-RT-f	CCTGAACAGGTCGCCAGAG	Forward primer for *orf24*
ORF24-RT-r	TGGTCGGCGCTCCTTCTCC	Reverse primer for *orf24*
ORF25-RT-f	CTTCAGCGAGGAAGTACCGG	Forward primer for *orf25*
ORF25-RT-r	TGGTGAAGTATTCGTCGCCG	Reverse primer for *orf25*
ORF26-RT-f	AACAGGCTCCCCTGGCAGGC	Forward primer for *orf26*
ORF26-RT-r	TGTCGGCGTTCTCGTAGACG	Reverse primer for *orf26*
ORF27-RT-f	CTGCAAGAACGGCACGAGGC	Forward primer for *orf27*
ORF27-RT-r	GGGTGAATTCTCCCTGCTGG	Reverse primer for *orf27*
ORF28-RT-f	TCTCGCCTTCGAGGGAGC	Forward primer for *orf28*
ORF28-RT-r	CGAGCGGTTCGCAGATCC	Reverse primer for *orf28*
ORF29-RT-f	GTGGGACGGGTATCGGG	Forward primer for *orf29*
ORF29-RT-r	TCACGTCTCCAGCCACTC	Reverse primer for *orf29*
ORF30-RT-f	TCTCTTTCGCACTCTGGC	Forward primer for *orf30*
ORF30-RT-r	CTGCGGTGGCGTACTTGG	Reverse primer for *orf30*
ORF31-RT-f	GGCGGGATCACCGGCAGG	Forward primer for *orf31*
ORF31-RT-r	GGCCCCGGTCCGCAGCCG	Reverse primer for *orf31*
ORF32-RT-f	ACTCTCGCGCCGGGTACC	Forward primer for *orf32*
ORF32-RT-r	TCTTCAACCAGGCCAAGC	Reverse primer for *orf32*
ORF33-RT-f	GTCCACGAGGCCAGGACG	Forward primer for *orf33*
ORF33-RT-r	CAGGCGTCTTCCTCGTCC	Reverse primer for *orf33*
ORF34-RT-f	ACTCGGATTAGCCGCCG	Forward primer for *orf34*
ORF34-RT-r	GCATGTGCAGCTGCTGGG	Reverse primer for *orf34*
ORF35-RT-f	TTGTCTCGATCGGCCAGC	Forward primer for *orf35*
ORF35-RT-r	GCAGCGACAGCCCGCTCC	Reverse primer for *orf35*
ORF36-RT-f	CGAGAACCACGCCTGGACCG	Forward primer for *orf36*
ORF36-RT-r	CTGTGAGGGGGGCGCCATCG	Reverse primer for *orf36*
ORF37-RT-f	GCACCGTCAGGGCTGAGAGC	Forward primer for *orf37*
ORF37-RT-r	GGAGTGGGCGAAGAGTGCCC	Reverse primer for *orf37*
ORF38-RT-f	GTAGGCCATATCCCCGAC	Forward primer for *orf38*
ORF38-RT-r	TCCGGTCGAGGCCCCAGG	Reverse primer for *orf38*
Glk-f	CGGCGGCACGAAGATC	Forward primer for glucokinase
Glk-r	GCGCAGCTTGTTGCCG	Reverse primer for glucokinase

Abbreviation: RT-PCR, reverse transcriptase PCR.

pUC19 did not grow on LB agar supplemented with A-500359B at concentrations ranging from 10 to 1000 μg ml^{-1}. On the other hand, *E. coli ΔtolC*/pUC19-*orf21* was resistant to A-500359B within the same concentration range, as shown in Figure 3b. Importantly, both *S. albus* J1074/pWHM3-*Ep-orf21* and *E. coli ΔtolC*/pUC19-*orf21* were not resistant to other tested aminoglycoside antibiotics, neomycin, kanamycin, G418, apramycin, gentamicin and streptomycin (data not shown). Therefore, it was concluded that ORF21 confers self-resistance to A-500359B and supports the fact that the A-500359s biosynthetic gene cluster has been cloned.

Expression analysis of A-500359s biosynthetic genes

A series of *S. griseus* SANK60196 mutants: an A-500359s high-producing strain (strain HP), an A-500359s low producer (strain 37-3) and A-500359s non-producers (strains 35-4 and 37-9) (unpublished data) were utilized to test the expression levels of *orfs* of the cloned region at various time points during A-500359s production. The production of A-500359A from strain HP was about 100-fold higher than that of strain 37-3 in a 7-day culture broth, and the gene expression pattern of A-500359s biosynthetic genes was compared between these two strains. The total RNA was prepared from 4- and 7-day-cultured mycelia and was used as a template for RT-PCR analysis. Specific oligonucleotide primers were designed to amplify all 38 *orfs*, as shown in Table 2. *glk*, used as a control, was expressed in all the tested strains and no differences in the *glk* expression were detected. Most of the genes that are likely to be involved in A-500359s biosynthesis, such as *orf7–14*, *-17*, *-18*, *-21–28*, *-30* and *-37*, were expressed in strains HP and 37-3. However, their expression levels in strain HP were significantly higher than those in strain 37-3. In addition, the expression of these same *orfs* could not be detected in the non-producing strains 35-4 and 37-9 (Figure 4).

DISCUSSION

We identified an NGDH gene, *orf*22, which is expressed in the A-500359s high-producing strain HP and not expressed in a mutant strain devoid of A-500359s production. Using this cloned NGDH gene, two contiguous cosmids (ccap2 and ccap13) were isolated from around 20 000 clones of a genomic library using the DIG

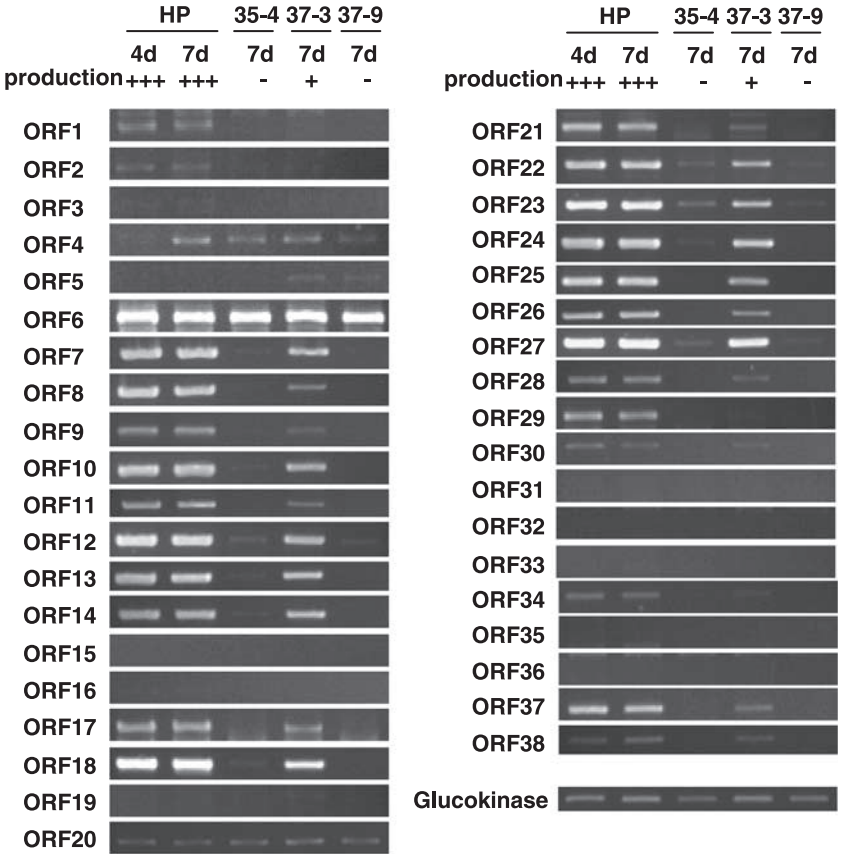

Figure 4 Gene expression analysis of 38 *orfs* in strains HP, 35-4, 37-3 and 37-9 by RT-PCR. HP, 35-4, 37-3 and 37-9 indicate the derivatives of the A-500359s producer. 4d and 7d are total RNA samples isolated from 4- and 7-day-cultured mycelia of *S. griseus* SANK60196 derivatives, respectively.

system. Sequencing analysis by the shotgun method identified 38 ORFs within the span of the 65-kb region, as shown in Figure 2 and Table 1.

To confirm the relationship between the cloned region and A-500359s biosynthesis, *orf21*, encoding a predicted aminoglycoside 3′-phosphotransferase, was heterologously expressed in *S. albus* J1074 and in *E. coli ΔtolC* to confirm its function as a mechanism for A-500359s resistance. Genes that confer self-resistance are frequently found in regions clustered with biosynthetic and regulatory genes, and this includes many examples of natural products the producing organisms of which utilize a phosphotransferase for self-resistance. For example, the neomycin resistance gene, *neo1* (AAA26699), from *Streptomyces fradiae*,[23] the ribostamycin resistance gene, *rph* (AJ748131), from *Streptomyces ribosidificus*,[24] the streptomycin resistance gene, *aphD* (AJ862840), from *S. griseus*[25] and the hygromycin resistance gene, *hyg21* (DQ314862), from *Streptomyces hygroscopicus*[26] are representative genes encoding phosphotransferases that confer selective resistance to the respective aminoglycoside. In addition to these aminoglycosides, the biosynthetic gene cluster of certain cyclic peptides also contain a gene encoding a phosphotransferase that confers resistance, including the viomycin resistance gene, *vph* (AY263398), from *Streptomyces vinaceus*[27] and the capreomycin resistance gene, *cph* (U13078), from *Streptomyces capreolus*.[28] As expected, the overexpression of *orf21* under a strong promoter permitted *S. albus* J1074 and *E. coli ΔtolC* to grow on agar plates and liquid media containing high levels of A-500359B (Figure 3), and significantly, the resistance was selective for A-500359B. This result strongly suggests that the 65-kb region including *orf21* is responsible for A-500359s biosynthesis and production.

To provide additional evidence that the A-500359s gene cluster was cloned, RT-PCR analysis was used to show that *orfs 7–14*, *17*, *18*, *21–30*, *34*, *36* and *37* were expressed in strains HP and 37-3, which were A-500359s high and low producers, respectively, but were not expressed in strains 35-4 and 37-9, which were A-500359s non-producers (Figure 4). Thus, the data support the fact that these *orf*s are required for A-500359s production. The minimal genes required for A-500359s biosynthesis were also deduced using RT-PCR and bioinformatics analyses. The A-500359s gene cluster is proposed to be contained within *orfs 7–30* and, in addition, *orf34* has an unknown function (a putative endonuclease), and *orf*36 and *orf*37 act as regulatory factors. Thus, it is proposed that the A-500359s gene cluster consists minimally of 26 *orf*s, with 18 *orf*s involved in biosynthesis, 6 *orf*s involved in resistance, regulation and transport (*orf*s 19–21, 30, 36 and 37), and 2 *orf*s of unclear function (*orf*s 29 and 34).

In conclusion, we have identified and cloned a gene cluster involved in the resistance and likely biosynthesis of A-500359s. Although the locus was identified using a probe for NGDH, it remains to be seen what role *orf*22 plays in A-500359s assembly. Despite this unknown function, we have shown that expression of the ORFs within this genetic locus is highly correlated with the production of A-500359s, and a gene (*orf*21) located within the cloned locus has been shown to confer selective resistance to A-500359s. Cloning of the A-500359s

gene cluster now permits a thorough functional characterization of the genes involved in A-500359s biosynthesis, which will ultimately facilitate combinatorial biosynthetic methods to prepare novel compounds and expand the molecular diversity of both natural and unnatural nucleoside antibiotics.

ACKNOWLEDGEMENTS

We thank Dr Ben Shen for his kind gifts in this work.

1 Takeuchi, S., Hirayama, K., Ueda, K., Sakai, H. & Yonehara, H. Blasticidin S, a new antibiotic. *J. Antibiot.* **11,** 1–5 (1958).
2 Iwasa, T., Suetomi, K. & Kusaka, T. Taxonomic study and fermentation of producing organism and antimicrobial activity of mildiomycin. *J. Antibiot.* **31,** 511–518 (1978).
3 Worthington, P. A. Antibiotics with antifungal and antibacterial activity against plant diseases. *Nat. Prod. Rep.* **5,** 47–66 (1988).
4 Kimura, K. & Bugg, D. H. Recent advances in antimicrobial nucleoside antibiotics targeting cell wall biosynthesis. *Nat. Prod. Rep.* **20,** 252–273 (2003).
5 Bormann, C., Möhrle, V. & Bruntner, C. Cloning and heterologous expression of the entire set of structural genes for nikkomycin synthesis from *Streptomyces tendae* Tü901 in *Streptomyces lividans*. *J. Bacteriol*. **178,** 1216–1218 (1996).
6 Chen, W. *et al.* Characterization of the polyoxin biosynthetic gene cluster from *Streptomyces cacaoi* and engineered production of polyoxin H. *J. Biol. Chem.* **284,** 10627–10638 (2009).
7 Lacalle, R. A., Tercero, J. A. & Jimenez, A. Cloning of the complete biosynthetic gene cluster for an aminonucleoside antibiotic, puromycin, and its regulated expression in heterologous hosts. *EMBO J.* **11,** 785–792 (1992).
8 Fernández-Moreno, M. A., Vallín, C. & Malpartida, F. Streptothricin biosynthesis is catalyzed by enzymes related to nonribosomal peptide bond formation. *J. Bacteriol.* **179,** 6929–6936 (1997).
9 Cone, M. C., Yin, X., Grochowski, L. L., Parker, M. R. & Zabriskie, T. M. The blasticidin S biosynthesis gene cluster from *Streptomyces griseochromogenes*: sequence analysis, organization, and initial characterization. *Chembiochem* **4,** 821–828 (2003).
10 McCarty, R. M. & Bandarian, V. Deciphering deazapurine biosynthesis: pathway for pyrrolopyrimidine nucleosides toyocamycin and sangivamycin. *Chem. Biol.* **15,** 790–798 (2008).
11 Li, L. *et al.* The mildiomycin biosynthesis: initial steps for sequential generation of 5-hydroxymethylcytidine 5′-monophosphate and 5-hydroxymethylcytosine in *Streptoverticillium rimofaciens* ZJU5119. *Chembiochem* **9,** 1286–1294 (2008).
12 Ohnuki, T., Muramatsu, Y., Miyakoshi, S., Takatsu, T. & Inukai, M. Studies on novel bacterial translocase I inhibitors, A-500359s. IV. Biosynthesis of A-500359s. *J. Antibiot.* **56,** 268–279 (2003).
13 Sambrook, J. & Russell, D. W. *Molecular Cloning: A Laboratory Manual* 3rd edn, (Cold Spring Harbor Laboratory Press: Cold Spring Harbor, NY, 2001).
14 Weber, J. M., Wierman, C. K. & Hutchinson, C. R. Genetic analysis of erythromycin production in *Streptomyces erythreus*. *J. Bacteriol.* **164,** 425–433 (1985).
15 Shen, B & Hutchinson, CR Deciphering the mechanism for the assembly of aromatic polyketides by a bacterial polyketide synthase. *Proc. Natl Acad. Sci. USA* **93,** 6600–6604 (1996).
16 Muramatsu, Y. *et al*. Studies on novel bacterial translocase I inhibitors, A-500359s. V. Enhanced production of capuramycin and A-500359A in *Streptomyces griseus* SANK60196. *J. Antibiot.* **59,** 601–606 (2006).
17 Decker, H. *et al*. A general approach for cloning and characterizing dNDP-glucose dehydratase gene from actinomycetes. *FEMS Microbiol. Lett.* **141,** 195–201 (1996).
18 Link, A. J., Phillips, D. & Church, G. M. Methods for generating precise deletions and insertions in the genome of wild-type *Escherichia coli*: application to open reading frame characterization. *J. Bacteriol.* **179,** 6228–6237 (1997).
19 Kieser, T., Bibb, M., Buttner, M., Chater, K. F. & Hopwood, D. A. *Practical Streptomyces Genetics* (The John Innes Foundation: Norwich, UK, 2000).
20 Sofia, H. J., Chen, G., Hetzler, B. G., Reyes-Spindola, J. F. & Miller, N. E. Radical SAM, a novel protein superfamily linking unresolved steps in familiar biosynthetic pathways with radical mechanisms: functional characterization using new analysis and information visualization methods. *Nucleic Acids Res.* **29,** 1097–1106 (2001).
21 Flatt, P. M. & Mahmud, T. Biosynthesis of aminocyclitol–aminoglycoside antibiotics and related compounds. *Nat. Prod. Rep.* **24,** 358–392 (2007).
22 Koronakis, V. TolC-the bacterial exit duct for proteins and drugs. *FEBS Lett.* **555,** 66–71 (2003).
23 Huang, F. *et al.* The neomycin biosynthetic gene cluster of *Streptomyces fradiae* NCIMB 8233: characterisation of an aminotransferase involved in the formation of 2-deoxystreptamine. *Org. Biomol. Chem.* **3,** 1410–1418 (2005).
24 Subba, B. *et al*. The ribostamycin biosynthetic gene cluster in *Streptomyces ribosidificus*: comparison with butirosin biosynthesis. *Mol. Cells* **20,** 90–96 (2005).
25 Distler, J. *et al*. Gene cluster for streptomycin biosynthesis in *Streptomyces griseus*: nucleotide sequence of three genes and analysis of transcriptional activity. *Nucleic Acids Res.* **15,** 8041–8056 (1987).
26 Palaniappan, N., Ayers, S., Gupta, S., Habib, e. I.-S. & Reynolds, K. A. Production of Hygromycin A analogs in *Streptomyces hygroscopicus* NRRL 2388 through identification and manipulation of the biosynthetic gene cluster. *Chem. Biol.* **13,** 753–764 (2006).
27 Yin, X., O'Hare, T., Gould, S. J. & Zabriskie, T. M. Identification and cloning of genes encoding viomycin biosynthesis from *Streptomyces vinaceus* and evidence for involvement of a rare oxygenase. *Gene* **312,** 215–224 (2003).
28 Felnagle, E. A., Rondon, M. R., Berti, A. D., Crosby, H. A. & Thomas, M. G. Identification of the biosynthetic gene cluster and an additional gene for resistance to the antituberculosis drug capreomycin. *Appl. Environ. Microbiol.* **73,** 4162–4170 (2007).

The Journal of Antibiotics (2009) 62, 333–334

www.nature.com/ja

NOTE

Isodeoxyhelicobasidin, a novel human neutrophil elastase inhibitor from the culture broth of *Volvariella bombycina*

Guang-Hua Xu[1], Young-Hee Kim[1], Soo-Jin Choo[1], In-Ja Ryoo[1], Chang-Ji Zheng[1,2], Soon-Ja Seok[3], Won-Gon Kim[1] and Ick-Dong Yoo[1]

The Journal of Antibiotics (2009) **62,** 333–334; doi:10.1038/ja.2009.24; published online 27 March 2009

Keywords: human neutrophil elastase; isodeoxyhelicobasidin; sesquiterpenoid; *Volvariella bombycina*

Elastin, an important structural protein of extracellular matrix (ECM), is the main component of elastic fiber, which provides resilience and elasticity to many tissues, such as the skin, lungs, ligaments and arterial walls.[1,2] Human neutrophil elastase (HNE), a serine protease primarily located in the azurophil granules of polymorphonuclear leukocytes, is the only enzyme capable of degrading ECM proteins, such as elastin, collagen, fibronectin, laminin and proteoglycan.[3] Biologically, elastase activity significantly increases with age and results in a reduced skin elastic property.[4]

In the course of our screening program for HNE inhibitors, we isolated a novel compound, isodeoxyhelicobasidin (**1**), from the culture broth of *Volvariella bombycina* (Figure 1). We report herein the fermentation, isolation, structure elucidation and biological activities of **1**.

The strain of *V. bombycina* (MKACC 53745) was provided by the Korea Agricultural Culture Collection of the National Institute of Agricultural Biotechnology, Suwon, Republic of Korea. The producing strain of *V. bombycina* pre-grown on a potato dextrose agar (PDA; Difco, Sparks, MD, USA) slant was inoculated into a 500-ml Erlenmeyer flask containing 100 ml of yeast peptone sucrose (YPS) medium consisting of 2% glucose, 0.5% polypeptone, 0.2% yeast extract, 0.1% KH_2PO_4 and 0.05% $MgSO_4{\cdot}7H_2O$ (pH 6.6), and cultured on a rotary shaker (153 r.p.m.) for 7 days at 27 °C. For fermentation, the seed culture was aseptically transferred into a 5-l jar fermenter containing 3.5 l of the above medium, and cultivation was carried out at 28 °C for 7 days with aeration of 2 l min^{-1} and agitation of 250 r.p.m.[5,6] The collected mycelial cake from the whole fermented broth (10 liters) was extracted with acetone and the extract was concentrated *in vacuo* to an aqueous solution, which was then extracted thrice with equal volume of EtOAc. The EtOAc layer (5 g) was loaded on a silica gel column and eluted with CH_2Cl_2–MeOH in a gradient mode (20:1 → 1:1), the active fraction was subjected to Sephadex LH-20 (GE Healthcare Bio-Sciences AB, Uppsala, Sweden) column chromatography and eluted with CH_2Cl_2–MeOH (1:1), and then purified by YMC C_{18} preparative HPLC (20×250 mm, flow rate=4 ml min^{-1}, MeOH–H_2O=85:15) to afford **1** (6 mg, t_R=33 min).

Compound **1** was obtained as a yellowish powder; $[\alpha]_D^{20}$–25.0 (*c* 0.2, MeOH); UV ($CHCl_3$) λ_{max} nm (log ε): 266 (4.02); IR (KBr) ν_{max} (cm^{-1}): 3434, 2964, 1650, 1633, 1368, 1304, 1210, 896; ^{1}H NMR ($CDCl_3$, 400 MHz): δ 7.55 (1H, s, 5-OH), 6.44 (1H, q, *J*=1.6 Hz, H-2), 2.93 (1H, m, H-8a), 2.04 (3H, d, *J*=1.60 Hz, H-15), 1.76-1.74 (1H, m, H-9a), 1.69-1.67 (1H, m, H-8b), 1.66-1.64 (1H, m, H-10a), 1.63-1.59 (1H, m, H-9b), 1.51-1.44 (1H, m, H-10b), 1.33 (3H, s, H-14), 1.12 (3H, s, H-12), 0.84 (3H, s, H-13); ^{13}C NMR ($CDCl_3$, 100 MHz): *ä* 188.9 (C-1), 184.8 (C-4), 152.1 (C-5), 139.0 (C-3), 138.4 (C-2), 126.3 (C-6), 51.5 (C-7), 46.3 (C-11), 41.6 (C-10), 39.1 (C-8), 27.8 (C-13), 25.9 (C-12), 24.2 (C-14), 21.3 (C-9), 14.5 (C-15); HR-ESI-MS (*m/z*): 247.1342 $[M\text{-}H]^-$ (calcd for $C_{15}H_{19}O_3$, 247.1340). The molecular formula of **1**, $C_{15}H_{20}O_3$, was determined by high-resolution mass spectrometry. The UV spectrum of **1** showed an absorption maximum at 266 nm, indicating the presence of 1,4-benzoquinone chromophore.[7,8] The IR spectrum revealed characteristic absorption bands for hydroxyl group at 3434 cm^{-1} and conjugated carbonyl group at 1650 cm^{-1}.[9] The ^{1}H NMR spectrum of **1** displayed an enolic hydroxyl proton at δ_H 7.55 (1H, s, 5-OH), a quinonoid proton at δ_H 6.44 (1H, q, *J*=1.6 Hz, H-2) and a quinonoid methyl at δ_H 2.04 (3H, d, *J*=1.6 Hz, H-15). In addition, it also displayed signals for three tertiary methyl and three methylene groups, which were attributed to cyclopentane ring bearing three tertiary methyl groups. The ^{13}C NMR spectrum of **1** exhibited 15 carbon resonances consisting of three tertiary methyls, one quinonoid methyl, three methylenes, two quaternary aliphatic carbons, two carbonyl groups, one quinonoid methine

[1]Chemical Biology Research Center, Korea Research Institute of Bioscience and Biotechnology, Yuseong-gu, Daejeon, Korea; [2]Key Laboratory of Natural Resources and Functional Molecules of Changbai Mountain, Affiliated Ministry of Education, Yanbian University College of Pharmacy, Yanji, Jilin, PR China and [3]Rural Development Administration (RDA), National Institute of Agricultural Science and Technology, Suwon, Korea
Correspondence: Dr I-D Yoo, Chemical Biology Research Center, Korea Research Institute of Bioscience and Biotechnology, 111 Gwahangno, Yuseong-gu, Daejeon 305-806, Korea.
E-mail: idyoo@kribb.re.kr
Received 10 February 2009; revised 3 March 2009; accepted 4 March 2009; published online 27 March 2009

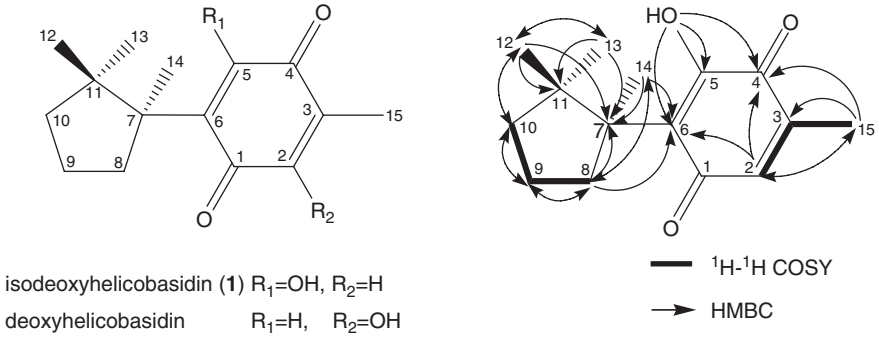

Figure 1 Structure, 1H-1H COSY and HMBC correlations of isodeoxyhelicobasidin (**1**).

Table 1 HNE inhibitory activity of isodeoxyhelicobasidin (1)[a]

	Inhibition ratio for HNE (%)					
Compound	*100 μM*	*30 μM*	*10 μM*	*3 μM*	*1 μM*	*IC_{50}[b] (μM)*
1	70.6 ± 0.7	64.4 ± 2.0	57.9 ± 0.8	38.3 ± 1.4	27.2 ± 0.3	9.0 ± 0.9
EGCG	65.9 ± 1.3	62.4 ± 0.8	47.3 ± 1.3	25.8 ± 1.4	17.3 ± 0.8	12.9 ± 0.3

Abbreviations: EGCG, epigallocatechin gallate; HNE, human neutrophil elastase.
[a]Results are expressed as means ± s.d. (n=3).
[b]IC_{50} indicates the concentration (μM) at which the inhibition percentage of HNE activity was 50%, and the values were determined by regression analysis.

and three quaternary aromatic carbons. All protonated carbons and their protons were assigned by ^{1}H-^{1}H COSY and heteronuclear multiple quantum correlation (HMQC) experiments. The above mentioned spectroscopic data suggested that compound **1** was a cuparene-type sesquiterpenoid,[10] and the gross structure was further confirmed by COSY and heteronuclear multiple-bond correlation (HMBC) experiments (Figure 1). The COSY correlation of the quinonoid methyl protons at δ_H 2.04 (H-15) with the quinonoid proton at δ_H 6.44 (1H, q, J=1.6 Hz, H-2) and HMBC correlations of H-15 with C-2 at δ_C 138.4, C-3 at δ_C 139.0 and C-4 at δ_C 184.8 suggested that the quinonoid methyl group was at C-5 and the quinonoid methine was at C-2. The hydroxyl proton at δ_H 7.55 (OH-5) was long-range coupled to C-4, C-5 at δ_C 152.1 and C-6 at δ_C 126.3 in HMBC spectrum. In addition, HMBC correlations of the tertiary methyl protons at δ_H 1.33 (H-14) with C-6, C-7 at δ_C 51.5 and C-8 at δ_C 39.1 were observed. These spectral data indicated that **1** was a derivative hydroxylated at C-5 and dehydroxylated at C-2 of deoxyhelicobasidin, which has been isolated from *Helicobasidium mompa* Tanaka.[11] The stereochemistry at C-7 of **1** was assigned as *S* configuration by comparison with deoxyhelicobasidin, which also showed a negative optical rotation. Thus, the structure of **1** was established to be (*S*)-5-hydroxy-3-methyl-6-(1,2,2-trimethylcyclopentyl)-1,4-benzoquinone and named as isodeoxyhelicobasidin.

The inhibitory activity of **1** on HNE was evaluated with earlier described procedure.[12] Briefly, each well of a 96-well plate containing 100 μl of the following reagents: 10 mM Tris-HCl buffer (pH 7.5), 1.4 mM MeO-Suc-Ala-Ala-Pro-Val-*p*-nitroanilide, 0.18 U HNE and the sample at various concentrations were incubated for 1 h at 37 °C in the dark. After the reaction was stopped by addition of 100 μl soybean trypsin inhibitor of 0.2 mg ml^{-1}, absorbance was immediately measured at 405 nm. Epigallocatechin gallate (EGCG) was used as a positive control. As a result, compound **1** dose-dependently inhibited HNE activity with an IC_{50} value of 9.0 μm, which was comparable to the positive control, EGCG (IC_{50}, 12.9 μm) (Table 1). Compound **1** also showed antibacterial activity against several gram-positive bacteria including *S. aureus* 503, methicillin-resistant *S. aureus* CCARM 3167 (MRSA), quinolone-resistant *S. aureus* CCARM 3505 (QRSA), *Bacillus subtilis* 1021, *Staphylococcus epidermidis* 3958 and *Streptococcus mutans* 3065 with MIC values of 3.1–12.4 μg ml^{-1}.[13] In conclusion, compound **1** was a new analog of helicobasidin and lagopodin B, which were earlier isolated from *H. mompa* Tanaka and *Coprinus cinereus*, respectively,[14,15] and the potent HNE inhibitory activity of **1** suggested that it could be useful for the development of anti-aging cosmetics.

ACKNOWLEDGEMENTS

This work was supported by a grant from the Korea Health 21 R&D Project, Ministry of Health & Welfare, Republic of Korea (A050432).

1 Wiedow, O., Schroder, J. M., Gregory, H., Young, J. A. & Christophers, E. Elafin: an elastase-specific inhibitor of human skin. Purification, characterization, and complete amino acid sequence. *J. Biol. Chem.* **265,** 14791–14795 (1990).
2 Xu, G. H., Ryoo, I. J., Kim, Y. H., Choo, S. J. & Yoo, I. D. Free radical scavenging and antielastase activities of flavonoids from the fruits of *Thuja orientalis*. *Arch. Pharm. Res.* **32,** 275–282 (2009).
3 Siedle, B. *et al.* Sesquiterpene lactones as inhibitors of human neutrophil elastase. *Bioorg. Med. Chem.* **10,** 2855–2861 (2002).
4 Robert, L. Extracellular matrix and aging: a review of mechanisms and interventions. *Cosmet. Toiletries* **116,** 61–70 (2001).
5 Oh, S. U., Yun, B. S., Lee, S. J., Kim, J. H. & Yoo, I. D. Atroviridins A–C and neoatroviridins A–D, novel peptaibol antibiotics produced by *Trichoderma atroviride* F80317. I. Taxonomy, fermentation, isolation and biological activities. *J. Antibiot.* **55,** 557–564 (2002).
6 Kim, J. P. *et al.* Melanocins A, B and C, new melanin synthesis inhibitors produced by *Eupenicillium shearii*. I. Taxonomy, fermentation, isolation and biological properties. *J. Antibiot.* **56,** 993–999 (2003).
7 Yates, P., Ardao, M. I. & Fieser, L. F. The infrared spectra of *p*-benzoquinones. *J. Am. Chem. Soc.* **78,** 650–652 (1956).
8 Bycroft, B. W. & Roberts-John, C. The structure of nidulin. *J. Org. Chem.* **28,** 1429–1430 (1963).
9 Correia-Alves, A., Moreira, M. M., Paul, M. I. & Cruz-Costa, M. A. A series of eleven dialkyl-hydroxy-*p*-benzoquinones from *Cyperus capitatus*. *Phytochemistry* **31,** 2825–2827 (1992).
10 Toyota, M., Koyama, H. & Asakawa, Y. Sesquiterpenoids from the three Japanese liverworts *Lejeunea aquatica*, *L. flava* and *L. japonica*. *Phytochemistry* **46,** 145–150 (1997).
11 Natori, S., Inoue, Y. & Nishikawa, H. The structures of mompain and deoxyhelicobasidin and the biosynthesis of helicobasidin, quinonoid metabolites of *Helicobasidium mompa* Tanaka. *Chem. Pharm. Bull.* **15,** 380–390 (1967).
12 Benedek, B., Kopp, B. & Melzig, M. F. *Achillea millefolium* L. s.l. - Is the anti-inflammatory activity mediated by protease inhibition? *J. Ethnopharmacol.* **113,** 312–317 (2007).
13 Zheng, C. J., Yu, H. E., Kim, E. H. & Kim, W. G. Viridicatumtoxin B, a new anti-MRSA agent from *Penicillium sp.* FR11. *J. Antibiot.* **61,** 633–637 (2008).
14 Natori, S., Nishikawa, H. & Ogawa, H. Structure of helicobasidin, a novel benzoquinone from *Helicobasidium mompa* Tanaka. *Chem. Pharm. Bull.* **12,** 236–243 (1964).
15 Bu'Lock, J. & Darbyshire, J. Lagopodin metabolites and artefacts in cultures of *Coprinus*. *Phytochemistry* **15,** 2004 (1976).

The Journal of Antibiotics (2009) 62, 335–338

www.nature.com/ja

NOTE

Macrolepiotin, a new indole alkaloid from *Macrolepiota neomastoidea*

Ki Hyun Kim[1], Ki Moon Park[2], Sang Un Choi[3] and Kang Ro Lee[1]

The Journal of Antibiotics (2009) **62,** 335–338; doi:10.1038/ja.2009.30; published online 17 April 2009

Keywords: Agaricaceae; cytotoxicity; indole alkaloid; *Macrolepiota neomastoidea*; macrolepiotin

The fungi of the genus, *Macrolepiota*, are grouped under the family *Agaricaceae* (division *Basidiomycota*) and comprise ~20 species. Various biological activities of the genus, *Macrolepiota*, have been reported, including anti-microbial, antioxidant and enzyme (trypsin, monophenolase) activities.[1–5] However, few species have been studied with regard to their secondary metabolites. Only several free amino acids, fatty acids and sterols have been reported from *Macrolepiota excoriata*, *Macrolepiota procera* and *Macrolepiota thacodes*.[6] Therefore, as part of a systematic study of Korean mushrooms,[7] we investigated the constituents of the fruiting bodies of the mushroom *Macrolepiota neomastoidea*, widely distributed throughout Korea and other East Asian countries. This is a poisonous mushroom known to cause severe gastrointestinal symptoms, including intestinal irritation, vomiting and profuse diarrhea.[8] Thus far, little work has been done on the chemical constituents of *M. neomastoidea*, except for the isolation of two compounds, lepiotins A and B.[9] Recently, we reported the isolation of lepiotin C and (*R*)-5-hydroxypyrrolidin-2-one, as well as lepiotins A and B.[10] As part of a continuing study, we have further isolated a new indole alkaloid named macrolepiotin (**1**), together with four known ergosterols, (22*E*,24*R*)-5α,8α-epidioxyergosta-6,9,22-triene-3β-ol (**2**),[11] (22*E*,24*R*)-5α,8α-epidioxyergosta-6,22-dien-3β-ol (**3**),[12] (24*S*)-ergost-7-en-3β-ol (**4**)[13] and (22*E*,24*R*)-5α,6α-epoxyergosta-9(14),22-diene-3β,7α-diol (**5**).[14] In this study, we describe the isolation and structural elucidation of **1** and the cytotoxic activities of compounds **1–5**.

MATERIALS AND METHODS

General

Optical rotations were measured on a Jasco P-1020 polarimeter (Jasco, Easton, MD, USA) in MeOH. IR spectra were recorded on a Bruker IFS-66/S FT-IR spectrometer (Bruker, Karlsruhe, Germany). UV spectra were recorded using a Schimadzu UV-1601 UV–visible spectrophotometer (Schimadzu, Kyoto, Japan). FAB and HR-FAB mass spectra were obtained on a JEOL JMS700 mass spectrometer (JEOL, Peabody, MA, USA). NMR spectra were recorded on a Varian UNITY INOVA 500 NMR spectrometer (Varian, Palo Alto, CA, USA) operating at 500 (^{1}H) and 125 MHz (^{13}C), respectively. Preparative HPLC was carried out using a Gilson 306 pump (Gilson, Middleton, WI, USA) with Shodex refractive index detector (Shodex, New York, NY, USA). Low-pressure liquid chromatography was carried out over a Merck Lichroprep Lobar-A Si 60 (Merck, Darmstadt, Germany) (240×10 mm) or a Lichroprep Lobar-A RP-18 (Merck) (240×10 mm) column using a FMI QSY-0 pump (Teledyne Isco, Lincoln, NE, USA). Silica gel 60 (Merck, 70–230 and 230–400 mesh) and RP-C_{18} silica gel (Merck, 230–400 mesh) were used for column chromatography. Spots were detected on a TLC under UV light or by heating after spraying with 10% H_2SO_4 in C_2H_5OH (v/v).

Mushroom material

The fresh fruiting bodies of *M. neomastoidea* were collected in November 2005 at Mt Jiri, Namwon of Jeonbuk Province, Korea. A voucher specimen (SKKU-2005-11) of the mushroom was deposited at the College of Pharmacy in Sungkyunkwan University, Korea.

Extraction and isolation

The air-dried and powdered fruiting bodies of *M. neomastoidea* (132 g) were extracted with 80% MeOH at room temperature to afford a methanolic extract (21.4 g). This extract was suspended in H_2O and partitioned with *n*-hexane, $CHCl_3$ and *n*-BuOH successively, and the solvent was removed thereafter to yield *n*-hexane (3.3 g), $CHCl_3$ (283 mg) and *n*-BuOH fractions (10.4 g). The *n*-hexane soluble fraction (3.3 g) was subjected to silica gel column chromatography with *n*-hexane-EtOAc (1:1) as the eluent to give seven fractions (H1–H7). Fraction H4 (75 mg) was further purified by RP-C_{18} preparative HPLC (Econosil RP-18 10 μ column, 250×22 mm; 100% MeOH) to give pure compounds **2** (6 mg) and **3** (35 mg). The $CHCl_3$ soluble fraction (283 mg) was subjected to a silica Lobar A-column with $CHCl_3$–MeOH (10:1) as the eluent to give seven fractions (C1–C7). Fraction C4 (55 mg) was further purified using a silica gel Waters Sep-Pak Vac 6cc ($CHCl_3$–MeOH, 22:1; Waters, Milford, MA, USA) to afford pure compounds **4** (4 mg) and **5** (3 mg). The *n*-BuOH soluble fraction (10.4 g) was subjected to a RP-C_{18} silica gel column chromatography with a gradient solvent system of MeOH–H_2O (0:1→1:1) as the eluent to give nine fractions (B1–B9). Fraction B8 (80 mg) was subjected to a RP-C_{18} silica Lobar A-column with 50% MeOH as the eluent to give two sub-fractions (B81–B82). Sub-fraction B81 (30 mg) was further

[1]Natural Products Laboratory, College of Pharmacy, Sungkyunkwan University, Suwon, Korea; [2]Department of Food Science and Biotechnology, Sungkyunkawn University, Suwon, Korea and [3]Bio-organic Science Division, Pharmacology Research Center, Korea Research Institute of Chemical Technology, Teajeon, Korea
Correspondence: Professor Dr KR Lee, Natural Products Laboratory, College of Pharmacy, Sungkyunkwan University, 300 Chonchon-dong, Jangan-ku, Suwon 440-746, Korea.
E-mail: krlee@skku.ac.kr
Received 6 February 2009; revised 19 March 2009; accepted 24 March 2009; published online 17 April 2009

purified by RP-C_{18} preparative HPLC, as described above to give the pure compound **1** (7 mg).

Physico-chemical properties

Macrolepiotin (**1**). Yellowish gum, $[\alpha]_D^{25}$: −6.5 (*c* 0.25, MeOH), UV λ_{max} (MeOH) nm (log ϵ) 231 (3.66), 280 (5.51), IR (KBr) 3443, 2253, 1662, 1028, 824, 761 cm^{-1}. ^1H- and ^{13}C-NMR spectral data are shown in Table 1. FAB-MS *m/z* 580 $[M+H]^+$. HR-FAB-MS (positive-ion mode) *m/z* 580.2665 ($[M+H]^+$, $C_{31}H_{38}N_3O_8$, calcd. for 580.2659).

Test for cytotoxicity *in vitro*

A sulforhodamin B bioassay (SRB) was used to determine the cytotoxicity of each compound against four cultured human cancer cell lines.[15] The assays were performed at the Korea Research Institute of Chemical Technology. The cell lines used were A549 (non-small-cell lung carcinoma), SK-OV-3 (ovary malignant ascites), SK-MEL-2 (skin melanoma) and HCT (colon adenocarcinoma). Doxorubicin was used as the positive control. The cytotoxicities of doxorubicin against A549, SK-OV-3, SK-MEL-2 and HCT cell lines were IC_{50} 0.16, 0.38, 0.04 and 0.82 μM, respectively.

Compound **1** was obtained as a yellowish gum, and was found to be positive for Dragendorff's reagent. Its molecular formula was determined to be $C_{31}H_{37}N_3O_8$ from the $[M+H]^+$ peak at *m/z* 580.2665 (calcd. for $C_{31}H_{38}N_3O_8$ 580.2659) in the positive-ion high-resolution (HR)-FAB-MS spectrum. The IR spectrum indicated that **1** possessed hydroxyl (3443 cm^{-1}) and carbonyl (1662 cm^{-1}) groups. Its UV spectrum revealed absorptions at 231 and 280 nm, suggesting chromophores of amide functional group and benzene rings in the molecule. The physico-chemical properties of **1** are summarized in the Materials and methods section. The ^1H- and ^{13}C-NMR spectral data of **1** are shown in Table 1.

Table 1 ^1H- and ^{13}C-NMR data of **1**

Position	δ_C	δ_H
1		10.93 (1H, s)
2	128.6	
3	107.5	
3a	126.1	
4	117.7	7.45 (1H, d, 7.5)
5	118.7	7.00 (1H, t, 7.5)
6	121.1	7.08 (1H, t, 7.5)
7	111.1	7.34 (1H, d, 7.5)
7a	136.2	
8	22.8	2.93 (1H, m), 3.18 (1H, m)
9	56.4	3.96 (1H, m)
10	169.4	
11	39.1	4.21 (1H, q, 7.5)
12	19.0	1.41 (3H, d, 7.5)
13	180.4	
1′		
2′	173.4	
3′	29.2	2.35 (1H, m), 2.60 (1H, m)
4′	23.5	2.02 (1H, m), 2.27 (1H, m)
5′	91.4	5.33 (1H, dd, 5.5, 1.0)
6′	129.3	
7′,11′	124.9	7.24 (2H, dd, 8.0, 2.0)
8′,10′	115.1	6.76 (2H, dd, 8.0, 2.0)
9′	155.2	
5′-OMe	52.6	3.16 (3H, s)
1″	64.3	3.76 (dd, 9.0, 6.5)
2″	37.2	2.05 (1H, m)
3″	28.5	1.42 (1H, m), 1.65 (1H, m)
4″	11.7	0.96 (3H, t, 7.5)
5″	15.0	1.01 (3H, d, 7.0)
6″	174.2	

NMR data were obtained in 500 MHz for ^1H and 125 MHz for ^{13}C in DMSO, and values in parentheses are coupling constants in Hz.

The ^1H-NMR spectrum (Table 1) of **1** showed signals for the presence of three methyl groups at δ_H 0.96 (t, H-4″), 1.01 (d, H-5″) and 1.41 (d, H-12), four methylene groups at δ_H 1.42, 1.65 (m, H-3″), 2.02, 2.27 (m, H-4′), 2.35, 2.60 (m, H-3′) and 2.93, 3.18 (m, H-8), five methine groups at δ_H 2.05 (m, H-2″), 3.76 (dd, H-1″), 3.96 (m, H-9), 4.21 (q, H-11) and 5.33 (dd, H-5′) and one methoxyl group at δ_H 3.16 (s, 5′-OMe). The 1,4-disubstituted aromatic protons were observed at δ_H 6.76 (dd, H-8′, 10′), 7.24 (dd, H-7′, 11′) and four 1,2-disubstituted aromatic protons were shown at δ_H 7.00 (t, H-5), 7.08 (t, H-6), 7.34 (d, H-7) and 7.45 (d, H-4). A signal of downfield resonance at δ_H 10.93 (s, H-1) with no heteronuclear multiple quantum coherence (HMQC) correlations with any carbon signal was assignable to the amide proton. An analysis of ^1H- and ^{13}C-NMR spectra together with HMQC indicated that 31 carbon signals of **1** were composed of 4 carbonyl carbons, 14 olefinic carbons (including 12 aromatic carbons, 2 quaternary carbons), 5 methine carbons (including 1 oxygenated methine carbon), 4 methylene carbons, 3 methyl carbons and 1 methoxyl carbon. Analysis of ^1H,^1H-COSY data, HMQC and heteronuclear multiple bond correlation (HMBC) experiments established the presence of three partial structures, namely lepiotin B (partial unit **A**), isoleucine (partial unit **B**) and indole derivative (partial unit **C**) (Figure 1).

The presence of lepiotin B (partial unit **A**) in **1** was apparent from the two sets of methine signals (δ_H/δ_C; 6.76/115.1, 7.24/124.9) on a 1,4-disubstituted aromatic ring, a methine signal (δ_H/δ_C; 5.33/91.4) adjacent to two hetero atoms and from a methyl signal (δ_H/δ_C; 3.16/52.6). The presence of a γ-lactam ring was confirmed from the HMBC correlations, in which correlations of H-5′ with C-2′ (δ_C 173.4), C-3′ (δ_C 29.2) and C-4′ (δ_C 23.5) were observed. This signal at H-5′ was further coupled with a methoxyl group (δ_C 52.6), which implied that the position of the methoxyl group was at C-5′. Therefore, the partial unit **A** was assigned as lepiotin B by the above evidence. The lepiotin B, having a γ-lactam and a phenol ring, was an unusual alkaloid, and the main constituent isolated from this mushroom.[9]

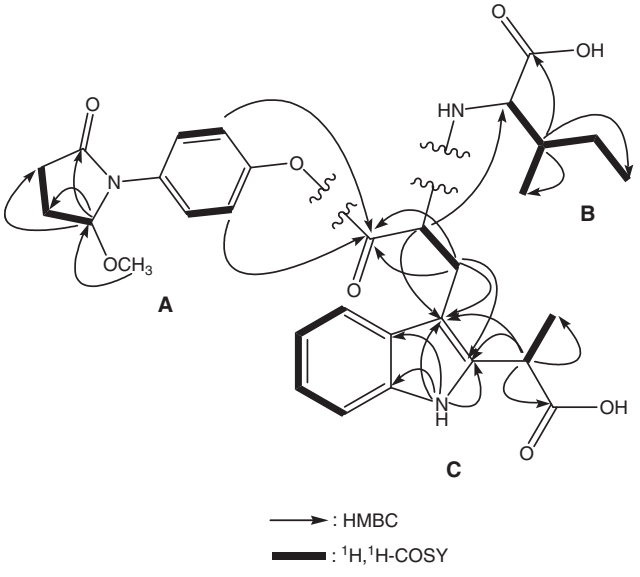

Figure 1 Key HMBC, ^1H,^1H-COSY correlations and partial units (**A**–**C**) of **1**.

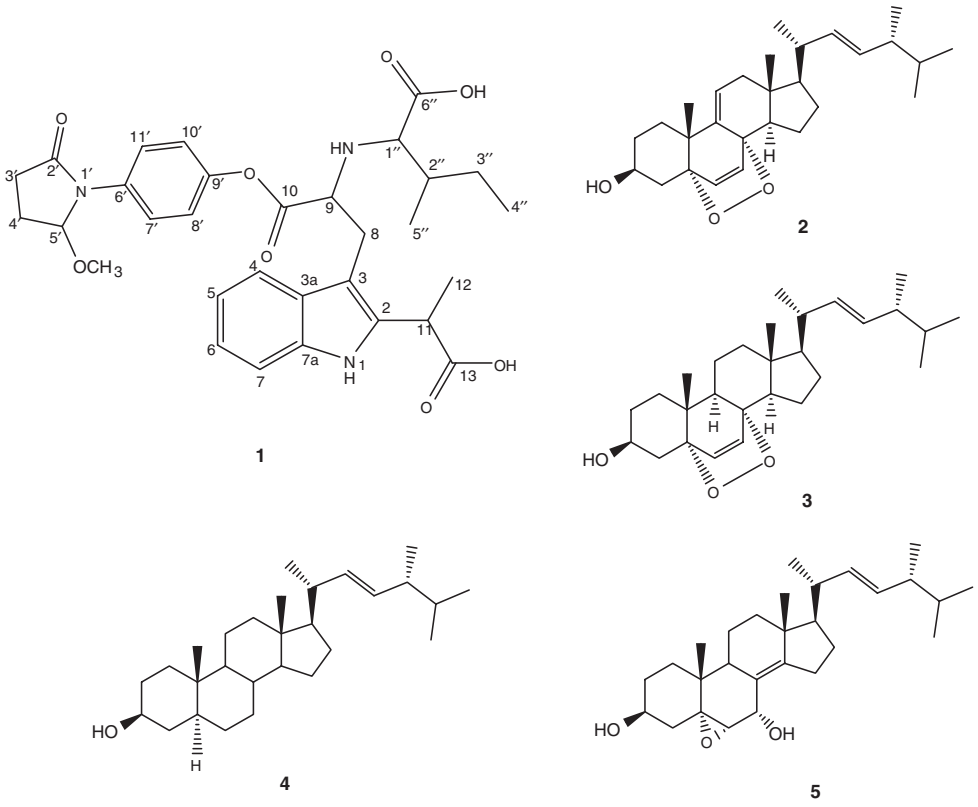

Figure 2 Structures of **1**–**5**.

Table 2 Cytotoxic activities of compounds (1–5) isolated from *Macrolepiota neomastoidea*

	IC_{50} (μM)			
Compound	*A549*	*SK-OV-3*	*SK-MEL-2*	*HCT-15*
1	>30.0	>30.0	>30.0	>30.0
2	25.6	17.5	11.8	17.1
3	14.0	17.9	12.7	10.0
4	>30.0	>30.0	>30.0	28.3
5	>30.0	16.5	>30.0	>30.0
Doxorubicin	0.16	0.38	0.04	0.82

IC_{50} value of compounds against each cancer cell line, which was defined as the concentration (μM) that caused 50% inhibition of cell growth *in vitro*.

A second partial unit **B** was assigned as isoleucine by the following NMR data. The ^{1}H-NMR spectrum clearly indicated the appearance of two methyl groups at C-4″ (δ_H 0.96) and C-5″ (δ_H 1.01), a methylene group at C-3″ (δ_H 1.42, 1.65), as well as two methine groups at C-1″ (δ_H 3.76) and C-2″ (δ_H 2.05). The NMR resonances were similar to those of the isoleucine,[16] which showed ^{1}H,^{1}H-COSY correlations between H-1″/H-2″, H-2″/H-5″, H-2″/H-3″ and H-3″/H-4″. In addition, correlations were observed between H-2″ (δ_H 2.05) and C-4″ (δ_C 11.7), C-5″ (δ_C 15.0) and C-6″ (δ_C 174.2) in the HMBC spectrum.

The remaining fragment consisting of $C_{14}H_{13}NO_3$ was elucidated as an indole derivative (partial unit **C**) by the interpretation of the ^{1}H,^{1}H-COSY, HMQC and HMBC data. The presence of the indole skeleton was apparent from 1,2-disubstituted aromatic ring signals (δ_H; 7.00 (t, H-5), 7.08 (t, H-6), 7.34 (d, H-7), 7.45 (d, H-4), δ_C; 111.1, 117.7, 118.7, 121.1, 126.1, 136.2). The downfield signal (NH-1) of an amide proton showed HMBC correlation to four quaternary olefinic carbons (C-2, 3, 3a, 7a) (Figure 1). In addition, ^{1}H,^{1}H-COSY correlation between the methyl proton signal at δ_H 1.41 (d, H-12) and the methine proton signal at δ_H 4.21 (q, H-11) and HMBC correlations between the methine proton signal at δ_H 4.21 (q, H-11) and C-2 (δ_C 128.6), C-3 (δ_C 107.5), C-12 (δ_C 19.0) and C-13 (δ_C 180.4) were observed. This suggested that the propionic acid was located at C-2. HMBC correlations from methylene proton signals at δ_H 2.93, 3.18 (m, H-8) to C-2 (δ_C 128.6), C-3 (δ_C 107.5), C-9 (δ_C 56.4) and C-10 (δ_C 169.4) suggested a connection between the indole skeleton and 2-amino propionic acid through carbon C-3. It was assumed that this indole derivative belonged to a small group of indolyl carboxylic acids, which were isolated from solvent extracts of indole-supplemented supernatants of *Escherichia coli* and *Corynebacteria*.[17] It presented a similar structure to 2-(2-tryptophanyl) lactic acid, obtained from the condensation reaction between tryptophan and pyruvic acid.[17]

The three partial structures **A**, **B** and **C** were built into a full structure from the HMBC correlations (Figure 1). The isoleucine function was attached at C-9 of the indole derivative by the HMBC correlation between H-9 (δ_H 3.96) and C-1″ (δ_C 64.3). Biogenetically, this resembled konbamidin,[18] and may be derived from 1 mol each of isoleucine and a third partial unit, the indole derivative. The ^{13}C-NMR chemical shift of C-10 at δ_C 169.4 indicated the presence of an ester bond. This connection was confirmed from the HMBC correlation between H-8′, 10′ (δ_H 6.76) and C-10 (δ_C 169.4). Using the above data, the structure of **1** was assembled as shown in Figure 2. The stereochemistry of **1** has not yet been determined and remains to be studied in detail.

Cytotoxic activities of the isolated compounds (**1**–**5**) were evaluated against the A549, SK-OV-3, SK-MEL-2 and HCT15 human tumor cell lines *in vitro* using the SRB assay. Compounds **2** and **3** showed moderate cytotoxicity against A549, SK-OV-3, SK-MEL-2 and HCT15 cell lines as shown in Table 2. The mechanism of cytotoxic activity of the ergosterol peroxide was not well studied, but the cytotoxicity of the peroxide compounds (**2** and **3**) was probably ascribed to the presence of the peroxide functional group.[19] Compounds **4** and **5** showed moderate cytotoxicity against HCT15 and SK-OV-3 cell lines, respectively.

ACKNOWLEDGEMENTS

The authors thank Drs EJ Bang, SG Kim, and JJ Seo at the Korea Basic Science Institute for the NMR and MS spectra measurements. This work was supported by the grant 'Classification of Poisonous Mushrooms and Study of Investigating Toxic Constituents, 2006' from the Rural Development Administration in Korea.

1 Dulger, B., Hacioglu, N., Aydin, G. & Uzun, Y. Antimicrobial activity of three Macrolepiota species from Turkey. *Asian J. Chem.* **20,** 3945–3948 (2008).
2 Vetter, J. Trypsin inhibitor activity of basidiomycetous mushrooms. *Eur. Food Res. Technol.* **211,** 346–348 (2000).
3 Barros, L., Baptista, P., Correia, D. M., Morais, J. S. & Ferreira, I. C. F. R. Effects of conservation treatment and cooking on the chemical composition and antioxidant activity of Portuguese wild edible mushrooms. *J. Agric. Food Chem.* **55,** 4781–4788 (2007).
4 Puttaraju, N. G., Venkateshaiah, S. U., Dharmesh, S. M., Urs, S. M. N. & Somasundaram, R. Antioxidant activity of indigenous edible mushrooms. *J. Agric. Food Chem.* **54,** 9764–9772 (2006).
5 Kolcuoglu, Y., Colak, A., Sesli, E., Yildirim, M. & Saglam, N. Comparative charaterization of monophenolase and diphenolase activities from a wild edible mushroom (*Macrolepiota mastoidea*). *Food Chem.* **101,** 778–785 (2006).
6 Senatore, F. Chemical constituents of some species of Agaricaceae. *Biochem. Syst. Ecol.* **16,** 601–604 (1988).
7 Kim, K. H., Choi, S. U., Park, K. M., Seok, S. J. & Lee, K. R. Cytotoxic constituents of *Amanita subjunquillea*. *Arch. Pharm. Res.* **31,** 579–586 (2008).
8 Lehmann, P. F. & Khazan, U. Mushroom poisoning by *Chlorophyllum molybdites* in the Midwest United States. Cases and a review of the syndrome. *Mycopathologia* **118,** 3–13 (1992).
9 Tomihisa, O., Hiroyuki, I., Genjiro, K. & Yoshiteru, O. Lepiotins A and B, new alkaloids from the mushrooms, *Macrolepiota neomastoidea* and *Chlorophyllum molybdites*. *Heterocycles* **47,** 883–891 (1998).
10 Kim, K. H., Lee, I. K., Park, K. M., Kim, W. K. & Lee, K. R. Isolation of γ-lactam alkaloids from the *Macrolepiota neomastoidea*. *Bull. Korean Chem. Soc.* **29,** 1591–1593 (2008).
11 Kazuko, Y., Mizuho, I., Shigenobu, A., Eiko, M. & Satoshi, K. Two new steroidal derivatives from the fruit body of *Chlorophyllum molybdites*. *Chem. Pharm. Bull.* **49,** 1030–1032 (2001).
12 Xu, M. L. *et al.* Cytotoxic constituents isolated from the fruit bodies of *Hypsizigus marmoreus*. *Arch. Pharm. Res.* **30,** 28–33 (2007).
13 Noboru, S. *et al.* Sterol analysis of DMI-resistant and sensitive strains of *Venturia inaequalis*. *Phytochemistry* **41,** 1301–1308 (1996).
14 Yue, J. M., Chen, S. N., Lin, Z. W. & Sun, H. D. Sterols from the fungus *Lactarium volemus*. *Phytochemistry* **56,** 801–806 (2001).
15 Skehan, P. *et al.* New colorimetric cytotoxicity assay for anticancer-drug screening. *J. Natl. Cancer Inst.* **82,** 1107–1112 (1990).
16 Krasnoff, S. B., Reategui, R. F., Wagenaar, M. M., Gloer, J. B. & Gibson, D. M. Cicadapeptins I and II: new aib-containing peptides from the entomopathogenic fungus *Cordyceps heteropoda*. *J. Nat. Prod.* **68,** 50–55 (2005).
17 Thomas, R. G. *et al.* Indolyl carboxylic acids by condensation of indoles with α-keto acids. *J. Nat. Prod.* **63,** 596–598 (2000).
18 Shinonaga, H., Shigemori, H. & Kobayashi, J. Konbamidin, a new indole alkaloid from the okinawan marine sponge *Ircinia* sp. *J. Nat. Prod.* **57,** 1603–1605 (1994).
19 Takei, T., Yoshida, M., Ohnishi-Kameyama, M. & Kobori, M. Ergosterol peroxide, an apoptosis-inducing component isolated from *Sarcodon aspratus* (Berk.) S. Ito. *Biosci. Biotechnol. Biochem.* **69,** 212–215 (2005).

The Journal of Antibiotics (2009) 62, 339–341

www.nature.com/ja

NOTE

Development of a molecule-recognized promoter DNA sequence for inhibition of *HER2* expression

Tsukasa Suzuki[1], Yukihiro Asami[1], Teruyuki Takahashi[1,2], Xiaofei Wang[1,2], Takayoshi Watanabe[1], Toshikazu Bando[3], Hiroshi Sugiyama[3], Noboru Fukuda[2] and Hiroki Nagase[1,2,4]

The Journal of Antibiotics (2009) **62,** 339–341; doi:10.1038/ja.2009.35; published online 15 May 2009

Keywords: cancer; EGFR; growth inhibition; HER2; HER2 transcription factor binding site; pyrrole–imidazole polyamide; transcription regulation

HER2 (also known as *ERBB2*, *NEU*) is one of the transmembrane tyrosine kinase receptor genes belonging to the *EGFR* family. Its expression is kept at a very low level in normal cells, but in tumors, over 30% of breast cancer is detected with extremely high levels of *HER2* mRNA. The overexpression of HER2 is frequently accompanied by tumor migration, low sensitivity to chemotherapy and an adverse prognosis.[1–5] Earlier studies have shown that HER2 protein overexpression and accumulation occurred mainly because of the resulting transcriptional deregulation, not because of the mRNA stabilization[6] and transcription-regulating sequences located in the upstream of the *HER2* coding region.[7] Thus, the inhibition of *HER2* transcription has been considered a useful method of cancer therapy. However, there is no report that a chemical reagent decreases *HER2* transcription in cancer cells. Hence, a compound that pre-transcriptionally deregulates *HER2* expression needs to be evaluated as a potentially useful *HER2* silencer for cancer therapy.

From studies of the double-stranded DNA minor groove recognition of naturally occurring antitumor/antiviral antibiotics, including duocarmycin A and distamycin A, pyrrole–imidazole polyamide (PI polyamide) has been discovered to be a designable DNA-recognition molecule in a sequence-dependent manner.[8–12] A PI polyamide compound composed of the aromatic amino acids, *N*-methylpyrrole (Py) and *N*-methylimidazole (Im), is able to recognize the complementary DNA and bind to the minor groove in a sequence-specific manner because the Py–Im pair recognizes the complementary cytosine–guanine (C–G) and the Im–Py combination will bind to guanine–cytosine (G–C), respectively.[13–17] A pairing of Py–Py or β-alanine–β-alanine (β–β) binds to adenine–thymine or thymine–adenine (A–T or T–A) base pairs.[14–18] The PI polyamide containing γ-aminobutyric acid and *N*, *N*-dimethylaminopropylamine as an internal guide residue was found to specifically bind as a hairpin to be designated a target site with ~300-fold enhancement relative to the binding affinities of the individual unlinked polyamide pair.[18] In addition, this compound has a different character from other gene-silencing tools, such as siRNA or antisense oligo nucleotides, because penetration in the living cells, cytosol import and nuclear transport of PI polyamide occur without any delivery system and may not be influenced by any catabolic enzymes or metabolic enzymes, such as nucleases and *P*450 enzymes, even in animals.[19–22] These findings highlight the advantages of PI polyamide as a suitable candidate compound for pre-transcriptional HER2 gene silencing. An earlier publication has also reported that PI polyamide compounds showed specific binding at the Ets-binding site of the HER2/neu promoter region and inhibition of HER2/neu promoter-driven transcription measured in a cell-free system using nuclear extract from a human breast cancer cell line, SKBR-3.[23] As far as we know, there was no report that showed inhibition of HER2/neu promoter-driven transcription and of cell growth in cancer cells using the PI polyamide compound. In this study, we designed and synthesized a novel PI polyamide compound targeting the HER2 transcription factor (HTF)-binding site, a relatively new activator protein-2-binding site that has been reported to contribute to HER2/c-erbB2 gene overexpression in tumor cell lines.[24,25]

First, we designed an eight-base-recognizing structure of PI polyamide (Figure 1a), which binds to the HTF-binding site inside the *HER2* promoter region (Figure 1b). Polyamide was synthesized, according to the method described earlier.[26]

Next, we performed a direct binding assay using Biacore2000 (GE Healthcare Ltd, Little Chalfont, UK) to see whether PI polyamide-*HER2* binds to a target sequence consisting of double-strand oligonucleotides containing the HTF-binding site. We confirmed that PI polyamide-*HER2* shows an approximately 10-times higher

[1]Division of Cancer Genetics, Department of Advanced Medical Science, Nihon University School of Medicine, Ooyaguchi-kamimachi, Tokyo, Japan; [2]Advanced Research Institute for the Sciences and Humanities, Nihon University, Chiyoda, Tokyo, Japan; [3]Department of Chemistry, Graduate School of Science, and, Institute for integrated Cell-Material Sciences, Kyoto University, Kyoto, Japan and [4]Department of Cancer Genetics, Roswell Park Cancer Institute, Buffalo, NY, USA
Correspondence: Dr Y Asami or Dr H Nagase, Division of Cancer Genetics, Department of Advanced Medical Science, Nihon University School of Medicine, Ooyaguchi-kamimachi, 30-1 Itabashi-ku, Tokyo 173-8610, Japan.
E-mails: 86331@ib.k.u-tokyo.ac.jp or nagase.hiroki@nihon-u.ac.jp
Received 24 March 2009; accepted 1 April 2009; published online 15 May 2009

Figure 1 Designed pyrrole–imidazole polyamide targeting *HER2* promoter region. (**a**) Targeting *HER2* promoter region. Bold lines are targeting sequences. Open circles: Py (*N*-methylpyrrole); black circles: Im (*N*-methylimidazole); ß: beta-alanine; Ac: Acetyl; Dp: *N*, *N*-dimethylaminopropylamine); γ-aminobutyric. (**b**) Chemical structure of PI polyamide-*HER2*.

Table 1 Kinetic constants for binding between PI polyamide-*HER2* and the *HER2* promoter region in a Biacore assay

Analyte	*Ligand*	k_a *(1/Ms)*	k_d *(1/s)*	K_A *(1/M)*	K_D *(M)*
PI poryamide-*HER2*	Match	4.01×10^4	1.93×10^{-3}	2.08×10^7	4.82×10^{-8}
	Mismatch	2.47×10^4	1.03×10^{-2}	2.40×10^6	4.16×10^{-7}

The kinetic constants were calculated from the surface plasmon resonance sensorgrams for the interaction between PI polyamide-*HER2* and biotin-labeled double-strand oligonucleotides hairpin DNA (100 nM) on a sensor chip SA. Match: 5′-CGGGGGTCCTGGAAGCCACAATTTTTTGTG GCTTCCAGGACCCCCG-3′. Mismatch: 5′-CGGGGGTCCTGGGGGCCACAATTTTTTGTGGCCCCCAGG ACCCCCG-3′. The concentration of PI polyamide-*HER2* varies at 0, 50, 100, 250, 1000 and 2000 nM. k_a, association rate constant; k_d, dissociation rate constant; K_A, association equilibrium constant; K_D, dissociation equilibrium constant.

preference for binding to a complementary DNA sequence, including the HTF-binding sites than those for binding to mutated DNA (Table 1).

Furthermore, we examined PI polyamide-*HER2* efficiency for cell proliferation at human breast and colon cancer cell lines, COLO205 (human, Caucasian, colon, adenocarcinoma cell line), HT29 (human, Caucasian, colon, adenocarcinoma grade II cell line), MCF-7 (human, Caucasian, breast, adenocarcinoma cell line) and MDA-MB-231 (human, Caucasian, breast, adenocarcinoma cell line). Cell culture conditions: COLO205 (ATCC number: CCL-222), HT29 (ATCC number: HTB-38), MCF-7 (ATCC number: HTB-22) and MDA-MB-231 (ATCC number: HTB-26) were cultured in RPMI 1640 containing 10% fetal bovine serum and 50 U ml^{-1} Penicillin, 50 μg ml^{-1} Streptomycin in 5% CO_2 in an incubator at 37 °C. Cell proliferation assay condition: colo205, MCF-7 and MDA-MB-231 cells were seeded on 96-well microplates (1.0×10^3 cells per well). Test compound was dissolved in 50% DMSO at an appropriate concentration and was treated for 72 h at 5% CO_2, 37 °C atmosphere. Living cells were detected by WST-8 (NacalaiTesque, Kyoto, Japan) using the maker's manual. The absorbance (A450) of each sample was measured by a Wallac 1420 multilabel counter (Amersham Biosciences, Piscataway, NJ, USA).) Consequently, PI polyamide-*HER2* showed cytostatic activity for all four cancer cells and, most significantly, for MDA-MB-231 cells (Figure 2a). These results suggested that PI polyamide-*HER2* binds to a complementary DNA sequence of the *HER2* promoter region containing an HTF-binding site and inhibited cell proliferation in various cancer cells. We therefore analyzed the expression level of *HER2/ErbB2* mRNA in the most responsive of MDA-MB-231 cells. Quantitative measurements using real-time PCR experiments were performed to evaluate whether PI polyamide-*HER2* is able to decrease the expression of *HER2* mRNA in MDA-MB-231 cells. (qRT-PCR experiments: MDA-MB-231 cultured in six-well plates (1.5×10^4 cells per well) were incubated in the presence of

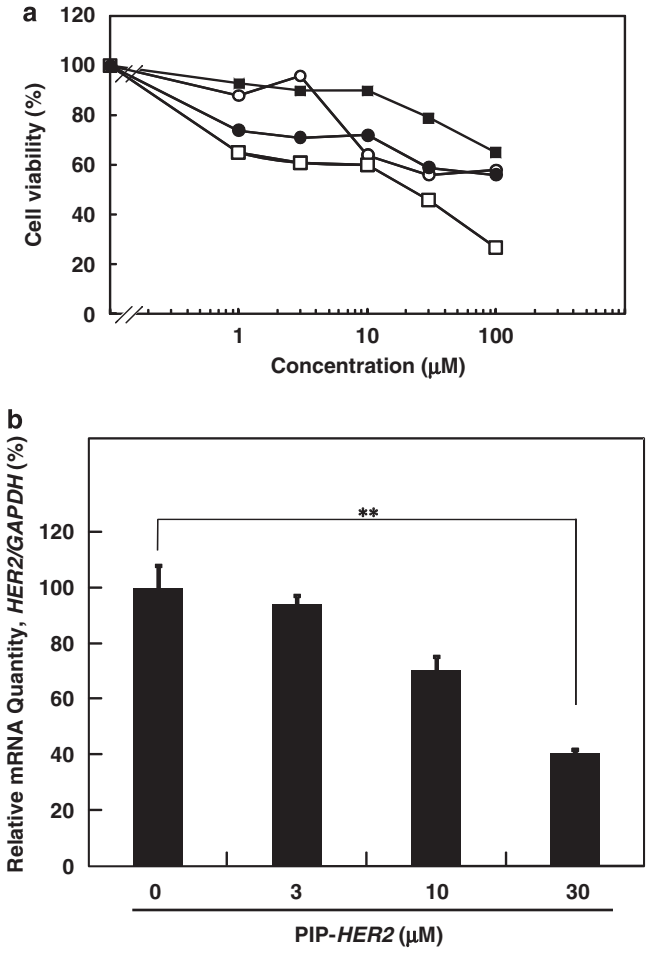

Figure 2 Effects of PI polyamide-*HER2* on cell growth and mRNA expression in MDA-MB-231 cell. (**a**) Effects of PI polyamide-*HER2* on the growth of COLO205, HT29, MCF-7 and MDA-MB-231 cells in a proliferation assay. Test compounds were dissolved in 50% DMSO at appropriate concentrations and treated for 72 h. Black squares: colo205 ($IC_{50}>100$ μM); black circles: HT29 ($IC_{50}<100$ μM); open circles: MCF-7 ($IC_{50}>100$ μM); open squares: MDA-MB-231 ($IC_{50}=30$ μM). (**b**) PI polyamide-*HER2* treatment decreased *HER2* expression in MDA-MB-231 cells. The cell had been treated with different concentrations of PI polyamide-*HER2* for 48 h, and *HER2* mRNA expression was determined by quantitative real-time PCR experiments. The *HER2* mRNA expression levels were expressed as a relative percentage to the control value. Data are expressed as the mean ± s.d. ($n=3$ for each group). The statistical significance of differences between control and experimental groups was determined by using a two-group two-tailed Student's *t*-test; $^{**}P<0.01$ was taken as the level of statistical significance.

some concentration of the test compound for 48 h in 37 °C in a 5% CO_2 atmosphere. After that, harvested cell lines were used for isolation of these total RNA with ISOGEN (NIPPON gene Co. Ltd, Tokyo, Japan) and cDNA made by reverse transcription PCR using Prime script RT reagent kit (Takara Bio Inc., Shiga, Japan). The abundance of *HER2* mRNA was determined by relative quantification that used 1% DMSO-treated cells as control, and GAPDH was measured as internal control with SYBR Premix EXTaq (Takara Bio Inc.) on Thermal Cycler Dice (Takara Bio Inc.). The results showed that PI polyamide-*HER2* induced dose-dependent suppression of *HER2* mRNA expression (Figure 2b). These findings provide a possible molecular basis to explain how PI polyamide-*HER2* inhibits cell proliferation in MDA-MB-231 cells.

It has been reported that the binding ability of PI polyamide for a target sequence depends on the recognition for linear combination of Watson–Crick base pairs.[16] PI polyamide-*HER2* should have approximately 13 000–50 000 capable target sites in a whole genome. Nevertheless, we think that the candidate-binding sites of PI polyamide-*HER2* must be more restricted because of the selective recognition of PI polyamide-*HER2* only at the non-histone binding to the minor groove region of double-helical DNA sequences. To overcome this off-target effect query, further comprehensive analysis is needed to investigate the global binding of PI polyamide-*HER2* using a Genome Precipitation assay in conjunction with microarray chip hybridization or with large-scale sequencing. A whole-genome gene-expression microarray may also help to track the off-target effect. Alternatively, improvement of specificity by a combinatorial modification of the PI polyamide-*HER2* compound may be needed.[27,28]

These observations indicate that PI polyamide-*HER2* induces the decrease of *HER2* mRNA expression and consequently inhibits cell proliferation in various cancer cells, including MDA-MB-231 cells. As far as we know, this is the first report that a chemical reagent decreases HER2 transcription in cancer cell and inhibits cell growth in various cancer cell lines. We, therefore, propose that *HER2* transcription can be controllable by means of PI polyamide-*HER2* administration and that PI polyamide-*HER2* may be a new type of chemical inhibitor for *HER2* silencing.

ACKNOWLEDGEMENTS

This work is supported by the Nihon University Multidisciplinary Research Grant for 2006; the Academic Frontier Project for 2006 Project for Private Universities: matching fund subsidy from MEXT to HN; the National Institute of Environmental Health Services to HN (ES012249-01); and National Cancer Institute Center Support Grant CA16056 (to Roswell Park Cancer Institute).

1 Press, M. F., Cordon-Cardo, C. & Slamon, D. J. Expression of the HER-2/neu proto-oncogene in normal human adult and fetal tissues. *Oncogene* **5,** 953–962 (1990).
2 Slamon, D. J. *et al.* Studies of the HER-2/neu proto-oncogene in human breast and ovarian cancer. *Science* **244,** 707–712 (1989).
3 Kraus, M. H., Popescu, N. C., Amsbaugh, S. C. & King, C. R. Overexpression of the EGF receptor-related proto-oncogene erbB-2 in human mammary tumor cell lines by different molecular mechanisms. *EMBO J.* **6,** 605–610 (1987).
4 Slamon, D. J. *et al.* Human breast cancer: correlation of relapse and survival with amplification of the HER-2/neu oncogene. *Science* **235,** 177–182 (1987).
5 Gusterson, B. A. *et al.* Prognostic importance of c-erbB-2 expression in breast cancer. International (Ludwig) Breast Cancer Study Group. *J. Clin. Oncol.* **10,** 1049–1056 (1992).
6 Pasleau, F., Grooteclaes, M. & Gol-Winkler, R. Expression of the c-erbB2 gene in the BT474 human mammary tumor cell line: measurement of c-erbB2 mRNA half-life. *Oncogene* **8,** 849–854 (1993).
7 Hurst, H. C. Update on HER-2 as a target for cancer therapy: the ERBB2 promoter and its exploitation for cancer treatment. *Breast Cancer Res.* **3,** 395–398 (2001).
8 Takahashi, I. *et al.* Duocarmycin A, a new antitumor antibiotic from *Streptomyces*. *J. Antibiot.* **41,** 1915–1917 (1988).
9 Arcamone, F., Penco, S., Orezzi, P., Nicolella, A. & Pirelli, A. Structure and synthesis of distamycin A. *Nature* **203,** 1064–1065 (1964).
10 Trauger, J. W., Baird, E. E. & Dervan, P. B. Extended hairpin polyamide motif for sequence-specific recognition in the minor groove of DNA. *Chem. Biol.* **3,** 369–377 (1996).
11 Gottesfeld, J. M., Neely, L., Trauger, J. W., Baird, E. E. & Dervan, P. B. Regulation of gene expression by small molecules. *Nature* **387,** 202–205 (1997).
12 Tao, Z. F., Fujiwara, T., Saito, I. & Sugiyama, H. Sequence-specific alkylation of DNA by duocarmycin A and its novel derivatives bearing PY/IM polyamides. *Nucleosides Nucleotides* **18,** 1615–1616 (1999).
13 Kielkopf, C. L., Baird, E. E., Dervan, P. B. & Rees, D. C. Structural basis for G.C recognition in the DNA minor groove. *Nat. Struct. Biol.* **5,** 104–109 (1998).
14 Dervan, P. B. Molecular recognition of DNA by small molecules. *Bioorg. Med. Chem.* **9,** 2215–2235 (2001).
15 Dervan, P. B. & Edelson, B. S. Recognition of the DNA minor groove by pyrrole–imidazole polyamides. *Curr. Opin. Struct. Biol.* **13,** 284–299 (2003).
16 Murty, M. S. & Sugiyama, H. Biology of *N*-methylpyrrole-*N*-methylimidazole hairpin polyamide. *Biol. Pharm. Bull.* **27,** 468–474 (2004).
17 Zhang, W., Bando, T. & Sugiyama, H. Discrimination of hairpin polyamides with an alpha-substituted-gamma-aminobutyric acid as a 5′-TG-3′ reader in DNA minor groove. *J. Am. Chem. Soc.* **128,** 8766–8776 (2006).
18 White, S., Baird, E. E. & Dervan, P. B. Effects of the A.T/T.A degeneracy of pyrrole–imidazole polyamide recognition in the minor groove of DNA. *Biochemistry* **35,** 12532–12537 (1996).
19 Fujimoto, K. *et al.* Sequence-specific protection of plasmid DNA from restriction endonuclease hydrolysis by pyrrole–imidazole–cyclopropapyrroloindole conjugates. *Nucleic Acids Res.* **30,** 3748–3753 (2002).
20 Best, T. P., Edelson, B. S., Nickols, N. G. & Dervan, P. B. Nuclear localization of pyrrole–imidazole polyamide–fluorescein conjugates in cell culture. *Proc. Natl Acad. Sci. USA* **14,** 12063–12068 (2003).
21 Nickols, N. G., Jacobs, C. S., Farkas, M. E. & Dervan, P. B. Improved nuclear localization of DNA-binding polyamides. *Nucleic Acids Res.* **35,** 363–370 (2007).
22 Fukasawa, A. *et al.* Pharmacokinetics of pyrrole–imidazole polyamides after intravenous administration in rat. *Biopharm. Drug Dispos.* **30,** 81–89 (2009).
23 Chiang, S. Y. *et al.* Targeting the Ets binding site of the HER2/neu promoter with Pyrrole–Imidazole polyamides. *J. Biol. Chem.* **275,** 24246–24254 (2000).
24 Grooteclaes, M. *et al.* A new cis element is involved in the HER2 gene overexpression in human breast cancer cells. *Cancer Res.* **59,** 2527–2531 (1999).
25 Vernimmen, D. *et al.* Identification of HTF (HER2 transcription factor) as an AP-2 (activator protein-2) transcription factor and contribution of the HTF binding site to ERBB2 gene overexpression. *Biochem. J.* **370,** 323–329 (2003).
26 Bando, T., Narita, A., Saito, I. & Sugiyama, H. Molecular design of pyrrole–imidazole hairpin polyamides for effective DNA alkylation. *Chemistry* **8,** 4781–4790 (2002).
27 Puckett, J. W. *et al.* Quantitative microarray profiling of DNA-binding molecules. *J. Am. Chem. Soc.* **129,** 12310–12319 (2007).
28 Bando, T., Narita, A., Iwai, A., Kihara, K. & Sugiyama, H. C-H to N substitution dramatically alters the sequence-specific DNA alkylation, cytotoxicity, and expression of human cancer cell lines. *J. Am. Chem. Soc.* **126,** 3406–3407 (2004).

The Journal of Antibiotics (2009) 62, 343

www.nature.com/ja

CORRIGENDUM

In vitro and in vivo antitrypanosomal activities of three peptide antibiotics: leucinostatin A and B, alamethicin I and tsushimycin

Aki Ishiyama, Kazuhiko Otoguro, Masahito Iwatsuki, Miyuki Namatame, Aki Nishihara, Kenichi Nonaka, Yuta Kinoshita, Yoko Takahashi, Rokuro Masuma, Kazuro Shiomi, Haruki Yamada and Satoshi Ōmura

The Journal of Antibiotics (2009) **62,** 343; doi:10.1038/ja.2009.41

Correction to: *The Journal of Antibiotics* (2009) **62**, 303–308; doi:10.1038/ja.2009.32

The authors of the above noted an error in publication of this paper (AOP and in this issue) in the name of the third author. The correct name of this author is Masato Iwatsuki.

The Journal of Antibiotics (2009) 62, 345

www.nature.com/ja

CORRIGENDUM

Development of a molecule-recognized promoter DNA sequence for inhibition of *HER2* expression

Tsukasa Suzuki, Yukihiro Asami, Teruyuki Takahashi, Xiaofei Wang, Takayoshi Watanabe, Toshikazu Bando, Hiroshi Sugiyama, Noboru Fukuda and Hiroki Nagase

The Journal of Antibiotics (2009) **62,** 345; doi:10.1038/ja.2009.42

Correction to: *The Journal of Antibiotics* (2009) **62**, 339–341; doi:10.1038/ja.2009.35

The authors of the above noted an error in the publication of this paper (AOP and in this issue) in the legend of Figure 1 and *y* axis of Figure 2. The corrected Figures 1 and 2 are shown below.

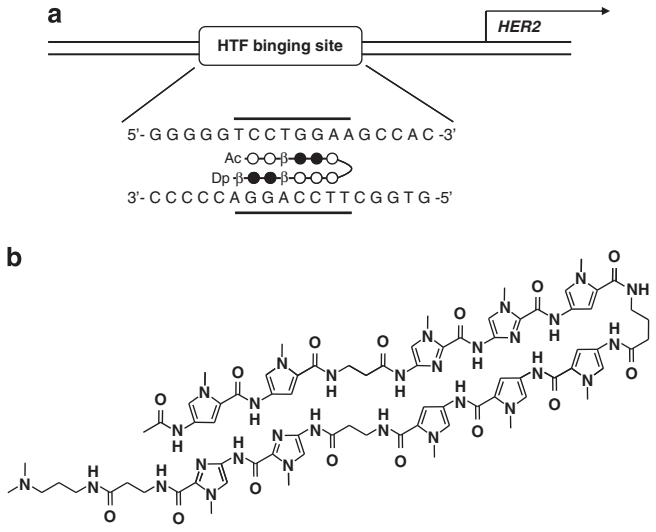

Figure 1 Designed pyrrole–imidazole polyamide targeting *HER2* promoter region. (**a**) Targeting *HER2* promoter region. Bold lines are targeting sequences. Open circles: Py (*N*-methylpyrrole); black circles: Im (*N*-methylimidazole); ß: beta-alanine; Ac: Acetyl; Dp: *N*, *N*-dimethylaminopropylamine;): γ-aminobutyric. (**b**) Chemical structure of PI polyamide-*HER2*.

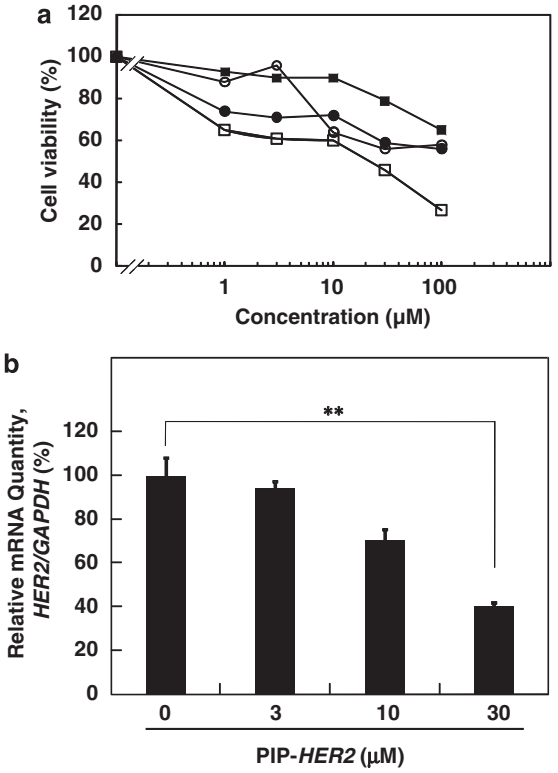

Figure 2 Effects of PI polyamide-*HER2* on cell growth and mRNA expression in MDA-MB-231 cell. (**a**) Effects of PI polyamide-*HER2* on the growth of COLO205, HT29, MCF-7 and MDA-MB-231 cells in a proliferation assay. Test compounds were dissolved in 50% DMSO at appropriate concentrations and treated for 72 h. Black squares: colo205 ($IC_{50}>100\,\mu M$); black circles: HT29 ($IC_{50}<100\,\mu M$); open circles: MCF-7 ($IC_{50}>100\,\mu M$); open squares: MDA-MB-231 ($IC_{50}=30\,\mu M$). (**b**) PI polyamide-*HER2* treatment decreased *HER2* expression in MDA-MB-231 cells. The cell had been treated with different concentrations of PI polyamide-*HER2* for 48 h, and *HER2* mRNA expression was determined by quantitative real-time PCR experiments. The *HER2* mRNA expression levels were expressed as a relative percentage to the control value. Data are expressed as the mean ± s.d. ($n=3$ for each group). The statistical significance of differences between control and experimental groups was determined by using a two-group two-tailed Student's *t*-test; $^{**}P<0.01$ was taken as the level of statistical significance.